UNIVERSITY OF CALGARY

The Characterization of Fibrous Sheath and Outer Dense Fiber Proteins of the Rat Sperm Tail

by

Carolyn Fitzgerald

A THESIS

SUBMITTED TO THE FACULTY OF GRADUATE STUDIES IN PARTIAL

FULFILLMENT OF THE REQUIREMENTS FOR THE DEGREE OF

MASTER OF SCIENCE

DEPARTMENT OF BIOCHEMISTRY AND MOLECULAR BIOLOGY

CALGARY, ALBERTA

DECEMBER, 2004

Thesis Abstract

The aim of this study was to further characterize three prominent proteins of the rat sperm tail, ODF14, FS14 and Spag5. FS14 and ODF14 were used to generate antibodies which were subsequently affinity-purified and used to screen a rat testicular cDNA library. Two cDNAs were isolated (designated 1017 and 1038) and it was determined that 1017 was homologous to mouse ornithine decarboxylase antizyme 3. However, it was found that 1038 resulted from a chimeric mRNA, consisting of sequences from two different chromosomes.

Spag5 was originally thought to be testis-specific and was identified due to its interaction with Odf1 using the yeast two hybrid system. Knock-out studies revealed no significant phenotype in mice and spag5 was found to be 73% similar to the human mitotic spindle protein, Astrin. We found that in spermatogenesis Spag5 does not appear to localize to either the axoneme or the meiotic spindle, but instead associates with ODF. In mitotic cells it colocalizes with Astrin in the mitotic spindle and the cytoplasm of rat IEC-18 cells

ACKNOWLEDGEMENTS

I would like to acknowledge the support of the following:

Dr. Frans van der Hoorn for his guidance and support for the duration of this thesis project

Dr. Dave Schriemer for his guidance and extra help with the mass spec work

Dr. J.B. Rattner for his guidance

Min Cheng, Yibing Ruan and Ying Zhang for their help and support

Dr. Richard Oko for his guidance

All of my family and friends for their support

TABLE OF CONTENTS

LIST OF FIGURES

Chapter 1: Introduction

1.a ***Spermatogenesis***

Spermatogenesis is a unique process which occurs within the seminiferous tubules within the testis. The testis is surrounded by a thick capsule of collagenous connective tissue which is called the tunica albuginea. The mediastinum testis is a thickening of the tunica albuginea on the posterior surface of the testis, which penetrates the organ and divides it into approximately 250 testicular lobes. Each of these lobes contains 1-4 seminiferous tubules, which are composed of a complex epithelium containing Sertoli cells and germinal cells (Johnson, 1970). Spermatogenesis begins with the spermatogonium (stem cell) which is next to the basal lamina. After sexual maturity, the spermatogonium undergoes a series of mitotic divisions. The spermatogonium divides to both differentiate and to renew the spermatogonium. In the rat, this division leads to type A and B spermatogonia. The type A cell is the renewed spermatogonium and the type B cell becomes a spermatocyte which will undergo meiosis (Clermont, 1966). The first meiotic division has six recognizable stages that the cells go through based on the appearance and arrangement of chromosomes which are called preleptotene, leptotene, zygotene, pachytene, diplotene and diakinesis. During the second meiotic division, the spermatocyte divides to form haploid round spermatids. These spermatids then undergo a series of morphological changes known as spermiogenesis, which results in mature spermatozoa (Clermont, 1966). The sequence of maturation changes that occur in a given area of the germinal epithelium between two successive appearances of a given cell association is called the cycle of the seminiferous epithelium (Leblond and Clermont, 1952). These stages exist because the germ cells in the seminiferous epithelium do not

separate during division, but remain attached via cytoplasmic bridges (Fawcett, 1959). The stages of the cycle can be identified by changes in the steps of spermatid development. In the rat, there are 14 stages in the cycle of the seminiferous epithelium (Leblond and Clermont, 1952). The stages and steps of the cycle of the rat seminiferous epithelium are depicted in figure 1.

1.b *Spermiogenesis*

Spermiogenesis is the third and final stage of spermatogenesis. Spermiogenesis is divided into four phases; the Golgi phase (steps 1-3 of the cycle), the cap phase (steps 4-7), the acrosomic phase (steps 8-14) and the maturation phase (steps 15-19). During the cap phase, the acrosomic granule forms and the centrioles migrate to the cell surface opposite to where the acrosome is being formed. Concurrently, the assembly of the axoneme is initiated. The acrosomic granule spreads over and covers the anterior half of the condensing nucleus, which is known as the acrosomal cap. During the acrosomic phase, the nucleus condenses and elongates and the acrosomal cap conforms to the shape of the spermatid head. The mitochondria begins to migrate to the middle piece of the sperm tail. During the last phase (maturation phase), the accessory components of the tail such as the outer dense fibers (ODF) and the fibrous sheath (FS) are formed. At the end of this phase, the residual bodies (cytoplasm) and all organelles except for the mitochondria in the middle piece are shed and engulfed by the Sertoli cells. Steps 7, 9, 14 and 18 of spermiogenesis are depicted in figure 2. The elongated spermatids are then released into the lumen of the seminiferous tubules as free cells to be transported to the epididymis for complete maturation. The cell morphological changes that occur during spermiogenesis are intricately linked to the complete reorganization of the microtubular

Figure 1: Stages of the cycle of the rat epithelium, with modifications from Dym and Clermont (1970). Each column, represented by a Roman numeral depicts cellular associations at each of the 14 stages of the cycle. The types of germ cells observed in developmental sequence are: A spermatogonia (A), Intermediate spermatogonia (In), B spermatogonia (B), preleptotene primary spermatocyte (Pi), leptotene primary spermatocyte (L), zygotene primary spermatocyte (Z), pachytene primary spermatocyte (P), diplotene spermatocyte (Di), and secondary spermatocyte (II). The nineteen steps of spermiogenesis are illustrated by spermatids (numbered 1-19) in the upper two rows.

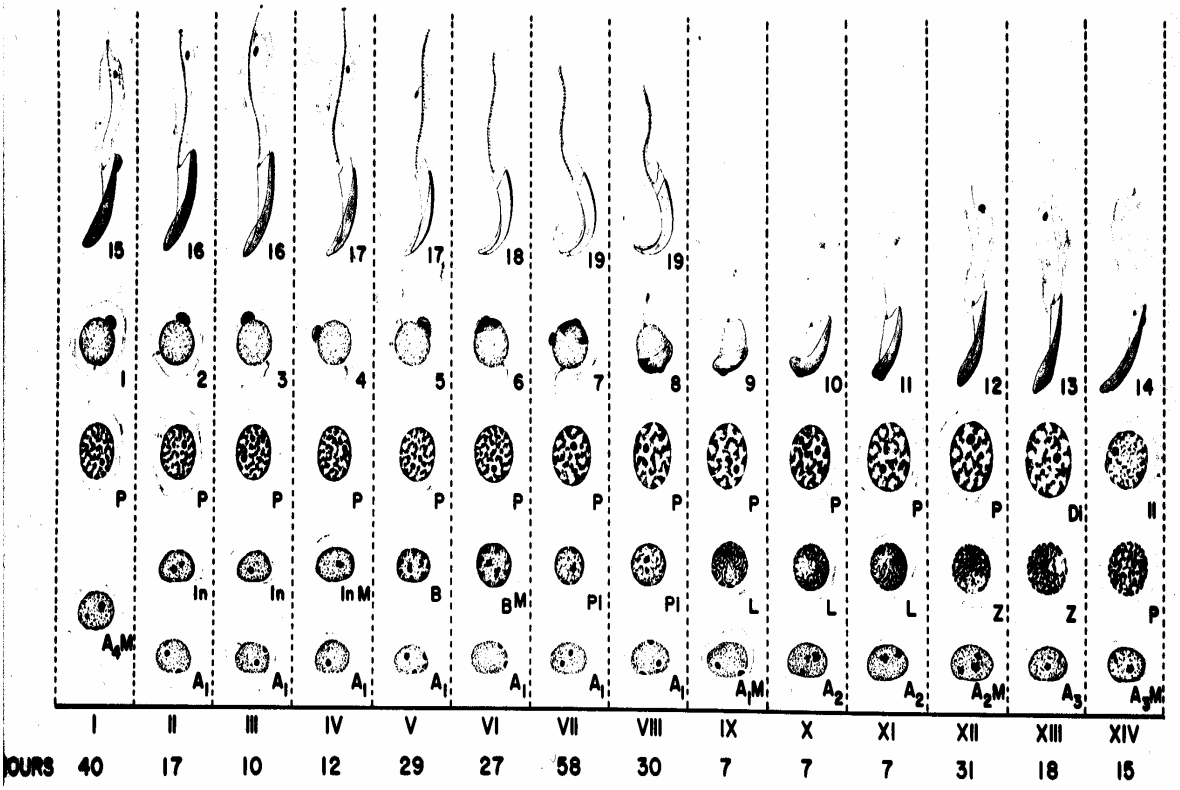
15
16
16
17
17
18
19
19
1
2
3
4
5
6
7
8
9
10
11
12
13
14
P
P
P
P
P
P
P
P
P
P
P
P
DI
II
In
In
In M
B
B M
PI
PI
L
L
L
Z
Z
P
A3M
A1
A1
A1
A1
A1
A1
A1
A1M
A2
A2
A2M
A3
A3M
I
II
III
IV
V
VI
VII
VIII
IX
X
XI
XII
XIII
XIV
OURS 40
17
10
12
29
27
58
30
7
7
7
31
18
15

Figure 2: Four steps of spermiogenesis are illustrated; steps 7, 9, 14 and 18. Cross-sections of the proximal and distal regions of the tail are shown with the various components such as outer dense fibers (ODF) and their anlagen (AODF), fibrous sheath (FS), the fibrous sheath longitudinal columns (LC) and its anlagen (ALC) and the fibrous sheath ribs. Note that until the end of step 14, the tail structures are enclosed within a periaxonemal compartment delimited in its proximal portion by a double plasma membrane that extends down to the annulus (An), near the connecting piece (CP). Early in step 15, the annulus slides along the axoneme while the ODF increase in diameter and the mitochondria migrate towards the tail. Other lettering: Man, manchette; AS, acrosomic system; N, nucleus; M, mitochondria; CB, chromatoid body; G, golgi apparatus; CA, centriolar adjunct. Adapted from Oko and Clermont, 1990.

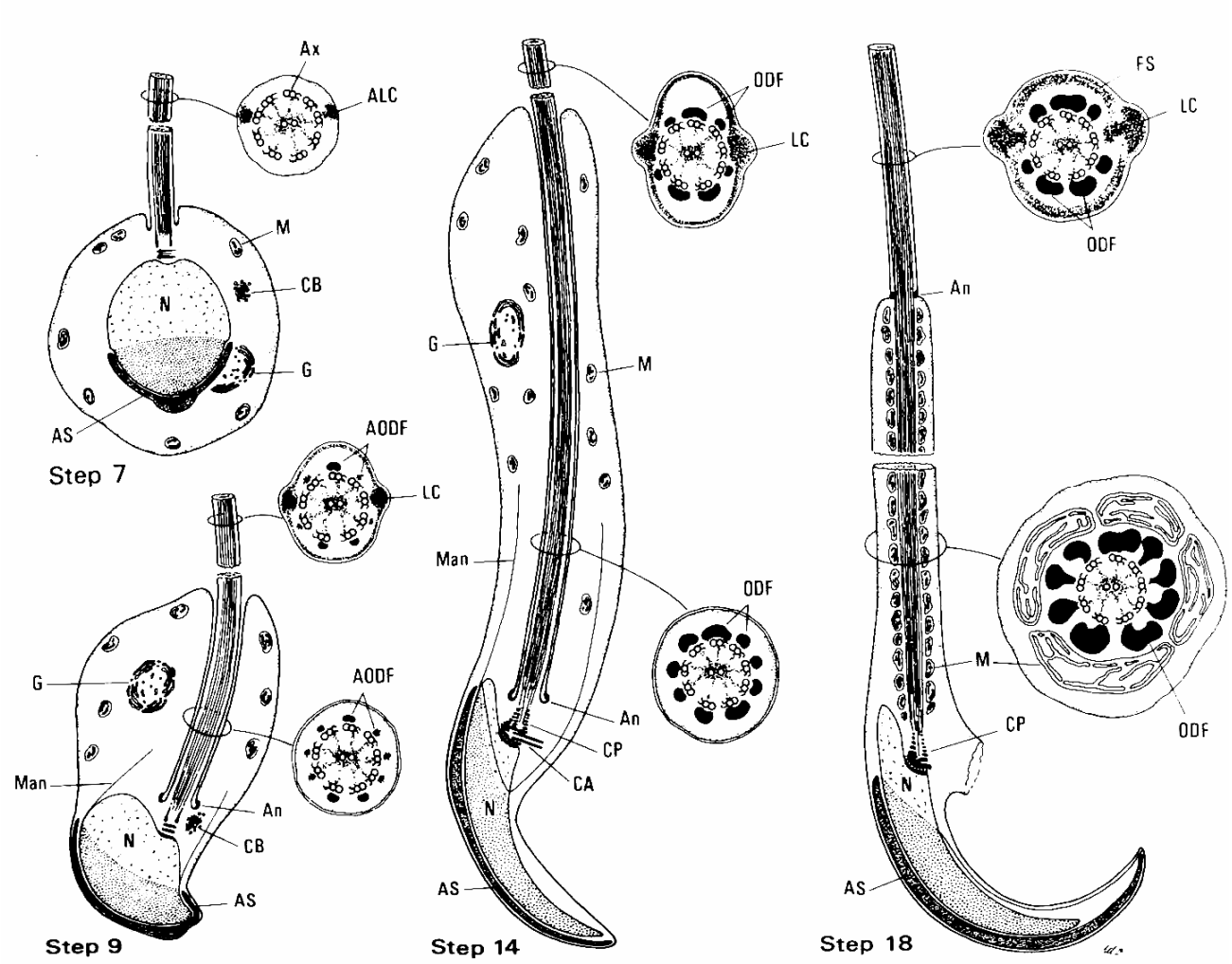
Ax
ALC
M
CB
N
G
AS
Step 7
AODF
LC
G
Man
AODF
An
CB
N
AS
Step 9
ODF
LC
G
M
Man
ODF
An
CP
CA
N
AS
Step 14
FS
LC
ODF
An
M
ODF
CP
N
AS
Step 18

cytoskeleton. The high plasticity of microtubules allows for the formation of the axoneme and the manchette, a cone-shaped microtubular structure that is implicated in sperm nuclear shaping and in caudal redistribution and compartmentalization of the cytoplasm. Testicular spermatids are not motile or fertile and require epididymal differentiation to be able to fertilize eggs. Epididymal sperm maturation appears to be the result of successive sequential events which occur only in different epididymal regions and has never been achieved under *in vitro* conditions. The main changes seen in the maturing spermatozoa in the epididymis are the ability to move, recognize and bind to the zona pellucida, and to fuse with the plasma membrane of the oocyte. Most of the changes in the spermatozoa in the epididymus occur on the surface of its plasma membrane (Dacheux *et al*, 2003).

1.c ***Structure of the Rat Sperm Tail***

The mammalian spermatozoa tail has four distinct segments: the connecting piece (adjacent to the head), the midpiece, the principal piece, and the short end piece. These sperm tail segments contain two unique cytoskeletal elements along the central axoneme called the outer dense fibers (ODF) and the fibrous sheath (FS) which distinguish the tail from simple flagella or cilia. Nine ODF extend through the midpiece (each associating with a specific microtubule doublet of the axoneme) and terminate in the end piece. The ODF is composed of a thin cortex surrounding a thick medulla. The protein composition of the ODF seems to be unique to the sperm. These ODFs are surrounded by a mitochondrial sheath in the midpiece. The mitochondria in the mitochondrial sheath (MS) are wrapped helically around the ODF. This structure is the energy generation system of the spermatozoa. In the principal piece, two longitudinal columns of the FS replace ODFs

3 and 8 and the transverse ribs of the FS surround the remaining ODF (Fawcett, 1975). The structure of the rat sperm tail is depicted in figure 3. Many studies have suggested that ODF functions as passive elastic structures, provide elastic recoil for the tail and possibly to protect the sperm against shear forces (Fawcett, 1975 and Baltz *et al*, 1990). The FS serves as a scaffold for both glycolytic enzymes and proteins of signaling cascades and possibly plays a role in the regulation of sperm motility (Eddy *et al*, 2003). Also associated with the sperm tail are the plasma membrane and a small amount of cytoplasm. The plasma membrane surrounding the MS is studded with diagonal or circumferential arrays of particles that follow the contour of the mitochondrial helix and are not present over the plasma membrane covering the cytoplasmic droplet (Friend and Fawcett, 1974). At the junction of the midpiece and the principal piece, the plasmalemma exhibits rows of particles in the outer part of the membrane. Covering the principal piece, the plasmalemma shows a double row of transmembrane particles called the zipper, which follow longitudinally over the FS opposite to ODF number 1 (Friend, 1977).

1.d ***Assembly of the Sperm Tail***

The process of spermiogenesis and how the tail is assembled is an intricate and detailed process. The initial formation of the tail elements described previously occurs in a portion of the cytoplasm that is secluded from the rest of the spermatid cytoplasm, called the periaxonemal compartment. This compartment is surrounded by a double plasma membrane in its proximal portion. The growth of the axoneme (during Golgi phase) is initiated by the distal centriole, which elongates in all growing cilia by the addition of alpha and beta tubulin at the distal ends of the microtubular singlets and

Figure 3: The rat spermatozoon has a sickle-shaped head and a tail that is 190 um long. The four regions of the tail are indicated, ie. The connecting piece (CP) which joins the head and the tail, the middle piece or midpiece (MP) showing the transversely oriented mitochondria, the principle piece (PP), and the end piece (EP). Cross-sections of all the regions of the tail are depicted showing the axoneme (microtubular doublets surrounding two microtubule singlets), the outer dense fibers, the fibroush sheath with the longitudinal columns and ribs, and mitochondria. The annulus is also shown at the junction of the midpiece and the principle piece. (adapted from Oko and Clermont, 1990).

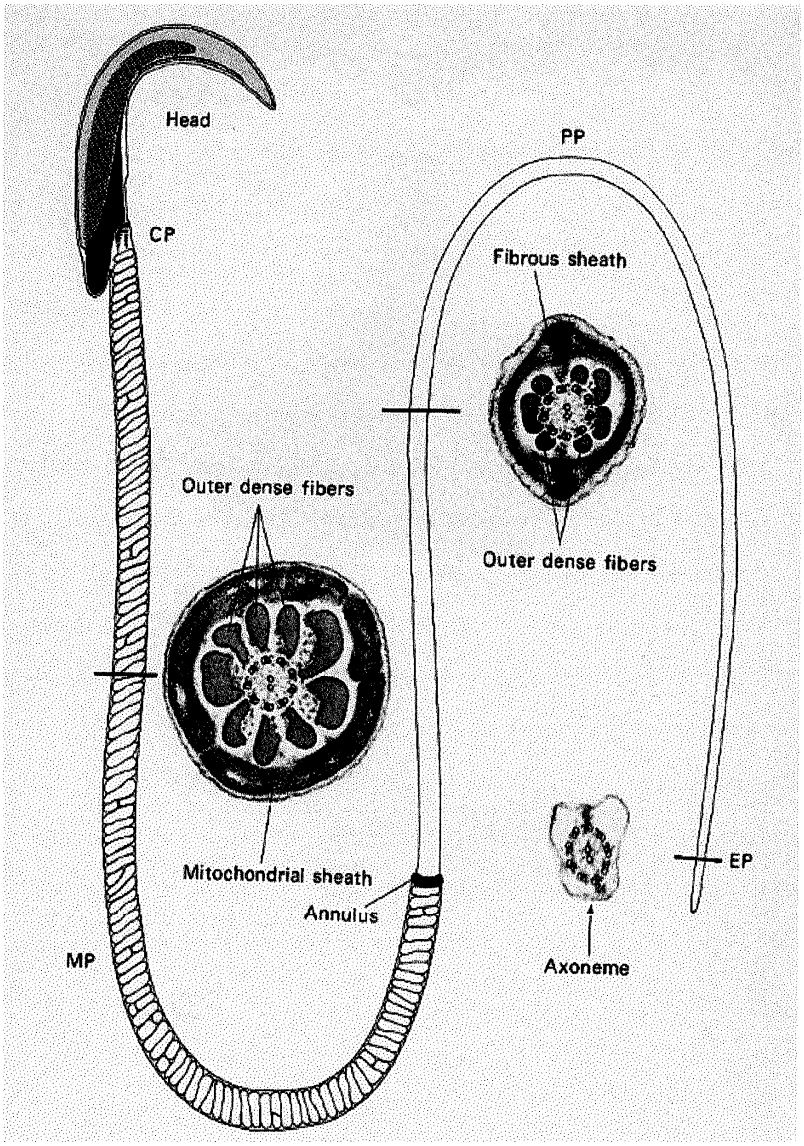
Head
CP
PP
Fibrous sheath
Outer dense fibers
Outer dense fibers
Mitochondrial sheath
Annulus
MP
EP
Axoneme

doublets (Rosenbaum *et al*, 1969). The connecting piece begins its formation during the cap phase. The centriole becomes associated with the implantation fossa at the periphery of the nucleus (Irons, 1983). There is also a thickening of the nuclear envelope where the implantation fossa is located and this structure is known as the basal plate. The material making up the capitulum and striated collar of the connecting piece gradually amasses around the two centrioles. During the cap phase, a microtubular structure known as the centriolar adjunct, grows out from the proximal centriole and reaches its full length in the acrosomic phase. The functional purpose for this adjunct is not known, but Irons suggests it might be for the transportation of protein from the cytoplasm to the forming neck piece (Irons, 1983). The biogenesis of the ODF occurs by the acrosomic phase and form next to each of the microtubular doublets of the forming axoneme in a proximal to distal direction along the tail. During the maturation phase, there is a rapid and massive increase in diameter of the ODF throughout its length (Irons and Clermont, 1982b, reviewed by Oko and Clermont, 1990). The FS precursor is laid down in a distal to proximal direction along the tail starting in the Golgi phase and ending in the acrosomic phase (Irons and Clermont, 1982a). Interestingly, the FS precursors are not immunologically identical to the mature FS components. Polyclonal antibodies against the mature FS do not recognize FS precursors at the light and ultrastructural level (Clermont *et al*, 1990 and Oko and Clermont, 1989).

1.e ***Microtubules and the Cytoskeleton***

The cellular cytoskeleton is a vital component of all eukaryotic cells, including somatic cells, oocytes and sperm cells. The cytoskeleton is responsible for a wide range

of functions including the maintenance of cellular integrity, organelle transport, cellular motility, meiosis and mitosis, membrane trafficking and the development of cell polarity and extensions. The cytoskeleton is composed of microtubules, actin filaments and intermediate filaments. Microtubules are implicated in a variety of different cellular processes, including spermatogenesis and mitosis. Microtubules are highly dynamic cylindrical structures assembled from alpha/beta tubulin heterodimers. Nucleation of microtubules occurs primarily at microtubule organizing centers (MTOC) or centrosomes, which are usually composed of a pair of centrioles embedded in a matrix of pericentriolar material (Dictenberg *et al*, 1998). The mitotic spindle is a bipolar microtubule-based structure which is responsible for chromosome segregation during mitosis (Compton, 2000). The basic element of the spindle is an antiparallel array of microtubules with their minus ends anchored at the spindle poles and their plus ends projecting towards the chromosomes. This lattice of microtubules serves as a track for motor proteins such as the dynein and kinesin superfamilies (Hirokawa *et al*, 1998a and Kim and Endow, 2000). The conventional view is that these motors bind to both microtubules and molecular cargo such as vesicles, and hydrolyze ATP to achieve motion along the MT “tracks”, thereby transporting the cargo within the cell. Motors have also been implicated in regulating the dynamics of MT assembly. Spindle microtubules are highly dynamic with a half life of 60-90 seconds, which is significantly more unstable than other microtubule based structures. This dynamic instability is necessary for proper spindle structure and regulation (Joshi, 1998; Saxton *et al*, 1984). Mitotic spindles organize at the time of nuclear envelope breakdown when two active MTOCs at opposite poles of the nucleus start to emanate microtubules. Spindle proteins can be divided into

three groups, microtubule-based motor proteins, microtubule-destabilizing factors and nonmotor microtubule-associated proteins (MAPs) which mostly have a role in the stabilization of microtubules. The role of multiple microtubule motors in spindle assembly has been the subject of intense investigation including bipolar kinesins, COOH-terminal kinesins, and cytoplasmic dynein (Sharp *et al*, 2000a). Dynein is thought to anchor astral microtubules to the cell cortex and, through its minus end-directed motor activity, maintain spindle pole positioning and promote spindle elongation. Dynein also localizes to the kinetochores during mitosis (Pfarr *et al*, 1990) and might be involved in chromosome segregation during anaphase (Sharp *et al*, 2000b). The role of nonmotor MAPs has only recently been investigated more thoroughly. One example of a nonmotor MAP family is the Dis1-TOG family. These MAPs have been shown to localize mainly to the centrosomes and spindle microtubules during mitosis. Biochemical studies have shown that Dis1-TOG proteins promote microtubule stability by stimulating growth at the plus end. Additionally, the Dis1-TOG family has been shown to stabilize the microtubule-kinetochore interaction (Garcia *et al*, 2001; He *et al*, 2001; Nakaseko *et al*, 2001). Multiple asters (MAST)/Orbit defines another emergent family of nonmotor MAPs that contains a NH_2-terminal domain also present in the Dis1-TOG family (Inoue *et al*, 2000 and Lemos *et al*, 2000). Members of the MAST/Orbit family have been found to be essential for spindle assembly (Pasqualone and Huffaker, 1994; Inoue *et al*, 2000; Lemos *et al*, 2000) and have been found to localize to the mitotic spindle, centrosomes and kinetochores (Lemos *et al*, 2000). The detailed morphogenesis of meiotic spindles has only been elucidated in a few female systems and in fewer male systems and shows a great variety in the number and location of MTOCs, differing from mitotic spindles

(Schatten *et al*, 1986; Messinger and Albertini, 1991). However, there are many motor and nonmotor proteins which have been implicated in both mitotic and meiotic spindles such as CENP-E in mouse (motor protein) (Parra *et al*, 2002), kinesin-like protein KLP67A in Drosophila (Gandhi *et al*, 2004) and many others. Research on motor and nonmotor microtubule-associated proteins is vast and extensive and with over thousands of publications on kinesins and dyneins for an example. An extensive review on these proteins is beyond the scope of this report. Suggested reviews of motor proteins: dynein and chromosome movement (Banks and Heald, 2001), kinesin motor domains (Sablin and Fletterick, 2004), MAPs, kinesins and microtubules (Maekawa and Schiebel, 2004).

1.f ***Microtubules and Spermatogenesis***

In spermatogenesis, microtubules are important structures in the cytoskeleton, mitotic spindles, meiotic spindles, the axoneme and the manchette, as already mentioned. Round spermatids contain a randomly cortical microtubule network, and display a normal centrosome consisting of a pair of centrioles along with a focus containing gamma-tubulin (Fouquet *et al*, 1998; Manandhar *et al*, 1998). The gamma-tubulin focus nucleates and organizes mainly acetylated microtubules (Fouquet *et al*, 1998). Polyglutamylation (Edde *et* al, 1990) and polyglycylation (Redeker *et al*, 1994) are two major modifications for both alpha and beta tubulin. These two modifications consist of the addition to a glutamyl residue located in the C-terminus of tubulin of at least 6 glutamates for polyglutamylation and 3-40 glycines for polyglycylation. Glycylation and glutamylation can coexist in one alpha-tubulin isoform and have been found in the axoneme of some mammalian species (Mary *et al*, 1996; Rudiger *et al*, 1995; Kan *et al*, 1995). The random

assortment of microtubules in round spermatids changes in the cap phase of spermiogenesis which the appearance of the manchette, which is a highly organized bundle of microtubules around the nucleus. Testis-specific tubulin isoforms have been found in the manchette, including a highly divergent testis-specific alpha-tubulin isoform (Hecht *et* al, 1988)and two coexpressed isoforms alpha3/7-tubulin and beta3/4-tubulin (Villasante *et al*, 1987; Lewis an Cowan, 1988). Also occurring around the time of the appearance of the manchette in the round spermatid is a polarity, where the Golgi apparatus, the associated acrosome and a giant lysosome are located at the cell anterior pole and the centrioles are positioned at the cell caudal pole. By step 18 elongated spermatids, the manchette is no longer present and the axoneme has fully formed.

1.g *The Outer Dense Fibers*

The molecular network that makes up the proteins of the sperm tail is relatively unknown. However, a few components of the ODF, ODF-associated proteins and FS have been characterized. The isolated ODF is composed of man proteins, (Oko, 1988) of which the 14-, 20-, 27-, and 84- kDa are the most prominent. The first ODF protein to be characterized was Odf1 (previously called RT7 (Vera *et al*, 1984 and van der Hoorn *et al*, 1990), Odf27 (Morales *et al*, 1994 and Shao and van der Hoorn, 1996), and rts5/1 (Burfeind and Hoyer-Fender, 1991). Odf1 was found to localize to the inner medulla of the ODFs (Morales *et al*, 1994). Characterization of Odf1 has also demonstrated that it has 16 C-terminal CGP repeats which are highly reminiscent of the *Drosophila* MST family. Odf1 was found to contain a leucine zipper in its N-terminus (Vera *et al*, 1984) and this was used as bait in protein interaction screens to identify Odf1-interacting

proteins. Leucine zippers are characterized by 4 or 5 leucines in the primary protein structure which are located every 7 amino acid residues. These leucines act as a zipper to bind two proteins together to make protein dimers. Leucine zippers were originally identified in DNA-binding proteins, such as transcription factors, but have been identified in many other proteins, such as the outer dense fiber proteins of the sperm tail. One of these Odf1-interacting proteins was Odf2 [formerly called Odf84 (Shao *et al*, 1997)]. Unlike Odf1, Odf2 was found to localize to the connecting piece and both the cortex and the medulla of the ODFs (Schalles *et al*, 1998). Another Odf1-interacting protein that was identified was Spag4. Spag4 is a 49-kDa protein that has a SAD1 homology domain (SAD1 is a MT binding protein in yeast speculated to aid motor protein binding to MTs) and localizes to the axoneme and the manchette, both microtubule-containing structures in male germ cells (Shao *et al*, 1999). It is not clear whether this binding is mediated by SAD1. Spag4 has been found to not interact with Odf2 and is spermatid specific. It is speculated that Spag acts as a link between ODFs (specifically Odf1) and the axoneme and may aid in Odf1 localization to the medulla of the ODF. Interestingly, Odf1, Odf2 and Spag4 all are under translational control. Both Odf1 and Spag4 are transcribed in round spermatids and then translated in elongating spermatids (Morales *et al*, 1994, Shao and van der Hoorn, 1996, Burfeind and Hoyer-Fender, 1991, Burmester and Hoyer-Fender, 1996). Odf2 is also transcribed in round spermatids, but transcription can be detected for this mRNA also in as early as pachytene spermatocytes. Odf2 is then also translated in elongating spermatids (Shao *et al*, 1997 and Schalles *et al*, 1998).

1.h *The Fibrous Sheath*

The isolated FS is also composed of many proteins, (Oko, 1988) of which the 14-, 27-, and 75- kDa are the most prominent. All of the major FS proteins cross-react in Western blots. The 75 kDa rat FS protein was found to be homologous to the mouse protein p82, which is also in the FS. P82 is first synthesized as a precursor protein of approximately 92 kDa (840 amino acids), but the mature form of the protein is 72 kDa. Although the major 72 kDa FS mouse protein was determined to be a novel cytoskeletal protein expressed during spermiogenesis, it was found to have regional domain sequence similarities to the A-Kinase anchoring proteins, which are responsible for anchoring protein Kinase A to the cytoskeleton (Carrera *et al*, 1994). P82 has also been called AKAP4, FSC1 and FS75 (Carrera *et al*, 1994, Carrera *et al*, 1996, El-Alfy *et al*, 1999, Fulcher *et al*, 1995, Turner *et al*, 2001, Visconti *et al*, 1997). Many other FS proteins have been characterized including, AKAP3 (also called FS95) (Turner *et al*, 2001, Visconti *et al*, 1997 and Mandal *et al*, 1999), TAKAP80 (Mei *et al*, 1997), glutathione *S*-transferase (Fulcher *et al*, 1995), glyceraldehydes 3-phosphate dehydrogenase-S (Bunch *et al*, 1998), type I hexokinase (Mori *et al*, 1998), ropporin (Fujita *et al*, 2000), rhophilin (Nakamura *et al*, 1999), FS39 (Catalano *et al*, 2001), and CABYR (Naaby-Hansen *et al*, 2002).

1.i *Spag5*

One other protein that was characterized due to its association with Odf1 was Spag5. Spag5 binds to Odf1 via leucine zippers in both proteins. Binding experiments demonstrated that Spag5 can interact with Odf1, Spag4 and itself, but it cannot bind to

Odf2. These results demonstrate that Spag5 has a leucine zipper motif involved in the interactions with itself and Odf1 and that these leucine zipper motifs determine specificity. Further sequence analysis revealed that Spag5 has two putative leucine zippers and deletion mutants were used to test whether one or both of these leucine zippers were responsible for Odf1-binding. These results suggest that the downstream leucine zipper is necessary but not sufficient for efficient interaction with Odf1 and that sequences upstream of the first leucine zipper are also required for the interaction between Odf1 and Spag5. However, Spag5 (unlike Odf1, Odf2 and Spag4) is not under translational control. Spag5 is transcribed in pachytene spermatocytes and round spermatids (more so in spermatocytes than spermatids) and it is also translated in both pachytene spermatocytes and round spermatids (Shao *et al*, 2001). A Spag5-null mouse was generated by homologous recombination, which lacked Spag5 mRNA and protein. However, male mice were viable and fertile and did not display an altered phenotype as a consequence of the knockout event. It was then suggested that if Spag5 plays a role in spermatogenesis, then it is likely compensated for by unknown proteins (Xue *et al*, 2002). Spag5 was also found to be 73% similar to the C-terminal 397 amino acids of Astrin, a human non-motor mitotic spindle protein. However, the Spag5 cDNA and protein that was used in these previous studies was actually only a partial Spag5. The full length Spag5 cDNA, gene and protein have since been sequenced and the original Spag5 was found to contain only the last 11 exons of the full 31 exon Spag5 gene in rat.

1.j *Astrin*

Astrin was identified by mass spectrometry of proteins that were associated with microtubules from a mammalian mitotic extract and was found to be 134 kDa in mass (Mack and Compton, 2001). Astrin has previously been called Deepest (Gruber *et al*, 2002) and hMAP126 (Chang *et al*, 2001). Silencing of Astrin by RNA interference in HeLa cells results in cell growth arrest and the formation of multipolar and disordered spindles (Gruber *et al*, 2002). Astrin associates with spindle microtubules as early as prophase (concentrates at spindle poles) but localizes throughout the spindle in metaphase and anaphase and associates with midzone microtubules in anaphase and telophase. Deletion analysis indicates that astrin's primary spindle-targeting domain is at the C terminus, although a secondary domain in the N terminus can target some of the protein to spindle poles (Mack and Compton, 2001). Recombinant astrin showed parallel dimers with head-stalk structures similar to motor proteins, although no sequence similarities were found to known motor proteins (Gruber *et al*, 2002). According to secondary structure predictions of Astrin, the sequence can be separated into several distinct domains. The N-terminal head domain (aa 1-481) of astrin is rich in proline (7.5%) together with serine and threonine residues, suggesting that astrin's function is regulated by phosphorylation *in vivo*. This hypothesis was supported by Chang, who found that astrin is a substrate of cdk1 *in vitro* (Chang, 2001). Also, there are four PXXP motifs in the head domain which may represent putative SH3-interaction sites suggesting that astrin could be a target for regulatory proteins (Alexandropoulos *et al*, 1995 and Yu *et al*, 1994). There are three regions (called PEST sequences) in astrin which are

frequently found in proteins underlying rapid degradation through ubiquitin-protein ligase complexes. This degradation is regulated through phosphorylation of the PEST sequence motifs (Rechsteiner and Rogers, 1996 and Rogers *et al*, 1986). Amino acids 482-903 of astrin are predicted to be essentially alpha-helical except for a short interruption. Most of this region shows the heptad repeat pattern of coiled-coil proteins, suggesting dimerization and formation of a rod-like structure (Gruber *et al*, 2002). Using CD spectroscopy and purified recombinant astrin protein, it was found that astrin has a domain structure resembling that of motor proteins with a large head domain, which lacks sequence similarity to motor domains, and a coiled coil domain responsible for formation of parallel dimers. These dimers oligomerize via their head domains into aster-like structures under physiological conditions.

1.k *ODF14 and FS14*

Two proteins that are both major proteins in total ODF and FS extracts are the 14 kDa FS protein (FS14) and the 14 kDa ODF protein (ODF14). Antibodies raised to ODF14 have been shown to cross-react with the 20-, and 27- kDa polypeptides on western blots. It has also been shown that antibodies raised against FS14 cross-react with the 75 kDa polypeptide of the FS. Additionally, it was shown that these two proteins (FS14 and ODF14) immunocrossreact with each other on western blots (Oko, 1988). Two cDNA clones were isolated from a rat testicular library using an antibody specific to FS14 and ODF14 that does not cross-react with other ODF or FS proteins. These clones were designated 1038 and 1017. These clones shared an identical amino terminal sequence, but differed in their carboxy termini. It was hypothesized that 1038 and 1017

encode the FS14 and ODF14 proteins. The amino terminal sequences of the FS14 and ODF14 proteins were sequenced and found to be identical. Developmental Northern blots were made using antisense 1038 and 1017 riboprobes on total testicular RNA extracts and revealed 1.0 kb transcripts for both which are first transcribed in late round spermatid development, just before condensation and elongation of the spermatid nucleus. Also, immunocytochemistry indicated that the ODF14 and FS14 proteins peak production and assembly late in elongating spermatids (Lawson, 1998). Therefore, it appears that ODF14 and FS14 are translationally regulated, similar to most ODF and FS proteins.

1.l ***Hypothesis and Research Aims***

The purpose of this study was to further characterize FS14, ODF14 and Spag5. The approach for Spag5 was to investigate its role in spermatogenesis and its relationship with Astrin in order to gain further insight into the apparent dual function of Spag5. Preliminary results led to the hypothesis that Spag5 bears a functional similarity to Spag4 due to its microtubule binding and Odf1 association as a bridge between the ODFs (specifically Odf1) and the axoneme. However, it was apparent that Spag5 also possibly had another separate function in the mitotic and/or meiotic spindle due to its homology to the human mitotic spindle protein, Astrin. Using a variety of approaches, including immunofluorescence, microtubule-binding assays, electron microscopy and immunocytochemistry, the apparent dual role of Spag5 was elucidated. ODF14 and FS14 are testis-specific and protein analysis thus far has been unable to distinguish between these two proteins, due to their identical amino terminal sequences and their immunocrossreactivity. Therefore the approach for FS14 and ODF14 was to investigate

the cDNAs 1038 and 1017 to determine where they originate from and if these clones encode either or both of FS14 and ODF14. The original hypothesis was that ODF14 and FS14 were alternatively spliced products of the same gene, due to their identical amino terminal sequence, but the results refute this claim.

Chapter 2: Materials and Methods

Elutriation: Spermatogenic Cell Dissociation and Isolation

Testes were removed from two rats and kept on ice. The tunica albuginea of all the testes was cut with sterile scissors and the seminiferous tubules were released into a 250 mL Erlenmeyer flask. To the testes, 40 mLs of media #1 [Dulbecco's Modified Eagle Medium (DMEM) with high glucose, glutamine and pyridoxine hydrochloride, Na Lactate, Na Pyruvate] and collagenase (0.5mg/mL) were added for 15 min at 32^{o}C and shaken periodically by hand. Krebs media (Elutriation media) was made the night before elutriation. The tubules were then settled to the bottom of the flask. The media was removed by tilting the flask with care not to disturb the tubules. The tubules were then washed three times with elutriation media fairly quickly. The tubules were resuspended in 40 mLs of Krebs media with 0.125mg/mL trypsin and 40 ug total DNase I (Stock: dissolve 1g of DNase I in 1 mL PBS=1 ug/ul). The tubules were allowed to sit for 15 min at 32^{o}C and were shaken periodically and pipetted up and down to ensure that a single cell suspension was found. The cells were checked under a microscope to ensure there were no cell clusters. After the 15 min incubation, 20 mg of trypsin inhibitor was added and pipetted up and down. The single cell suspension was filtered through a nylon filter (pre-wet with ddH_2O) into a 50 mL centrifuge tube. The cells were spun for 10 min at 1,500 rpm at room temperature and were rinsed twice with Krebs media. The final cell pellet was resuspended in 20 mL of Krebs media (with 100ug DNase I) and loaded into a 60 mL syringe where it was loaded into the elutriation equipment. Elutriation was performed as described previously and fractions containing spermatocytes, round spermatids and a mix of round and elongating spermatids were isolated.

Isolation of Rat Sperm Tails and ODF

Total sperm was collected from rat epididymides and washed twice by centrifugation at 500 x g at 4^{o}C for 10 min in 25 mM Tris-buffered saline (TBS pH 7.5). The pellet was then sonicated on ice to separate the heads from the tails. The pellet was then washed twice in TBS and then resuspended in TBS containing 80% sucrose and centrifuged at 200 000 x g for 1 h in a 60 Ti angle rotor (Beckman Mississauga, ON). The tails were collected from the inside wall of the tube (the heads are located on the outside wall) and resuspended in sucrose and the whole step was repeated to gain >99% purity of the sperm tails. Some of this tail fraction was used directly in Western blotting and some was used to isolate ODF and FS according to previously published protocols (Oko, 1998; Oko and Clermont, 1990; Oko, 1988).

Spermatocyte and Spermatid Nuclear RNA Isolation

Elutriated cells were transferred to a 7 mL glass homogenizer on ice. 3 mL of cold buffer [10 mM HEPES (pH 8), 50 mM NaCl, 0.5 M sucrose, 1 mM EDTA (pH 8), 0.5 mM spermidine, 0.15 mM spermine], and Nonidet P-40 to a final concentration of 0.1%. The cells were homogenized 10 times with an A pestle to assist in breaking up the cells and releasing the nuclei. The homogenate was transferred to a 15 mL polypropylene tube and centrifuged for 10 in at 3,000 rpm at 4^{o}C to pellet the nuclei. RNA was isolated from the nuclei according to the TRIzol reagent protocol previously described. This RNA was treated with DNase I (Roche) to ensure there was no DNA contamination.

RNA, DNA and Protein Isolation from Tissues

Tissue samples were homogenized in 1 mL of TRIzol Reagent per 50-100 mg of tissue using a power homogenizer. The homogenized samples were incubated for 5 min at 15-30^{o}C to permit the complete dissociation of nucleoprotein complexes. 0.2 mL of chloroform was added to the samples per 1 mL of TRIzol reagent and shaken by hand for 15 sec and then incubated for 2 to 3 min at the same temperature. The samples were centrifuged at 12,000 X g for 15 min at 4^{o}C. The aqueous phase was transferred to a new tube and 0.5 mL of isopropyl alcohol was added per 1 mL of TRIzol reagent in order to precipitate the RNA. The samples were incubated at 15-30^{o}C for 10 min and then centrifuged at 12,000 X g for 10 min at 4^{o}C. The RNA pellet was washed once with 75% ethanol and centrifuged at 7,500 X g for 5 min at 4^{o}C, briefly air-dried and resuspended in RNase-free water. The RNA pellet was treated with DNase I (Roche) to ensure there was no DNA contamination. After the addition of chloroform and after the use of the aqueous phase for RNA isolation, the interphase and phenol phases were saved and used to isolate DNA and protein. To isolate DNA, 0.3 mL of 100% ethanol per 1 mL of TRIzol used in the beginning step was added and mixed by inversion. The samples were then incubated at 15-30^{o}C for 3 min and then centrifuged at 2,000 X g for 5 min at 4^{o}C.The supernatant was removed for protein isolation and the DNA pellet was washed twice in a solution containing 0.1 M sodium citrate in 10% ethanol (1 mL per 1 mL of TRIzol used initially). The DNA pellet was stored in the washing solution for 30 min at 15-30^{o}C and centrifuge at 2,000 X g for 5 min at 4^{o}C . Following two washes, the DNA

pellet was suspended in 75% ethanol for 10-20 min at 15-30^{o}C and centrifuged at 2,000 X g for 5 min at 4^{o}C. The DNA was air-dried for 10 min and dissolved in 8 mM NaOH such that the concentration of DNA was 0.2-0.3 ug/ul. The supernatant removed from the DNA pellet was used to precipitate protein with the addition of 1.5 mL of isopropanol per 1 mL of TRIzol. The sample was incubated for 10 min at 15-30^{o}C and then centrifuged at 12,000 X g for 10 min at 4^{o}C. The protein pellet was washed 3 times in a solution containing 0.3 M guanidine hydrochloride in 95% ethanol. The pellet was stored in the wash solution for 20 min at 15-30^{o}C and centrifuged at 7,500 X g for 5 min at 4^{o}C.The protein pellet was vacuum-dried for 10 min and dissolved in 1% SDS by pipetting. The sample was incubated at 50^{o}C to assist in solubilizing the pellet.

Microtubule isolation from tissue

Rat brain and testis were washed with 1XBRB80 (80mM PIPES pH6.9, 2mM EGTA, 2mM $MgCl_2$), put into liquid nitrogen, dissected into 400mg sections, placed into microfuge tubes and put into liquid nitrogen again. The tissues were then homogenized in with a mortar and pestle (washed with 1XBRB80) in 1mL of 1XBRB80 (containing a protein inhibitor cocktail containing 1ug/mL aprotinin, 10ug/mL leupeptin, 1ug/mL pepstatin, 2mM PMSF, 2mM benzamidine and 1mM DTT) per 400mg piece of tissue. The tissues were crushed until no visible chunks remained and the homogenate was placed on ice for 15 minutes. The homogenate was then spun in the TL-100 Ultracentrifuge at 27,000 x g for 20 minutes at 4^{o}C to removed clumps of tissue and other cellular debris. The pellet was discarded and the supernatant removed to a new tube and spun at 89,000 x g for 30 minutes at 4^{o}C to remove smaller debris. The supernatant was

transferred to a new tube containing, 20ul 50mM $MgCl_2$, 10ul 100mM GTP (promotes polymerization of MTs), 20ul 1M Glucose (filtered), 3ul 5U/ul Hexokinase, protein inhibitor cocktail and 1ul 1M DTT and immediately, 0.029 mM Taxol was added to a 1 in 100 dilution. The tube was then covered with parafilm and incubated for 5 min in a 33^{o}C waterbath. Next, 0.29mM taxol was added to the same dilution and incubated for another 5 min. Lastly, 2.9mM taxol was added to the same dilution and AMP-PNP to a final concentration of 1mM and incubated at 33^{o}C for 15 min. 10ul was removed for gel analysis. A ¼ volume of glycerol cushion (40% glycerol, 1mM GTP, 1mM AMP-PNP, 10uM taxol, 1XBRB80) was underlayed and samples were spun at 89,000 x g for 30 min at 4^{o}C. The supernatant was removed and the cushion was washed 3X with 200ul of 1XBRB80. The cushion was then removed carefully (so as to not disturb the tubulin pellet) and the pellet was resuspended in 200uL of 1XBRB80 (5uL was taken for gel analysis). The microtubules then sat on ice for 15 min to allow for depolymerization. Once again, $MgCl_2$, GTP, hexokinase, protein inhibitors and DTT were added and the microtubules were allowed to polymerize again with the 3 step taxol incubations and centrifugation. The depolymerization and polymerization steps were repeated a third time. The final products (microtubules plus associated proteins) were resuspended in 100uL 1XBRB80 and 10% glycerol.

Microtubule isolation from cells (including all MT-associated proteins)

To test the proteins' native association with MTs in cells, a protocol was developed to isolate MTs including all associated proteins. Rat IEC-18 cells were scraped off of a 90-mm dish and resuspended in 1mL of 1XBRB80 buffer containing a protease

inhibitors cocktail (see previous MT isolation procedure) as well as 1mM AMP-PNP and 20uM taxol. The suspension was sonicated for 10 sec and followed quickly by centrifugation at 3,000 rpm for 5 min at room temperature to remove cell debris and large organelles. The supernatant was transferred to an ultracentrifuge tube and spun at 27,000 x g for 30 min at 22^{o}C through a 40% glycerol cushion. The MT pellet was resuspended in 1XBRB80 buffer.

Antibody Affinity Purification

Polyclonal Anti-Spag5 was affinity purified through two columns of CNBr-activated Sepharose 4B (Pharmacia Biotech Catalogue No.17-0430-01). In one column, the beads were coupled to pure MBP protein and in the second column, the beads were coupled to purified MBP-Spag5 protein. Initially, the freeze-dried CNBr-activated sepharose 4B powder was mixed with 1mM HCl to produce the gel slurry which was subsequently de-gassed. The ligand was coupled to the beads (gel slurry) in 5 mL of coupling buffer (0.1M $NaHCO_3$ pH8.3, 0.25M NaCl in PBS) per gram of initial powder and mixed end-over-end for 1 hour at room temperature or overnight at 4^{o}C. The beads were then washed 5 times with coupling buffer. The remaining active groups were blocked for 2 hours at room temperature or overnight at 4^{o}C with 10mL of 0.1M Tris-HCl ph8.0. The excess adsorbed protein was washed away with coupling buffer followed by at least 3 cycles of alternating pH (0.1M acetate buffer, 0.5M NaCl ph4.0 and 0.1M Tris-HCl, 0.5M NaCl ph8.0). The anti-Spag5 serum was diluted (3mL serum + 3mL PBS) and then run through the MBP-sepharose coupled column 3 times. The flow through from the MBP column was then run through the MBP-Spag5-sepharose coupled

column 3 times. Both columns were washed 5 times with PBS. The purified antibody was then eluted from the MBP-Spag5 column with 6mL of 0.1M glycine in PBS pH 2.8 (0.25mLx2, then 0.5mL fractions) and then 10mL of 0.1M glycine in PBS pH 1.8 (0.25mLX2, then 0.5mL fractions). These fractions were then tested by Western blotting and used in subsequent experiments.

Rat Testis and Epididymis Tissue Preparation, Immunocytochemistry and Electron Microscopy

Adult male Sprague-Dawley rats were anesthetized and perfused through the abdominal aorta and heart either with 0.5% glutaraldehyde and 4.5% paraformaldehyde in 0.1M phosphate buffer containing 50mM lysine (pH 7.4 for electron microscopy) or in Bouin fixative (for light microscopy) in order to fix the testis and epididymides. Tissues were prepared for light microscopy at the Calgary Laboratory Services (Anatomic Pathology Research Laboratory Services). Tissues meant for Lowicryl embedding (for electron microscopy) were immersed in the respective fixatives for 2 hours at $4^{o}C$, washed three times in phosphate buffer, and incubated with phosphate buffer containing 50mM NH_4Cl for 1 h at $4^{o}C$. Tissues were then washed in buffer, dehydrated in graded methanol up to 90% and then infiltrated and embedded in Lowicryl K4M (Chemische Werke Lowi, Waldkraiburg, Germany). Thin sections were mounted on Formvar-coated nickel grids (Polysciences Inc., Warrington, PA) for immunogold labeling. Tissues fixed in Bouin fixative were washed extensively in 75% ethanol before being dehydrated in ethanol and embedded in paraffin. Paraformaldehyde-fixed tissues were washed in phosphate buffer, dehydrated and embedded in paraffin. For light microscopy immunocytochemistry, rat testis paraffin sections were deparaffinized and hydrated

though a graded series of ethanol concentrations before immunoperoxidase localization with the affinity purified anti-Spag5 antibody by standard procedures (Oko, 1998). Spag5 antibody was also incubated with MBP-Spag5 protein and precipitated with beads in order to determine antibody specificity. This antibody was then used in immunocytochemistry. For electron microscopy, ultrathin Lowicryl sections of rat testis and epididymides on Formvar-coated nickel grids were immunogold labeled according to a procedure established previously (Oko *et al*, 1996). The preparation of tissue for electron microscopy as well as immunogold labeling was performed in Richard Oko's lab, Department of Anatomy and Cell Biology, Queen's University.

In vitro Translation

The Spag5 product was subcloned into pBS-ATG (Shao *et al.*, 1997), which provides an in frame initiation codon for in vitro translation, as an *EcoR*I and *Sal*I fragment. In vitro translations were performed using T7 (RNA polymerase) TNT system (Promega) in the presence of ^{35}S-Met as described previously (Shao *et al.*, 1997)

Microtubule binding assay

The TNT reaction described above was combined with ~10ug (0.1 ug/ul) of isolated microtubules and BRB80 buffer (to a final concentration of 1X), 1mM AMP-PNP, 20uM Taxol and incubated at 33^{o}C for 15 minutes. The mixture was then underlayed with an equal volume of glycerol cushion and spun at 27,000 x g, for 30min at 22^{o}C. The supernatant was discarded and the cushion washed 3 times with 100ul of 1X BRB80, which was then also removed, leaving the pellet. This whole procedure was

repeated once and the pellet diluted in 20ul of 1X SDS loading buffer for SDS-PAGE analysis.

Cell Transfections

Mouse 3T3 fibroblasts were grown to about 50% confluency on the day of transfection. The Spag5 insert from pBS-ATG/spag5 was cut out with *EcoR*I and *Sal*I and ligated into the same sites in the pEGFP-C2 vector. Mouse 3T3 fibroblasts were transfected with pEGFP-C2/spag5 using the LipofectAMINE PLUS^{TM} Reagent (Life Technologies).

Immunofluorescence

IEC-18 cells (CRL-1589), which are normal rat epithelial ileum cells (including cells which were transfected with GFP-Spag5), were grown on coverslips to approximately 60-70% confluency. Cells were then fixed for 10 minutes in methanol, treated for 10 minutes with 0.5% Triton X-100 in phosphate buffered saline (PBS) and then washed for 10 minutes in 0.05% Tween (in PBS). Primary and secondary antibodies were diluted in PBS containing 1% bovine serum albumin (BSA). The fixed cells on the coverslips were placed on a layer of parafilm in a humidified chamber and 50ul of primary antibody was added to each coverslip and incubated for 1 hour at 37^{o}C. The coverslips were immersed in PBS containing 0.05% Tween 20 for 10 minutes at room temperature with occasional, gentle agitation. Coverslips were put back in to the humidified chamber and 50ul of secondary antibody was added to each coverslip and incubated for 1 hour at 37^{o}C. Secondary antibodies were Alex Fluor 488 goat anti-rabbit

IgG (highly cross-adsorbed, from Molecular Probes), Cy3-conjugated AffiniPure Goat Anti-mouse IgG (H+L) secondary antibody from Jackson ImmunoResearch Laboratories Inc., and Cy3-conjugated AffiniPure Goat Anti-rabbit IgG (H+L) from Jackson ImmunoResearch Laboratories Inc.

Deconvolution Microscopy

Images were captured on the Leica DM RXA2 microscope with the Roper (Princeton Instruments) cooled scientific CCD camera using the Winview software (Roper Princeton Instruments) with an in-house developed C++ COM-object which provides integrated control of the camera, microscope and light source shutter. The Leica microscope contains a motorized filter cube holder, objective lens turret and stage X,Y,Z movement. Sections were captured every 100nm and the resulting Z-stacks were deconvolved using software from MicroTome Nearest Neighbour Deconvolution VayTek Inc.

Immunoprecipitation

Astrin polyclonal antibody (4 uL) and Spag5 affinity purified antibody (50 uL) were each added separately to 5 ug of rat total testis protein and mixed gently for one hour at 4^{o}C in order to couple the antigen to the antibody. To precipitate the immune complexes, 25 uL of Protein A Sepharose CL-4B beads (Pharmacia Biotech) were added to each mixture and mixed gently for one hour at 4^{o}C. The pellet was washed three times with 1 mL lysis buffer and once with wash buffer (50 mM Tris, pH 8). The samples were centrifuged at 12,000 X g for 20 sec between each wash and the supernatant discarded. The final pellet was suspended in 30 uL sample buffer and heated at 95^{o}C for 3 min to

dissociate the complexes from the beads. The samples were spun at 12,000 X g for 20 sec to remove the beads. The samples were then used for Western blotting.

Western Blotting

Total rat testis protein, sperm tail protein, ODF protein and fractions 50 (containing a mixture of round and elongating spermatids), 90 (containing round spermatids) and 220 (containing spermatocytes) of elutriated cells were run on a 10% SDS-PAGE and transferred to polyvinylidene fluoride (PVDF) membrane. The blots were blocked in TBS-TN (TBS+Tween+NP40) + 5% milk powder overnight at 4^{o}C. The blots were incubated in primary antibody diluted in blocking buffer for 1 h at room temperature. Affinity purified anti-Spag5 was used at 1/5 dilution and anti-Astrin (kind gift from Dr. Duane Compton, Dartmouth Medical School) was used at 1/100 dilution. The blots were then washed 3 times for 10 min in TBS-TN. The filters were incubated in goat anti-rabbit secondary antibody conjugated to horse radish peroxidase at 1/12000 dilution. The filters were next washed as previously described and developed with Enhanced Chemiluminescence and exposed to X-ray film (Kodak XARS).

RT-PCR

Isolated total RNA was reverse transcribed to a single strand cDNA using the SUPERSCRIPT^{TM} Preamplification System for First Strand cDNA (Life Technologies). Total RNA was isolated from rat brain, colon, epididymus, heart, kidney, liver, lung, small intestine, smooth muscle, and testis. These reactions were primed with Spag5 specific primers. Total testis RNA was also isolated from 5 day, 10 day, 15 day, 21 day, 25 day, 31 day old rats, and adult rats. RT-PCR was also performed on these samples

using the same Spag5 specific primers. Total testis RNA was also used to amplify the 1038 and 1017 mRNA. This was performed using a primer common to both sequences in the 5' end (pr678 - 5'GAGAAACTGCCTTGTACCAGGTCC 3') and two gene-specific primers in the 3' end [1038 (pr338) – 5'GCCTCTAGCCATGTTCCTCAAGC 3' and 1017 (pr117) – 5'GTGGAAGTCTAACTGAACT 3'). RNA was also isolated from the nuclei of elutriated sperm cells (elongating spermatids, round spermatids and spermatocytes) and used to amplify a sequence further upstream in the genomic sequence of the 3' end of 1038 that differs from the 3' end of 1017 (prom1038 - 5'CCACGTTAAGGCCGACTTACCTG 3').

Northern Blotting

Total RNA isolated from rat and mouse was run through a 1.5% agarose gel, containing 2.2 M formaldehyde according to the protocol in Molecular Cloning, Sambrook and Russell (2001). Before the RNA was run on the gel, a denaturation reaction was set up containing 20ug RNA, 2ul of 10X MOPS electrophoresis buffer [0.2M MOPS (pH 7), 20mM sodium acetate, 10mM EDTA (pH 8), 4ul formaldehyde, 10ul formamide and 1ul ethidium bromide (200 ug/mL). The RNA reactions were incubated for 1 hour at 55^{o}C. The samples were then chilled for 10 min in ice water and then centrifuged for 5 sec. 2 ul of 10X formaldehyde gel-loading buffer was added to each sample and put back on ice. The samples were loaded in the gel and run in 1X MOPS electrophoresis buffer for 4 hours at 5 V/cm until the bromophenol blue migrated about 8 centimeters. The gel was photographed on a UV transilluminator aligned to a transparent ruler. The gel was next treated for transferring to Duralon-UV^{TM} membrane

(Stratagene). The gel was rinsed in DEPC-treated water, soaked in 5 gel volumes of 0.05 N NaOH for 20 min and soaked in 10 gel volumes of 20X SSC for 40 min. The RNA was then transferred over night by capillary action using 20X SSC. After transfer, the RNA was cross-linked to the membrane by UV irradiation (254 nm for 1 min at 1.5 J/cm^2). Presence of RNA on the membrane was checked by visualizing under UV light. The membrane was incubated at 68^oC for 2 hours in 20 mLs of prehybridization solution [0.5 M sodium phosphate (pH 7.2), 7% (w/v) SDS, 1 mM EDTA (pH7)]. Probes against the common (chromosome 2) region of both 1017 and 1038 and the unique (chromosome 4) region of 1038 were made by PCR. The probes were radiolabelled by using a dNTP mix of cold dNTPs (dATP, dTTP and dGTP) and radiolabelled alpha-^{32}P(dCTP). The probes were denatured for 5 min at 100^oC and then chilled on ice. The probes were added directly to the prehybridization solution and incubated overnight at 42^oC. After hybridization, the membrane was washed in 1X SSC containing 0.1% SDS at room temperature for 10 min. The membrane was then washed in 0.5X SSC containing 0.1%SDS at 68^oC for 10 min. This wash step was repeated 2 more times. The membrane was then dried on blotting paper and exposed for 24 hours to Kodak X-OMAT AR X-ray film at -70^oC.

BLAST searches

The rat, mouse and human genomes were accessed in the NCBI database and searched using the full-length 1017 sequence, as well as the uncommon 3' 1038 sequence. These same sequences (1017 and 1038) were also used to search ESTs for both rat and mouse using advanced BLAST. The full-length Spag5 sequence was also used to

search the rat and human genomes. Matches were determined using the two parameters given by the search algorithm, namely the identity/length of the matching sequence, and the E value (expected number of chance hits with the same identity and length).

Radiation Hybrid Mapping

Radiation hybrid mapping was based on PCR using genomic DNA from hybrid cells as the PCR template and was carried out at the CIHR Genome Resource Facility, The Centre for Applied Genomics at the Hospital for Sick Children in Toronto, Ontario, Canada. For this experiment, the T55 panel was used, which consists of rat cells that have been irradiated and fused with hamster cells. These hamster cells contain a random selection of rat chromosome fragments. Linked markers are likely to be retained on the same fragment, while unlinked markers are likely to be separated by at least one break. The T55 panel contains a map of the rat genome using 5255 genetic markers. The C-terminal 400 base pairs of the 1038 clone were mapped using the T55 panel. The primers used were the following : 5' GGAGAGAATGTGGGGAATACCAG 3'; 5' GCCTCTAGCCATGTTCCTCAAGC 3' (to amplify a 400 bp fragment corresponding to 439-739bp in the 1038 clone). The N-terminal 336 base pairs of both 1017 and 1038 were mapped using the T55 panel as well. The primers used for the N-terminal sequences were: 5'GAGAAACTGCCTTGTACCAGGTCC 3'; 5'CCCTGCCACTTAGGAAATTCTCTC 3' (to amplify 336 bp spanning exon 1 and intron 1 of the putative chromosome 2 gene). Twenty five nanograms of hybrid DNA was used in PCR analysis as recommended. For linkage analysis, PCR typing results were

submitted to the Otsuka GEN Research Institute database : http://ratmap.ims.u-tokyo.ac.jp/menu/RH.html.

MALDI-TOF Mass Spectrometry

Matrix-assisted laser desorption ionization-time of flight (MALDI-TOF) mass spectra were obtained for both the FS14 and ODF14 proteins. Total ODF and FS fractions were run on a 10%-20% gradient polyacrylamide gel, stained with Coomassie Brilliant Blue dye and the 14 kDa bands were excised. The gel pieces were washed three times for fifteen minutes with 50% acetonitrile/25mM ammonium bicarbonate with gentle shaking. The gel pieces were soaked in 400uL 100% acetonitrile for five minutes. The acetonitrile was removed and the gel pieces were dried in a speed-vac for 20-30 minutes. A solution of 10ug/ul of trypsin in 25mM ammonium bicarbonate was made and 15uL was added to each gel piece. The samples were incubated at 37^{o}C for 16-24 hours. The next day, 100uL 50% acetonitrile/5% TFA was added and the tube was agitated gently for an hour. The sample was spun in a microcentrifuge for five minutes and the supernatant was carefully removed (contains majority of peptides). The supernatant was dried in a speed-vac. The sample was then mixed with a matrix (α-cyano-4-hydroxycinnamic acid), spotted on to a metal plate, dried and analyzed by MALDI-TOF.

CHAPTER 3: SPAG5 RESULTS

3.a *Astrin and Spag5 Protein Immunoprecipitations*

The original spag5 protein used to generate the MBP-Spag5 fusion protein was found to be 73% similar to the C-terminus of astrin, a human non-motor mitotic spindle protein. In order to determine whether Spag5 and Astrin are the same protein or if they come from the same gene, a cross immunoprecipitation (IP) using total rat testis protein was performed, followed by Western blotting. Both IPs (anti-Spag5 and anti-Astrin) pulled down proteins that were recognized by the other antibody (anti-Astrin and anti-Spag5 respectively).The proteins that were identified (approximately the same for both blots) were of the sizes ~25 kDa, ~30 kDa, ~35 kDa, ~45 kDa, ~54 kDa, ~72 kDa and are depicted in figure 4. On the Spag5 blot (Figure 4, panel B), a protein of approximately 47 kDa is barely visible. In figure 4, panel A (Astrin blot), the major band appears to be about 54 kDa. However, in panel B (Spag5 blot), there is a large band that appears to span from under 54 kDa almost to 72 kDa. This does not match panel A exactly since there is only a faint band at approximately 72 kDa in the Astrin blot. This difference will be further analyzed in the discussion. From this data it was concluded that Spag5 and Astrin are the same proteins, Astrin is the human protein and Spag5 is the rat protein.

3.b *Spag5 colocalizes with Astrin to the mitotic spindle and the ER in IEC-18 cells*

Immunoprecipitation studies revealed that Spag5 and Astrin antibodies recognize each other, so it was important to colocalize these two proteins in cells to further support that spag5 and astrin are the same proteins. Rat IEC-18 cells were fixed and co-stained

Figure 4: Western blot of proteins immunoprecipitated from rat testis protein with affinity purified anti-Spag5 and anti-Astrin. In lane A, proteins were immunoprecipitated from total rat testis protein with affinity purified polyclonal anti-Spag5 and blotted with polyclonal anti-Astrin. In lane B, proteins were immunoprecipitated from total rat testis protein with polyclonal anti-Astrin and blotted with affinity purified polyclonal anti-Spag5. Note the similar banding pattern in both lanes. This experiment was repeated three times.

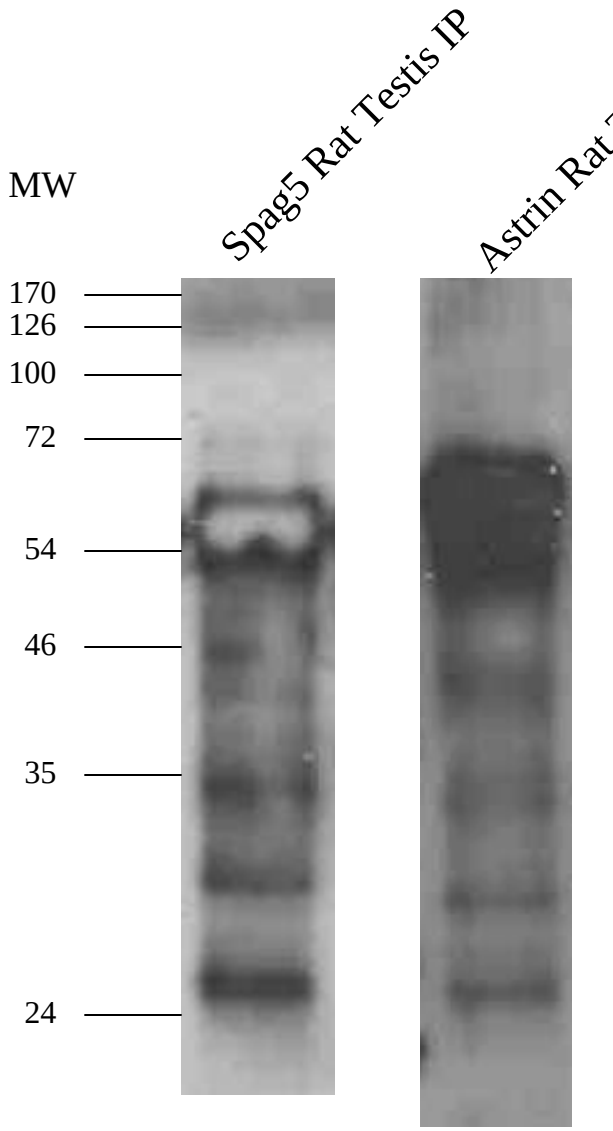
MW
Spag5 Rat Testis IP
Astrin Rat Testis IP
170
126
100
72
54
46
35
24
Anti-Astrin
Anti-Spag5
A.
B.

for Spag5, ER, golgi and mitochondria (Figures 5). The Spag5 pattern visualized under confocal microscopy was a punctate pattern in the cytoplasm of interphase cells, with an apparent localization with the mitotic spindle in mitotic cells. This pattern was similar to the pattern identified in HeLa cells stained for Astrin (Mack and Compton, 2001 and Gruber *et al*, 2002), therefore, co-localization immunofluorescence (IF) experiments were performed. To address the punctate patterning of Spag5 and Astrin in the cytoplasm, colocalization IF experiments were performed with mitochondria, golgi and ER. Spag5 did not appear to colocalize with golgi or mitochondria, however Spag5 seemed to colocalize to the ER (Figure 5). This finding will be further analyzed in the discussion. Spag5 does colocalize with Astrin in both mitotic and interphase cells, however, this colocalization is not 100% (Figure 6). In interphase cells, there is little to no Spag5 detected in the nucleus, while some Astrin is detected in the nucleus. Also, some signal for both Astrin and Spag5 in the cytoplasm of interphase cells does not colocalize. The question still remained as to what Spag5 and Astrin were associating with in the cytoplasm. In mitotic cells, it was obvious that both Spag5 and Astrin were localizing to the spindle. The function of the Spag5/Astrin association with the mitotic spindle will be discussed in the next chapter. Together these results show that antibodies against Spag5 may be a subset of Astrin detectable with the particular antibody generated.

3.c ***Spag5 and Astrin Genomic Structure and Localization***

The Spag5 rat gene is localized on rat chromosome 10 (Figure 7, top panel). It is preceded by two genes, Fructose-bisphosphate aldolase C (brain type aldolase) and the Phosphatidylinositol-glycan biosynthesis (class S protein) genes. Spag5 consists of 31

Figure 5: Confocal microscopy of rat IEC18 cells using affinity-purified anti-Spag5 antibodies to detect endogenous Spag5 protein (green), MitoTracker to detect mitochondria (red), anti-Golgi antibodies (red), and anti-Bip to detect endoplasmic reticulum (ER) (red). Immunofluorescence results show that some Spag5, but not all co-localizes with ER (as evidenced by the yellow color in the merged image) in interphase cells. No co-localization as observed with mitochondria or Golgi. Magnification: 100x.

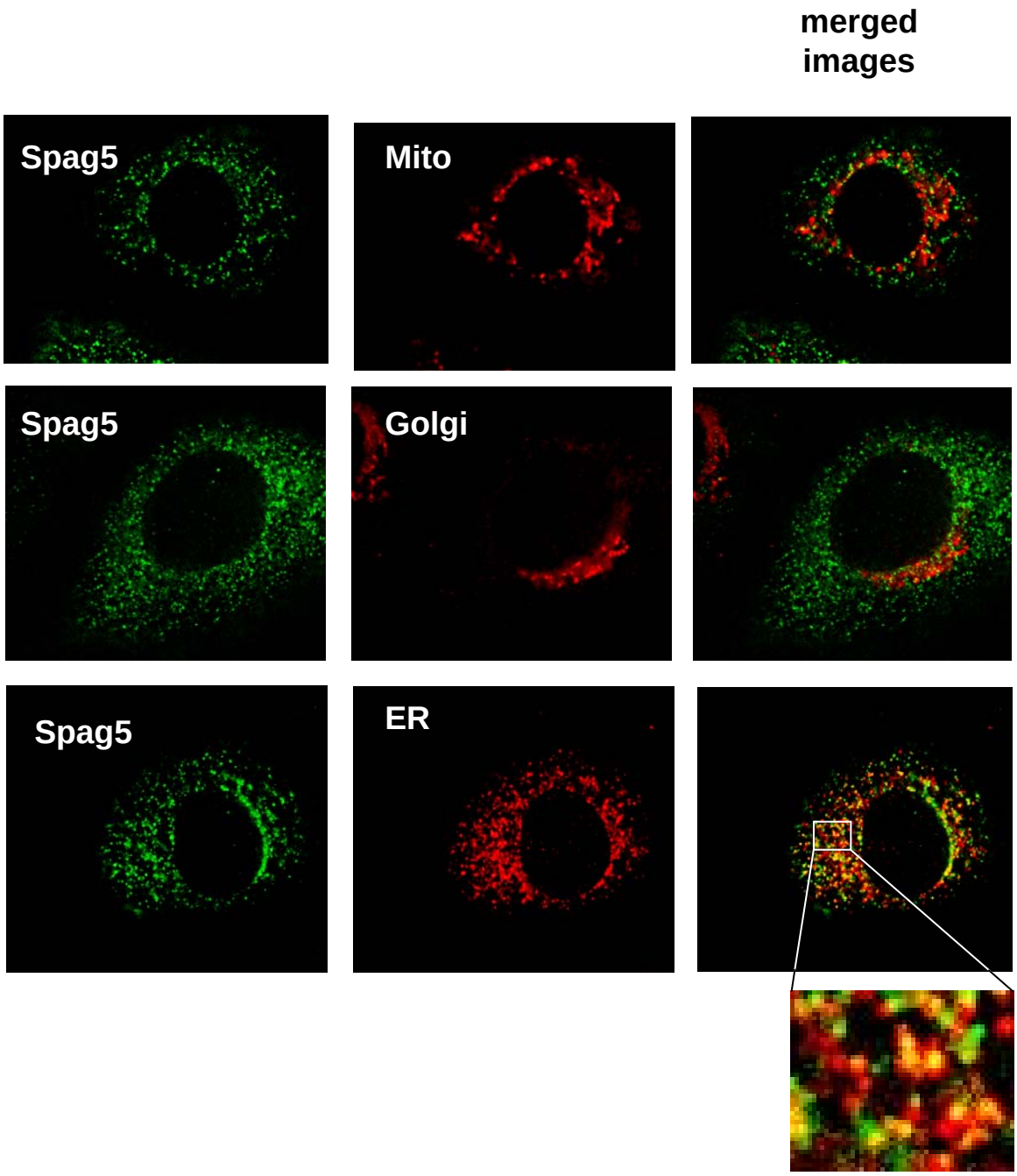
merged images
Spag5
Mito
Spag5
Golgi
Spag5
ER

Figure 6: Rat IEC18 cells were used in confocal microscopy using affinity-purified anti-Spag5 antibodies and anti-astrin polyclonal antibody to analyze possible overlap in subcellular location. In interphase cells (top row) Spag5 (red) and astrin (green) show a punctate pattern typical for some spindle and centrosomal proteins in interphase cells: the patterns overlap to some degree (yellow color). In a cell in anaphase (bottom row, right hand cell) Spag5 and astrin patterns also overlap, but not completely. An accumulation of Spag5 and astrin is observed in between the areas of separating DNA, the future site of cytokinesis. Note that Spag5 is excluded from the nucleus, in contrast to astrin. Magnification: 100x

Merged images

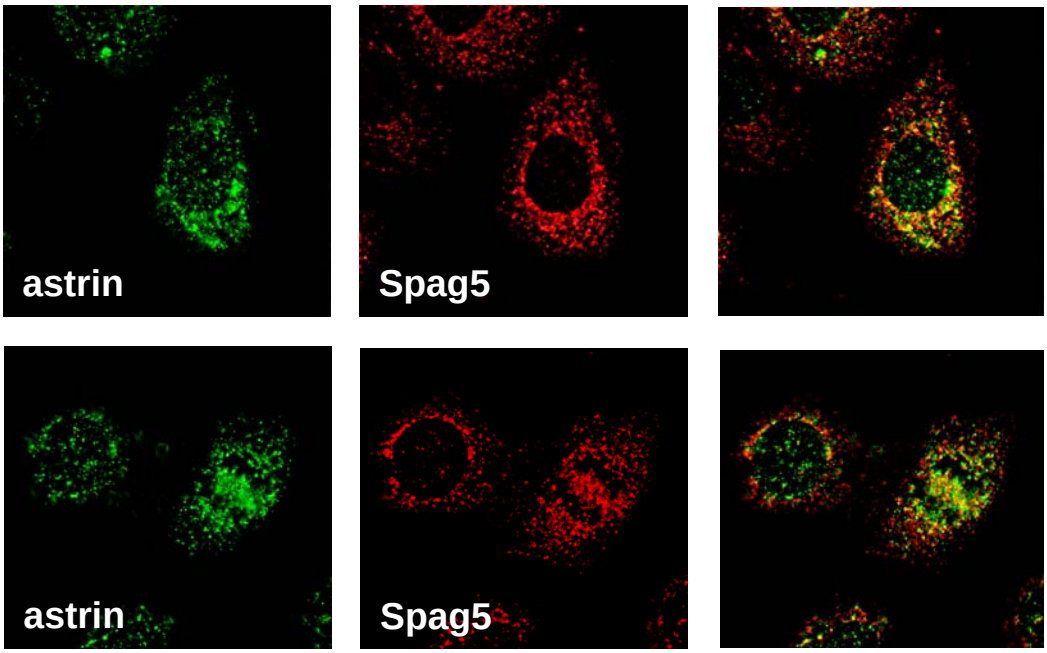

exons of which the last 11 exons were used to generate the MBP-Spag5 fusion protein that was used to make the anti-Spag5 polyclonal antibody. The Astrin human gene is localized on human chromosome 17 and is called the Spag5 gene (Figure 7, bottom panel). It is preceded by the same two genes as the rat Spag5 gene and it consists of 24 exons. Two Astrin fusion proteins were generated in order to make two polyclonal Astrin antibodies. The amino-terminal 609 amino acids (corresponding to the first 8 exons of the Astrin gene) and the carboxy-terminal 586 amino acids (corresponding to the last 16 exons of the Astrin gene) of the Astrin protein were expressed in bacteria as fusion proteins with glutathione *S*-transferase (Mack and Compton, 2001). The original Spag5 protein (last 11 exons of the Spag5 gene) was found to be 73% similar to the Astrin protein. Thus, Spag5 and Astrin represent the rat and human homologues of the same gene, in a conserved genomic surrounding. Experiments described below demonstrate however that the antibodies generated define an overlapping but partially distinct set of Spag5/Astrin proteins. An alignment of the full Spag5 and Astrin proteins is shown in figure 8.

3.d ***Spag5 localizes to cytoplasm of spermatocytes and round spermatids and the tails of elongating spermatids***

Spag5 associates with the mitotic spindle, it was of interest to localize Spag5 in the rat testis and to see if Spag5 also associates with meiotic spindles. Rat testis sections were stained with affinity purified anti-Spag5. Many different stages of the seminiferous epithelium were identified. In all stages that were identified, the most darkly stained cells were elongating spermatids with the Spag5 antibody also picking up a dark signal in the cytoplasm of primary spermatocytes, and a faint signal in the cytoplasm of secondary

Figure 7: The full length Spag5 mRNA sequence was used to search the ENSMBL rat genome database to determine the size and location of the Spag5 gene. These results are depicted in the top panel. The flanking genes, fructose-bisphosphate aldolase C (brain type aldolase) and the phosphatidylinositol-glycan biosynthesis (class S protein) are also indicated. The full length Astrin mRNA sequence was used to search the ENSEMBL human genome database to determine the size and location of the Astrin gene. These results are depicted in the bottom panel. The Astrin gene is called the Spag5 gene in human and is flanked by the same genes as the Spag5 gene in the rat genome. The rat Spag5 gene is located on rat chromosome 10 and the human Astrin gene is located on human chromosome 17

Spag 5 Gene - Rat

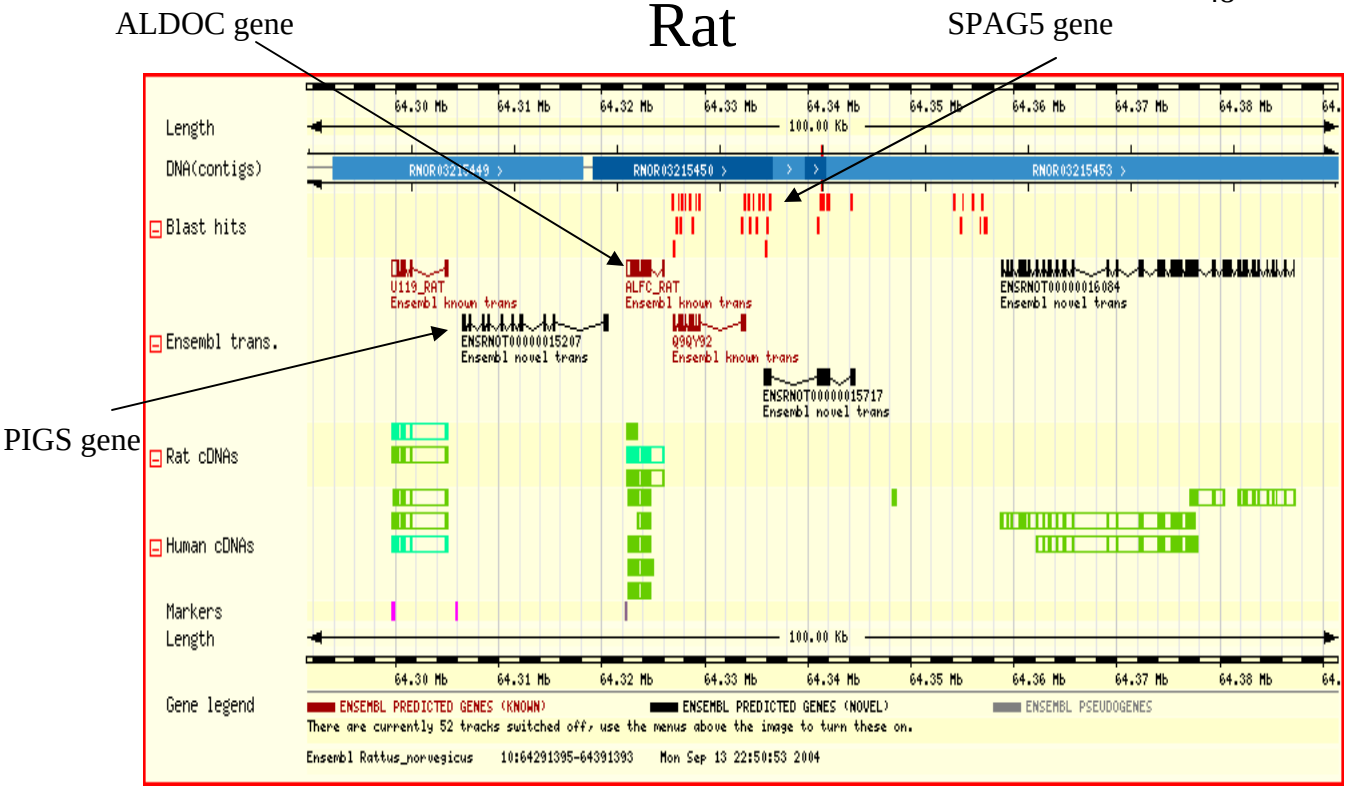

Astrin Gene - Human

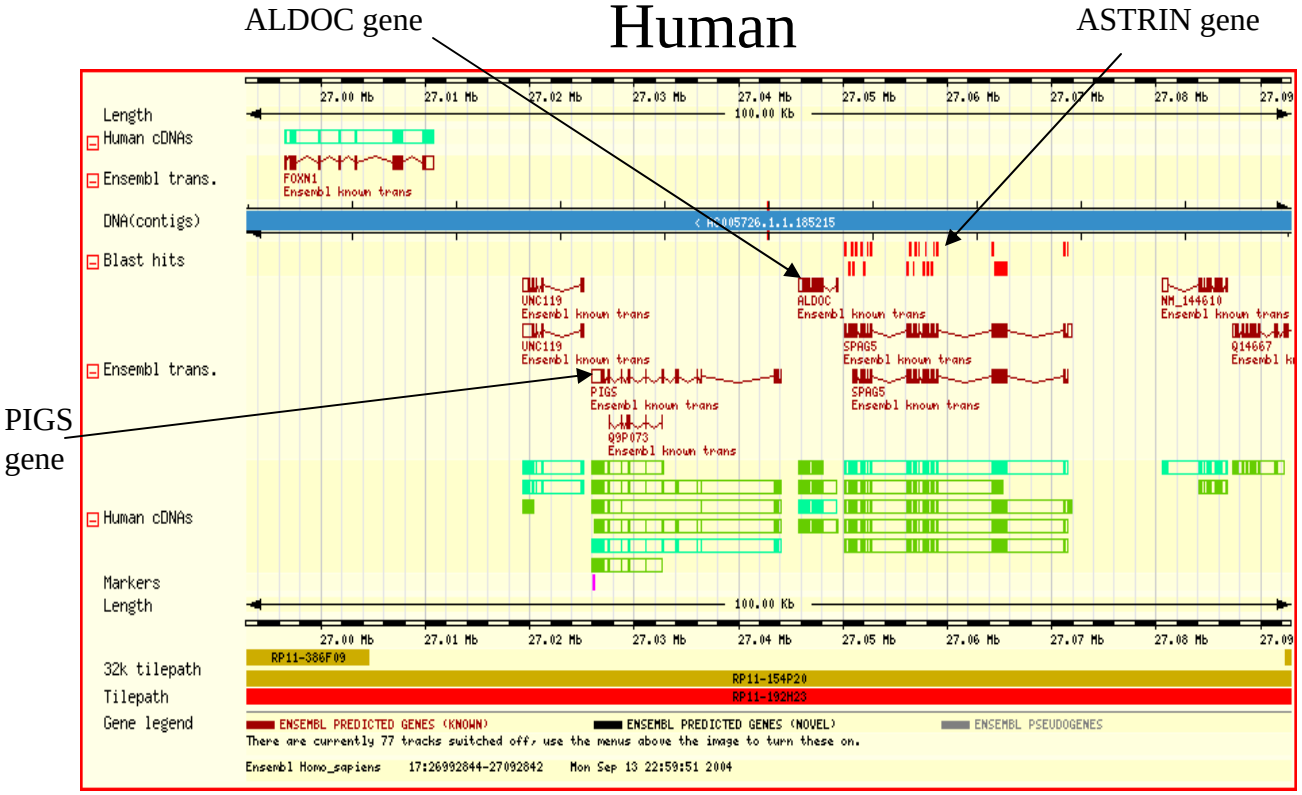

Figure 8: The astrin and spag5 protein sequences were aligned to demonstrate the amount of similarity between the two proteins. Note the differing amino terminal sequences between astrin and spag5 and the more similar carboxy terminal sequences. Spag5 comes from a gene of 31 exons and astrin comes from a gene of 24 exons. The differing number of exons likely accounts for the difference in the amino terminal sequence.

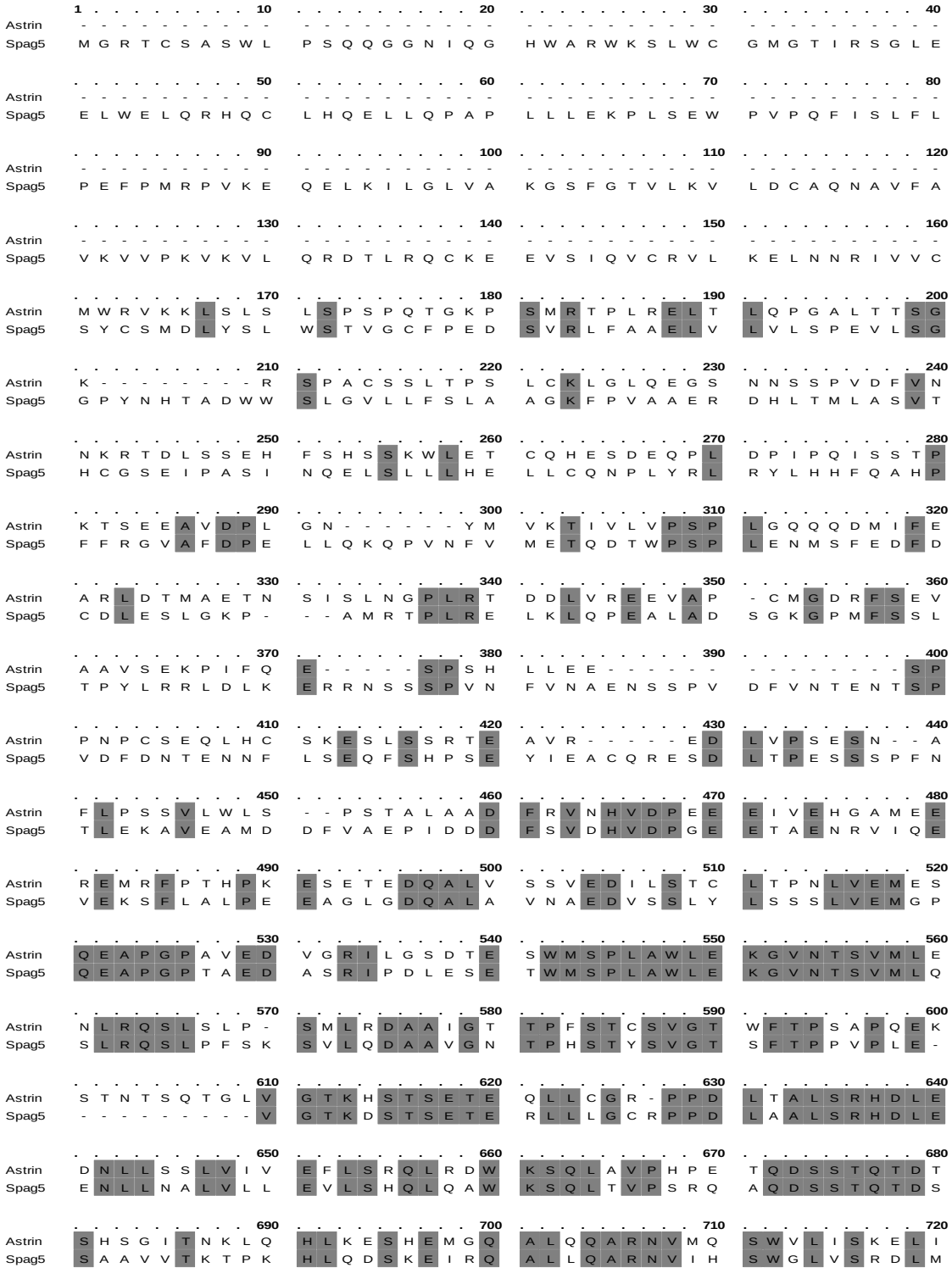
1 . . . . . 10 . . . . . 20 . . . . . 30 40
Astrin -
Spag5 M G R T C S A S W L P S Q Q G G N I Q G H W A R W K S L W C G M G T I R S G L E
. . . . . 50 . . . . . 60 . . . . . 70 80
Astrin -
Spag5 E L W E L Q R H Q C L H Q E L L Q P A P L L L E K P L S E W P V P Q F I S L F L
. . . . . 90 . . . . . 100 . . . . . 110 120
Astrin -
Spag5 P E F P M R P V K E Q E L K I L G L V A K G S F G T V L K V L D C A Q N A V F A
. . . . . 130 . . . . . 140 . . . . . 150 160
Astrin -
Spag5 V K V V P K V K V L Q R D T L R Q C K E E V S I Q V C R V L K E L N N R I V V C
. . . . . 170 . . . . . 180 . . . . . 190 200
Astrin M W R V K K L S L S L S P S P Q T G K P S M R T P L R E L T L Q P G A L T T S G
Spag5 S Y C S M D L Y S L W S T V G C F P E D S V R L F A A E L V L V L S P E V L S G
. . . . . 210 . . . . . 220 . . . . . 230 240
Astrin K - - - - - - - - R S P A C S S L T P S L C K L G L Q E G S N N S S P V D F V N
Spag5 G P Y N H T A D W W S L G V L L F S L A A G K F P V A A E R D H L T M L A S V T
. . . . . 250 . . . . . 260 . . . . . 270 280
Astrin N K R T D L S S E H F S H S S K W L E T C Q H E S D E Q P L D P I P Q I S S T P
Spag5 H C G S E I P A S I N Q E L S L L L H E L L C Q N P L Y R L R Y L H H F Q A H P
. . . . . 290 . . . . . 300 . . . . . 310 320
Astrin K T S E E A V D P L G N - - - - - - Y M V K T I V L V P S P L G Q Q Q D M I F E
Spag5 F F R G V A F D P E L L Q K Q P V N F V M E T Q D T W P S P L E N M S F E D F D
. . . . . 330 . . . . . 340 . . . . . 350 360
Astrin A R L D T M A E T N S I S L N G P L R T D D L V R E E V A P - C M G D R F S E V
Spag5 C D L E S L G K P - - - A M R T P L R E L K L Q P E A L A D S G K G P M F S S L
. . . . . 370 . . . . . 380 . . . . . 390 400
Astrin A A V S E K P I F Q E - - - - - S P S H L L E E - - - - - - - - - - - - S P
Spag5 T P Y L R R L D L K E R R N S S S P V N F V N A E N S S P V D F V N T E N T S P
. . . . . 410 . . . . . 420 . . . . . 430 440
Astrin P N P C S E Q L H C S K E S L S S R T E A V R - - - - - E D L V P S E S N - - A
Spag5 V D F D N T E N N F L S E Q F S H P S E Y I E A C Q R E S D L T P E S S S P F N
. . . . . 450 . . . . . 460 . . . . . 470 480
Astrin F L P S S V L W L S - - P S T A L A A D F R V N H V D P E E E I V E H G A M E E
Spag5 T L E K A V E A M D D F V A E P I D D D F S V D H V D P G E E T A E N R V I Q E
. . . . . 490 . . . . . 500 . . . . . 510 520
Astrin R E M R F P T H P K E S E T E D Q A L V S S V E D I L S T C L T P N L V E M E S
Spag5 V E K S F L A L P E E A G L G D Q A L A V N A E D V S S L Y L S S S L V E M G P
. . . . . 530 . . . . . 540 . . . . . 550 560
Astrin Q E A P G P A V E D V G R I L G S D T E S W M S P L A W L E K G V N T S V M L E
Spag5 Q E A P G P T A E D A S R I P D L E S E T W M S P L A W L E K G V N T S V M L Q
. . . . . 570 . . . . . 580 . . . . . 590 600
Astrin N L R Q S L S L P - S M L R D A A I G T T P F S T C S V G T W F T P S A P Q E K
Spag5 S L R Q S L P F S K S V L Q D A A V G N T P H S T Y S V G T S F T P P V P L E -
. . . . . 610 . . . . . 620 . . . . . 630 640
Astrin S T N T S Q T G L V G T K H S T S E T E Q L L C G R - P P D L T A L S R H D L E
Spag5 - - - - - - - - - V G T K D S T S E T E R L L L G C R P P D L A A L S R H D L E
. . . . . 650 . . . . . 660 . . . . . 670 680
Astrin D N L L S S L V I V E F L S R Q L R D W K S Q L A V P H P E T Q D S S T Q T D T
Spag5 E N L L N A L V L L E V L S H Q L Q A W K S Q L T V P S R Q A Q D S S T Q T D S
. . . . . 690 . . . . . 700 . . . . . 710 720
Astrin S H S G I T N K L Q H L K E S H E M G Q A L Q Q A R N V M Q S W V L I S K E L I
Spag5 S A A V V T K T P K H L Q D S K E I R Q A L L Q A R N V I H S W G L V S R D L M

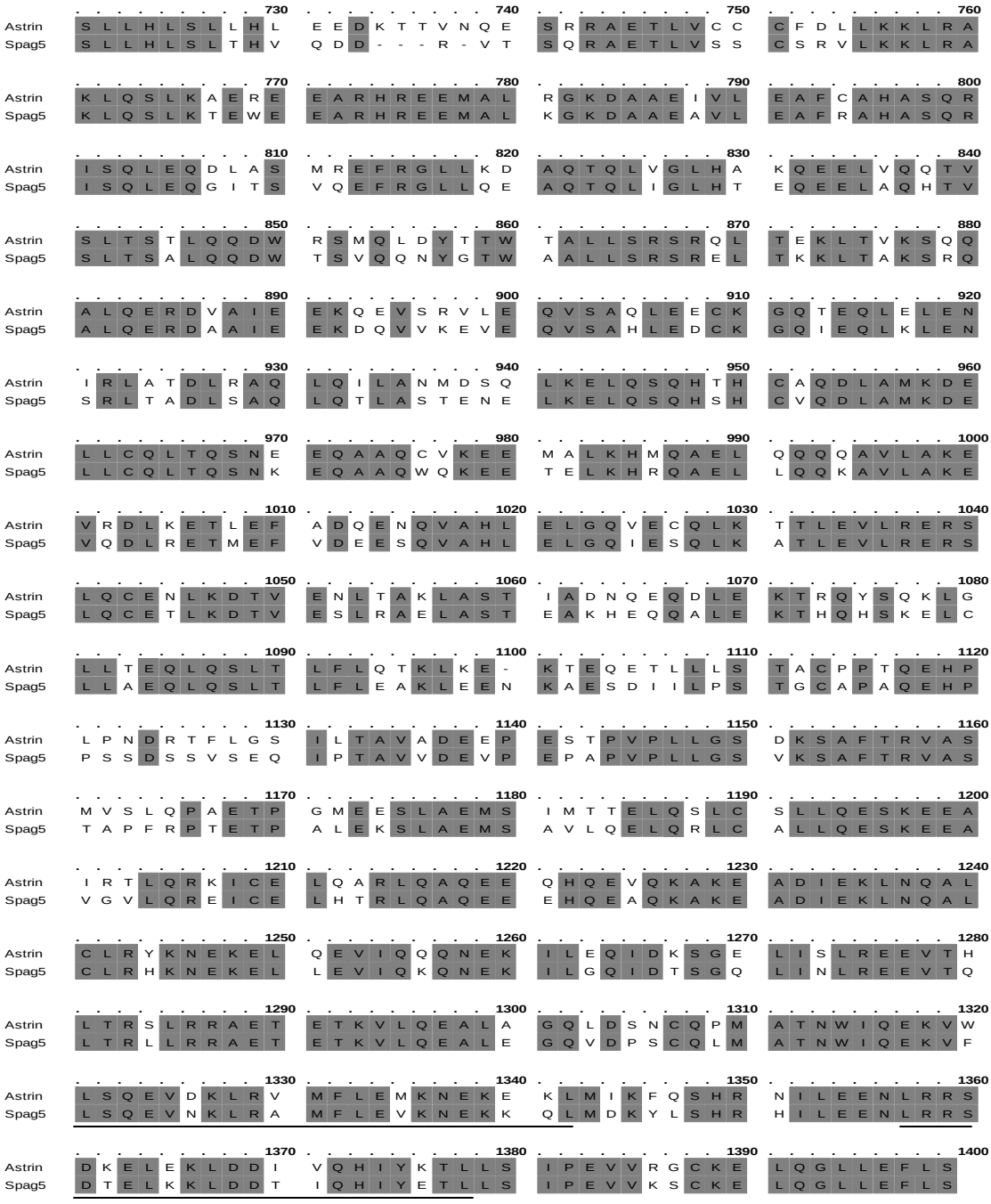
Astrin
Spag5

spermatocytes and round spermatids. The signal detected in elongating spermatids was predominantly in the tail. Cross-sections of rat seminiferous tubules stained with anti-Spag5 are depicted in figure 9. These results support previous results by Shao *et al* (2001) where they used immunoprecipitation of Spag5 from elutriated germ cells. Shao found that Spag5 protein is synthesized in pachytene spermatocytes and round spermatids, with little if any de novo synthesis observed in elongating spermatids. Since it was determined that Spag5 is a form of Astrin, it was of interest to investigate whether Spag5 associates with the meiotic spindles in spermatogenesis. Meiotic spindles are visible under light microscopy sections of seminiferous tubules, however, no staining of these structures with anti-Spag5 was identified (Figure 10, inset). As a negative control for these experiments, anti-Spag5 antibody was pre-incubated with MBP-Spag5 protein and then used in the same experiments (Figure 9, panels B and D). Little to no Spag5 signal was detected using this antibody.

3.e *Spag5 binds to microtubules in vitro and in IEC-18 cells*

Although we did not find binding of Spag5 to meiotic spindles, we pursued the possibility of Spag5 binding microtubules *in* vitro and in mitotic cells, because we colocalized Spag5/Astrin to mitotic spindles (Figure 6). This possibility was tested both *in vitro* and in the rat IEC-18 cell line. Spag5 was *in vitro* transcribed and translated in the pBluescript (ATG) vector, producing a protein product of approximately 50 kDa. This protein product was analyzed for any microtubule binding capacity. Spag4 was used as a positive control (described in Shao *et al*, 1999) and Ras was used as a negative control (known to not bind microtubules *in vitro*). Spag5 was found to bind to microtubules *in*

Figure 9: Staining of rat seminiferous tubules with anti-Spag5 antibody (affinity-purified). Panels A and C show stages VIII, V and VII of the seminiferous epithelium stained with anti-Spag5. Spag5 signal is detected in the tails of elongating spermatids with a faint signal in the cytoplasm of spermatocytes and round spermatids. Panels B and D show stages V and IV of the seminiferous epithelium stained with anti-Spag5 that was pre-incubated with MBP-Spag5 protein (blocking). Little stain is seen using the blocked antibody. Magnification for panels A and B: 20X. Magnification for panels C and D: 10X.

A.

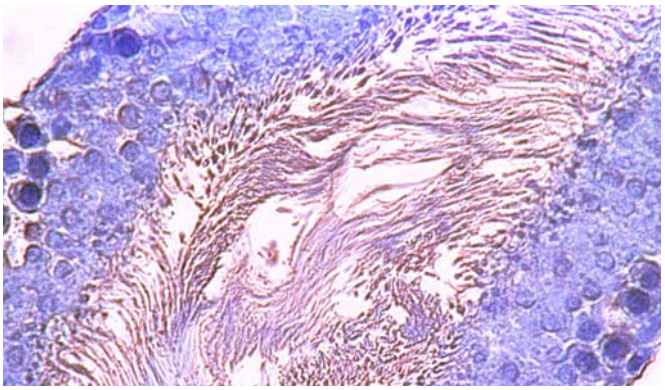

S VIII

B.

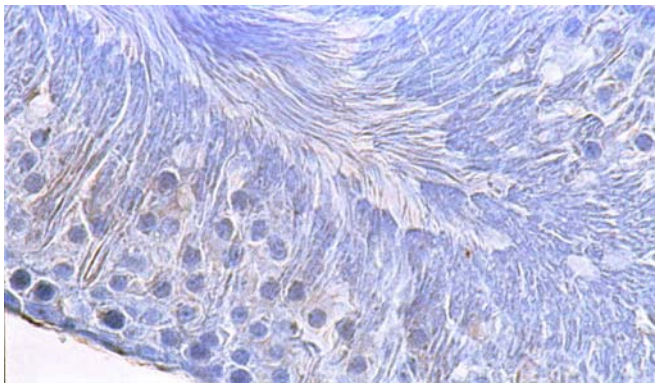

S V

C.

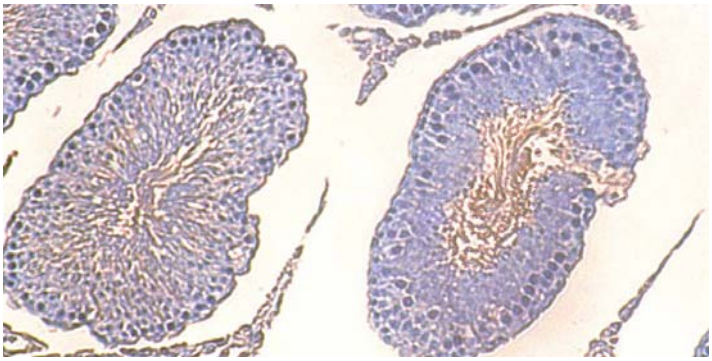

S V **S VII**

D.

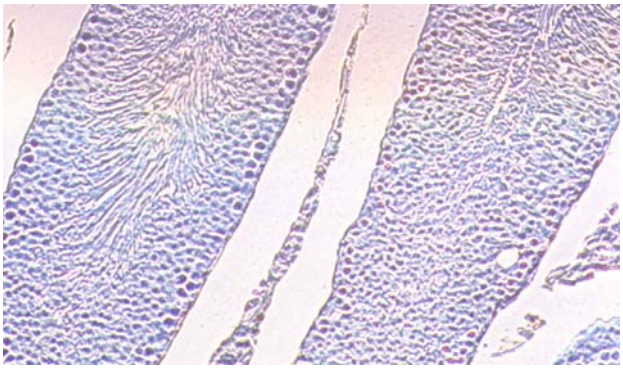

S IV

Figure 10: Staining of rat seminiferous tubules with anti-Spag5 (affinity-purified). Rat testis section staining shows a stage VIII cross-section (with inset). Most Spag5 signal detected in elongating spermatids, the cytoplasm of primary spermatocytes and a faint signal in the cytoplasm of secondary spermatocytes and round spermatids. Magnification: 20X.

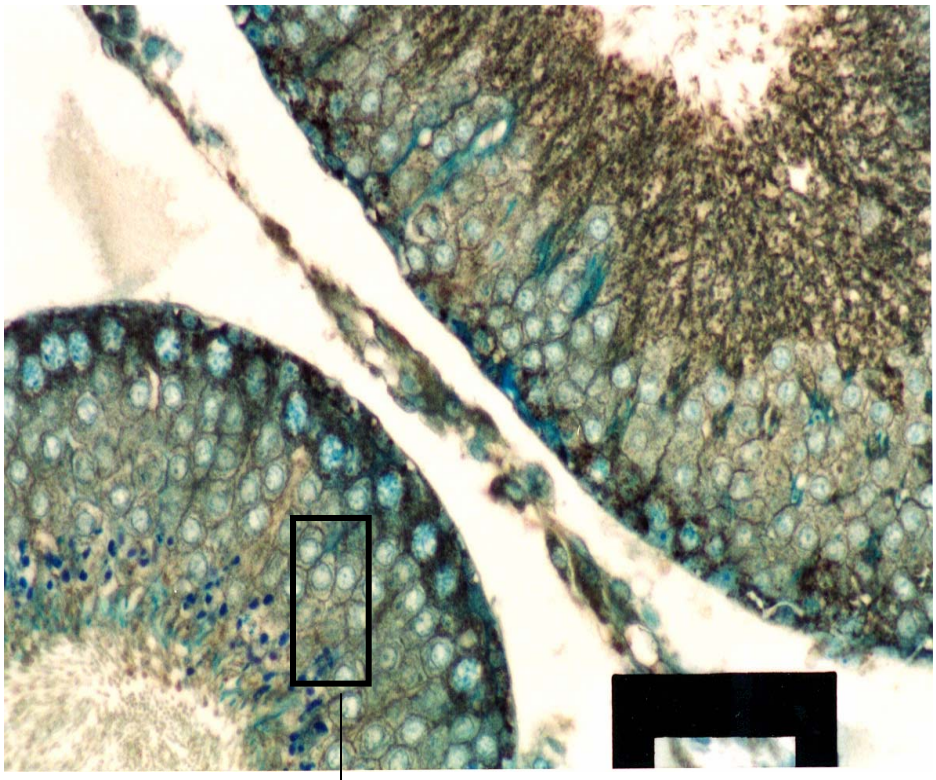

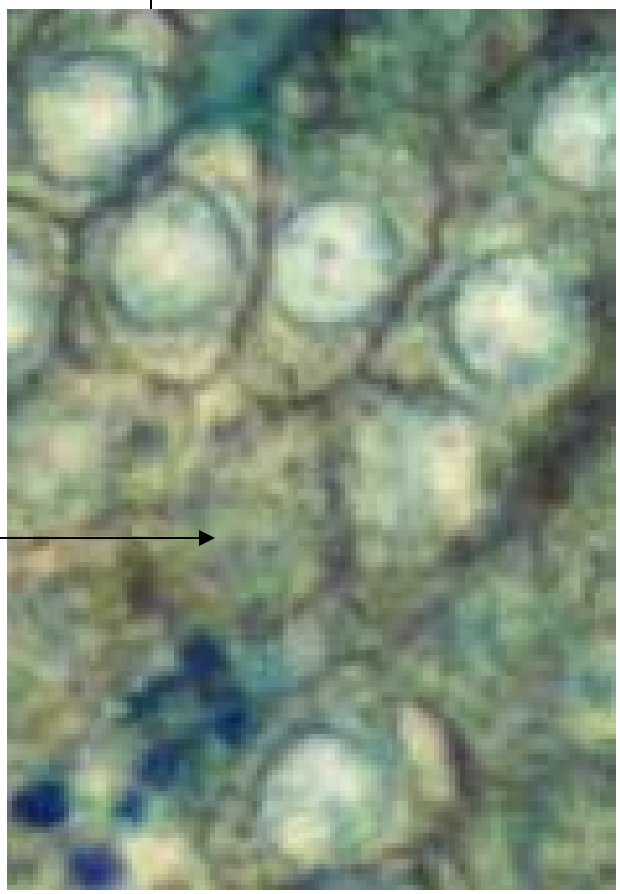

Meiotic Spindle

vitro (Figure 11A, lanes i and j), leading to the hypothesis that Spag5 has a similar role to Spag4 in the rat sperm tail (binding to ODF and axoneme). The *in vitro* transcribed and translated Spag5 that was detected in this assay was approximately 50 kDa in size (Figure 11A, lanes a and b). Two different Spag5 plasmids were used to generate Spag5 protein, one with an internal start codon and one without. Due to the similarity between Spag5 and Astrin (non-motor mitotic spindle protein) it was also hypothesized that this microtubule-binding capacity of Spag5 is necessary for its interaction with the mitotic spindle in somatic cells and/or meiotic spindles.

To test the Spag5's native association with MTs in cells, a protocol was developed to isolate MTs, which retain the components on MTs *in vivo.* These microtubules were subjected to SDS-PAGE (12%) transferred to PVDF membrane and blotted both with affinity-purified Spag5 antibody and an Astrin polyclonal antibody. The Spag5 blot generated one major band at ~54 kDa, with one minor band and ~110 kDa (Figure 11B). The Astrin blot generated multiple bands of sizes ~27 kDa, ~31 kDa, ~34 kDa, ~42 kDa, ~47 kDa, ~54 kDa, ~68 kDa, ~73 kDa and ~110 kDa. The major Astrin bands were the 27 kDa and the 47 kDa bands (Figure 11B). The two bands visualized on the Spag5 blot matched three bands of the same size on the Astrin blot (54 kDa and 110 kDa). Anti-Astrin appears to detect all of the proteins that Spag5 identifies, while also identifying many different proteins of different sizes. Both the similarities and differences between Spag5 and Astrin will be discussed in the next chapter.

Figure 11: Spag5 binds to microtubules, both *in vitro* and in IEC-18 rat cells. In panel A, HA-tagged Spag5 (lanes a, e and i), Spag5 (lanes b, f and j), Spag4 (lanes c, g and k) and ras (lanes d, h and l) were translated in vitro and incubated with brain microtubules. MT complexes were pelleted through cushions and analyzed ("pellet"). Supernatants were also analyzed, as were input (1^{st} supernatant) materials. Note that Spag5 binds MT, as does Spag4, in contrast to ras, which does not, as expected. In panel B, both affinity purified polyclonal anti-Spag5 antibody and polyclonal anti-Astrin antibody were used to blot microtubules isolated from rat IEC-18 cells (with all MT-associated proteins still intact). Note that both anti-spag5 and anti-astrin detect MT-associated proteins from IEC-18 cell.

A.

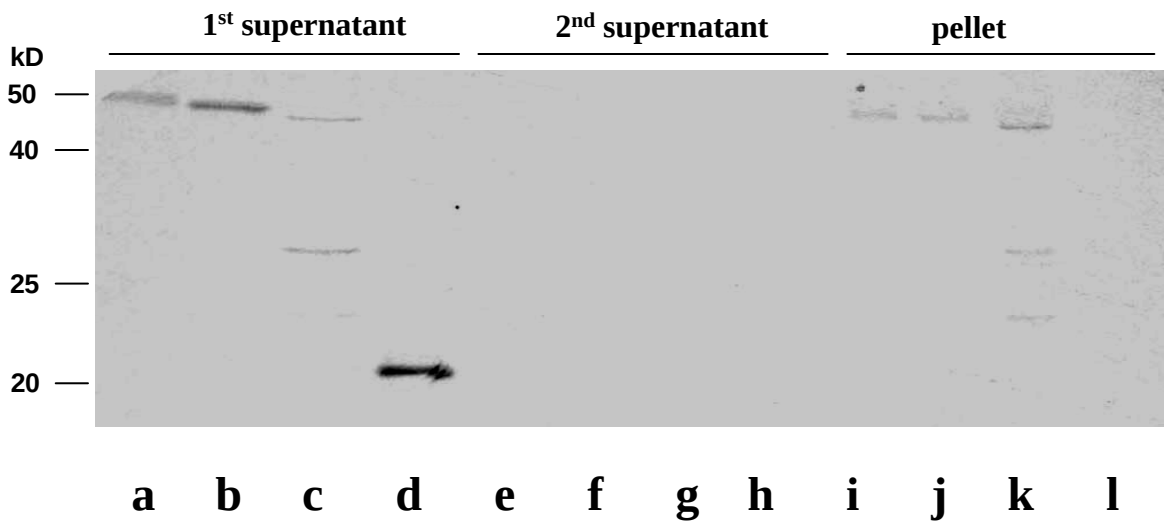
1st supernatant
2nd supernatant
pellet
kD
50
40
25
20
a b c d e f g h i j k l

B.

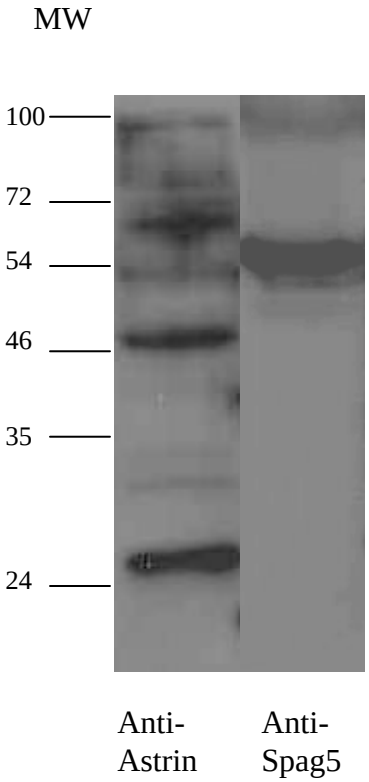
MW
100
72
54
46
35
24
Anti-Astrin
Anti-Spag5

3.f *Spag5 localizes to the ODF, but not the axoneme in rat sperm tails*

Light microscopy results indicated that Spag5 localizes to elongating spermatid tails and the cytoplasm of spermatocytes and round spermatids, but not to meiotic microtubules. Thus Spag5 could possibly associate with non-microtubule structures in sperm tails, such as the ODF, FS or mitochondrial sheath. Electron microscopy experiments were done to localize Spag5 at the ultra-structural level. Rat testis sections as well as rat epididymal fractions were fixed and immunogold-labeled for Spag5 and visualized under electron microscopy. Cross-sections and longitudinal sections of both elongating spermatid tails (Figure 12) and mature epididymal sperm tails (Figure 13) were immunogold-labelled for Spag5. Spag5 does not appear to localize to the axoneme, but instead mainly to the ODF. Infrequently, gold particles are identified over the FS, mitochondrial sheath and the axoneme, but this observation is not consistent over all of the sections. It is possible that the tissue preparation could result in modifying the axoneme so that any possible Spag5 epitope was not available. Therefore, further work would need to be completed to verify that Spag5 does not localize to the axoneme. A graphical representation of quantification of the electron microscopy results is depicted in figure 14. The ultra-structural analysis thus suggests that Spag5/Astrin behaves as an ODF-associated protein in elongating spermatids.

3.g *Spag5 mRNA is expressed in many different tissues*

In previous studies, Northern blot analysis was used to investigate the RNA expression of Spag5 in various tissues and was found to only be expressed in testis (Shao *et al*, 2001). However Astrin was reported to be expressed in a variety of cell types. We

confirmed that Spag5/Astrin is expressed in IEC-18 cells (Figures 5 and 6). Therefore, we conducted RT-PCR experiments and found that Spag5 is transcribed in many different tissues (Figure 15). Beta-actin primers were used to analyze the quality and quantity of cDNA. These results support a hypothesis that Spag5 has a role in somatic cells, separate from its role in spermatogenesis. In addition to the expected transcript size, many different tissues contain smaller than expected Spag5 fragments, which may derive from differentially spliced variants. RT-PCR was also performed on testis RNA isolated from rats ranging in age from 5 days old to adult. The Spag5 transcript does not appear until after day 15 (Figure 16), which was surprising since all adult tissues express Spag5 RNA (see Discussion).

3.h *Spag5 and Astrin Protein Analysis*

RT-PCR results determined that Spag5 is expressed in many different tissues, so it was important to determine whether the protein is also present in different tissues. One other result from RT-PCR was the detection of smaller PCR products and it was of interest to determine whether there are also other protein variants of different sizes. Also, electron microscopy revealed that Spag5 associates with the ODF, so it was of interest to determine whether Spag5 is an integral ODF protein or if it just associates with the ODF. In order to answer all of the above points, protein analysis of both Spag5 and Astrin was performed. Spag5 protein was analyzed by Western blotting in three somatic cell lines (IEC-18, NIH 3T3, HeLa), ODF, rat spermatids and rat spermatocytes. Spag5 detects multiple bands in spermatocytes and spermatids of sizes ~25 kDa, ~30 kDa, 54 kDa, ~80 kDa, 110 kDa, 150 kDa and ~180 kDa (Figure 17A, lanes 8 and 9). The bands decrease

Figure 12: Immuno-electron microscopy analyses of rat elongating spermatids in rat testis sections using affinity-purified anti-Spag5 antibodies. Gold label is predominantly surrounding the ODF, but some label is over the axoneme and mitochondrial sheath. Note the rounded mitochondria forming the mitochondrial sheath on the developing midpiece of the tail. Panel A shows a longitudinal section of a developing midpiece (X 75,000) and Panel B shows a cross-section of a developing midpiece (X 50,000). ODF, outer dense fibers; AX, axoneme; M, mitochondrial sheath

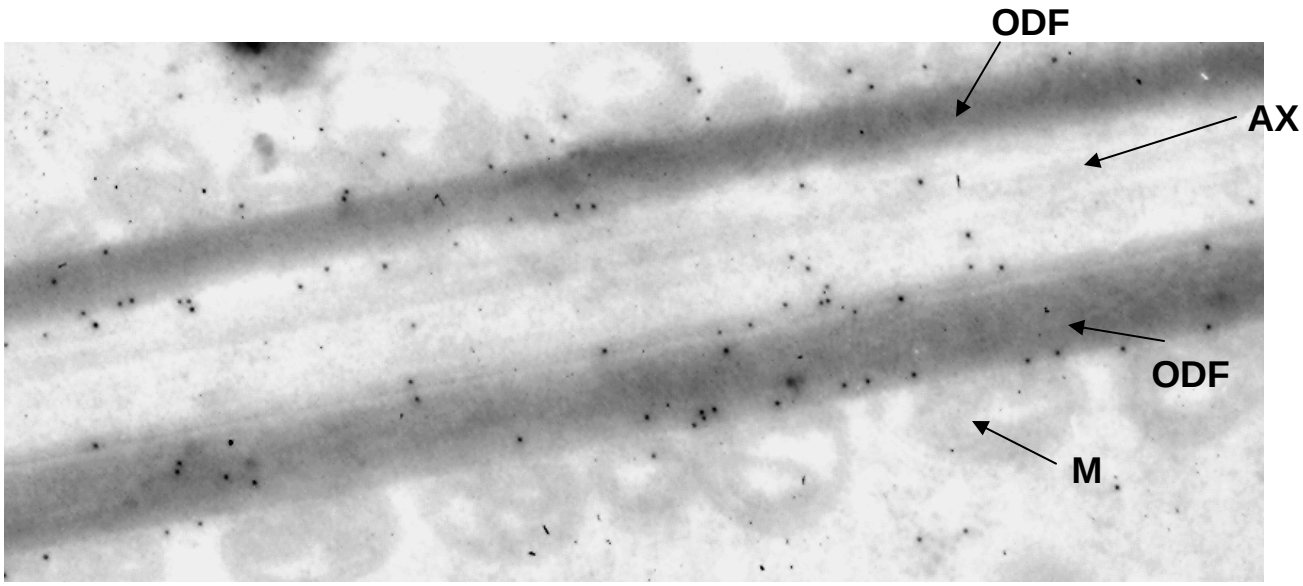

A.

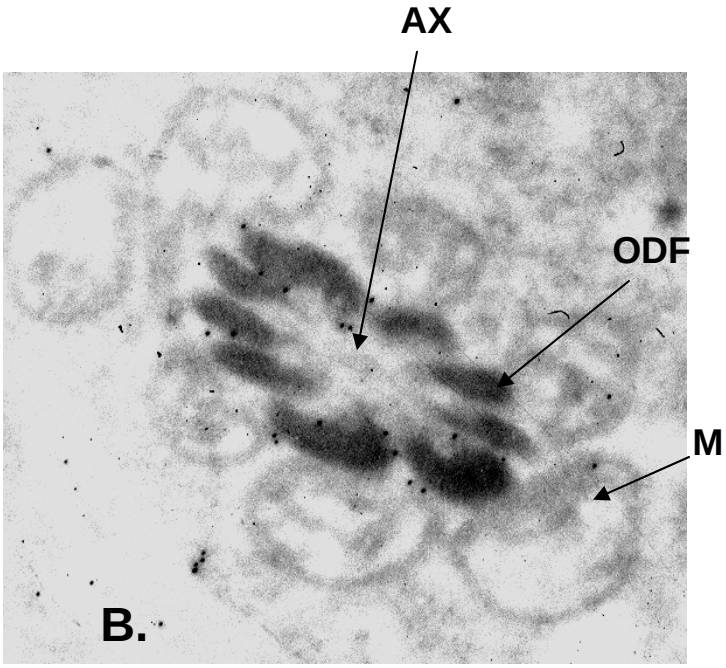

Figure 13: Immuno-electron microscopy analyses of mature rat spermatozoa from epididymal sections using affinity-purified anti-Spag5 antibodies. Gold label is predominantly surrounding the ODF, but some label is detected over the FS, axoneme and the mitochondrial sheath. Panel A shows a midpiece cross-section (X 75,000); panel B shows two principal piece cross-sections (X 50,000); panel C shows a midpiece longitudinal section(X 50,000); panel D shows a midpiece cross-section negative control which was labeled with secondary antibody only. ODF, outer dense fibers; FS, fibrous sheath; AX, axoneme; M, mitochondrial sheath.

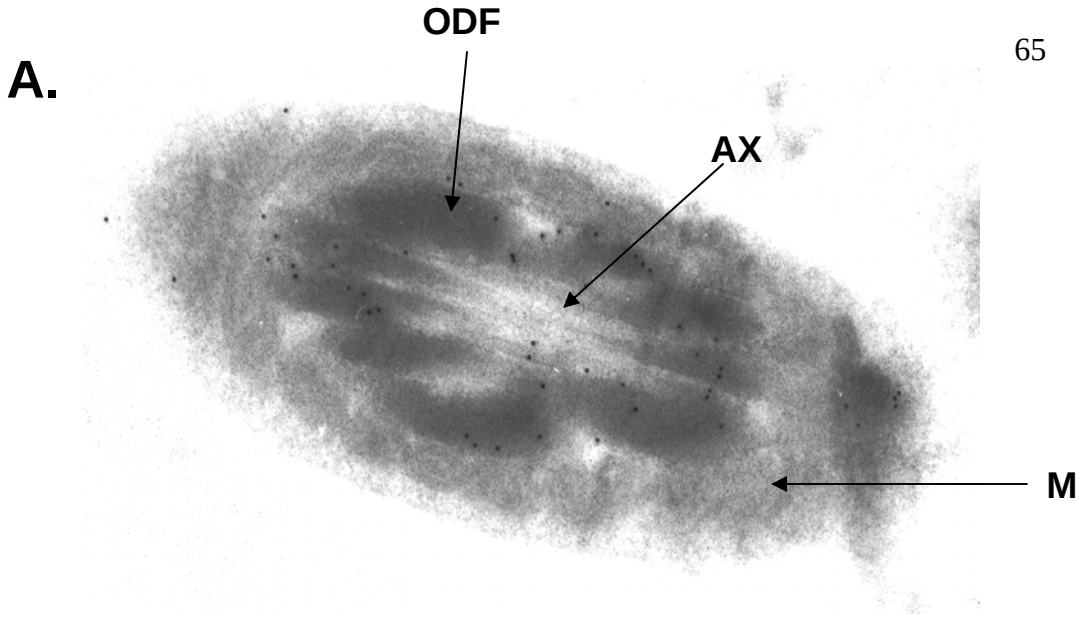
A.
ODF
AX
M

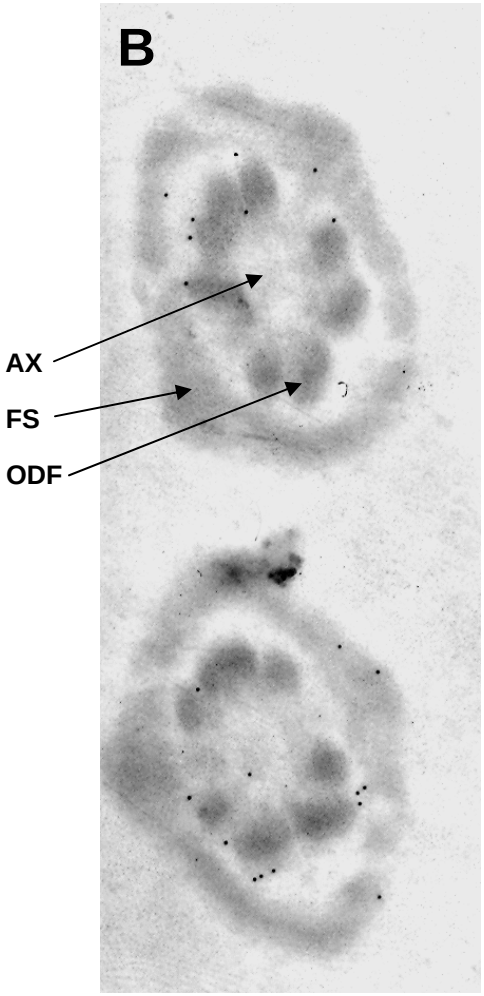
B
AX
FS
ODF

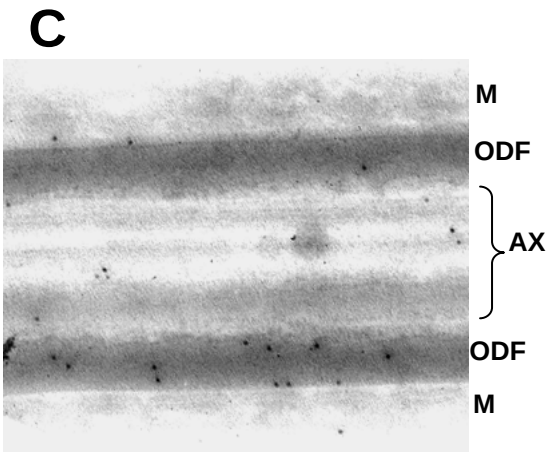
C
M
ODF
AX
ODF
M

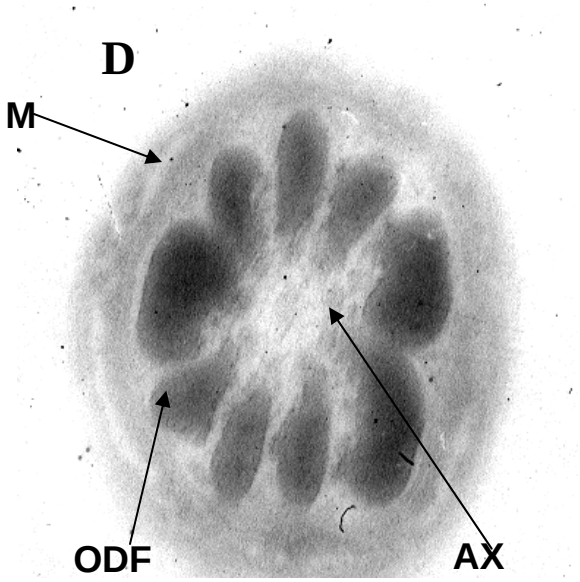
D
M
ODF
AX

Figure 14: Graphical representation of electron microscopy results. A total of ten electron micrographs were analyzed for the number of gold particles localized over four different subcellular structures in the rat sperm tail. Gold particles were counted over the outer dense fibers (ODF), fibrous sheath (FS), axoneme (Ax) and the mitochondrial sheath (MS). The most gold particles were found localized over the ODF (250) with the lowest number of particles found on the FS (12). Both the axoneme and the MS had significantly more gold particles than the FS (65 and 75) but these numbers were significantly less then the ODF.

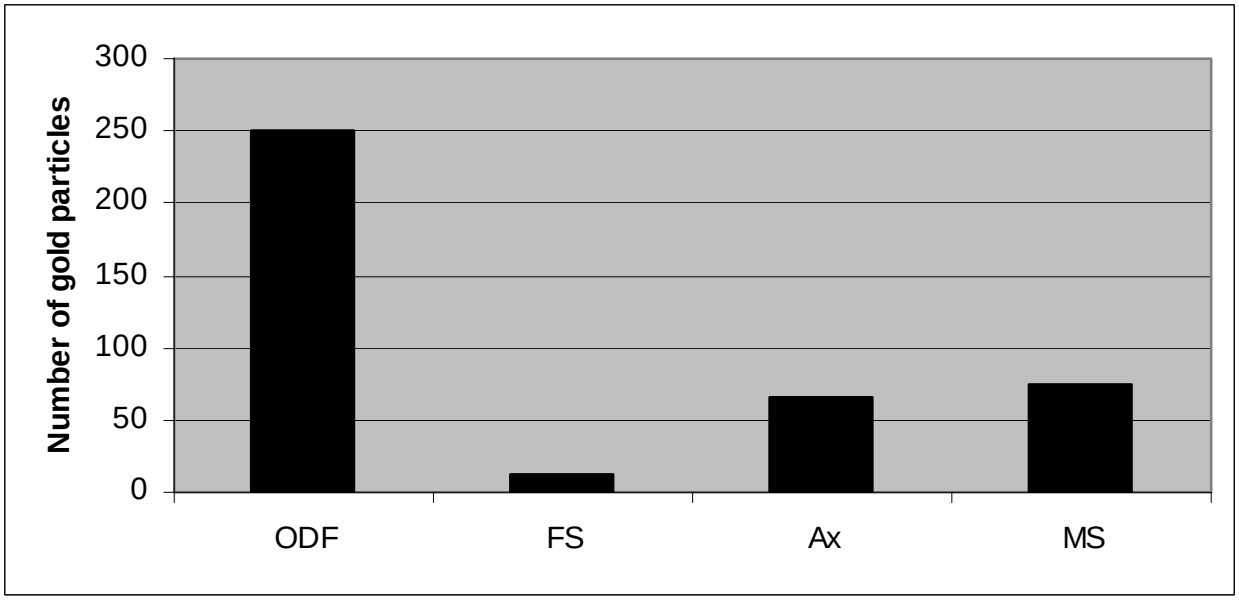
Number of gold particles
300
250
200
150
100
50
0
ODF
FS
Ax
MS

in intensity from spermatocytes to spermatids until the only band present in rat sperm tails is the 54 kDa band (Figure 17A lanes 3 and 4). This data suggests that there is possibly processing of the Spag5 protein after it is translated in spermatocytes. Additionally, blotting of protein extracts from 3T3 cells, HeLa cells, and IEC-18 cells with anti-Spag5, yields two bands in all blots of sizes ~30 kDa and ~54 kDa (Figure 17A, lanes 5, 6 and 7). However, no Spag5 bands were detected in purified ODF (Figure 17A, lanes 1 and 2). Two different extracts of ODF and sperm tails were used for authenticity. Spag5 protein binds Odf1 *in vitro* (Shao *et al*, 2001), however, results indicate that Spag5 is not part of the integral ODF proteins and is lost during the ODF isolation process. Western blots of total rat testis protein and rat sperm tail protein was compared between Spag5 and Astrin. The Spag5 antibody detected five bands in total rat testis protein at ~27 kDa, ~55 kDa, ~100 kDa, ~130 kDa and ~170 kDa (Figure 18A). The same Spag5 antibody detected only one band in rat sperm tail protein at ~55 kDa (Figure 18A). When the same protein extracts were blotted with the Astrin antibody, multiple bands were also detected. In rat testis protein, bands were detected at ~27 kDa, ~32 kDa, ~35 kDa, ~40 kDa, ~47 kDa, ~55 kDa, ~70 kDa, ~100 kDa, and ~110 kDa (Figure 18B). However, Astrin detected three bands in rat sperm tails at ~20 kDa, ~47 kDa, ~70 kDa. Some of these bands match bands of the same sizes in the Spag5 blots, but there are many bands detected in the Astrin blots that are not detected in the Spag5 blots. The band sizes that were detected in both Spag5 and Astrin total testis blots were 27 kDa, 55 kDa and 100 kDa. There were no similar band sizes in sperm tail protein since Spag5 only detected one band of ~55 kDa and this band was not obvious in the Astrin blot. Looking at the both Astrin blots in figure 18B, it is possible that the 47 kDa and 70 kDa bands in sperm

tails could correspond in actuality to the 47 kDa and 55 kDa bands in the testis (proteins could be post-translationally modified), but more work would need to be done to determine this.

3.i *Spag5 overexpression in mouse 3T3 fibroblasts*

Most of the spag5 experiments that were undertaken were dealing with endogenous spag5 protein and mRNA. We decided to overexpress spag5 in mouse 3T3 fibroblasts to see if we could repeat the immunoflourescence observations. Spag5 was overexpressed in mouse 3T3 cells using the Spag5-GFP vector. Spag5 expression was detected by the green GFP signal. Spag5 was only found in the cytoplasm of the cells with no mitotic spindle localization identified (Figure 19, panels B and C). The Spag5 signal appeared to be perinuclear and diffuse with no punctate signal visualized. These results are not consistent with endogenous immunofluorescence of Spag5 in rat IEC-18 cells, and may indicate the limited usefulness of using GFP-spag5 constructs. These differing results will be further analyzed in the discussion.

Figure 15: Spag5 mRNA synthesis was analyzed by RT-PCR. Total RNA was isolated from the indicated tissues and cDNA was made using random primers and reverse transcriptase (RT).

Top panel) PCR was performed using Spag5-specific primers and 35 cycles.

Bottom panel) beta-actin primers were used to analyze the quality and quantity of cDNA in each sample. Note that Spag5 mRNA is detected in all tissues. Also note that some tissues (colon, liver, intestine and testis) produce smaller than expected Spag5 PCR fragments, which may derive from differentially spliced smaller mRNA variants.

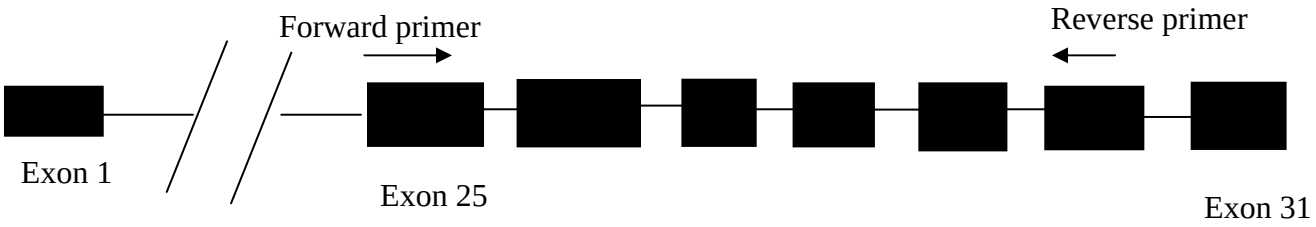
Forward primer
Reverse primer
Exon 1
Exon 25
Exon 31

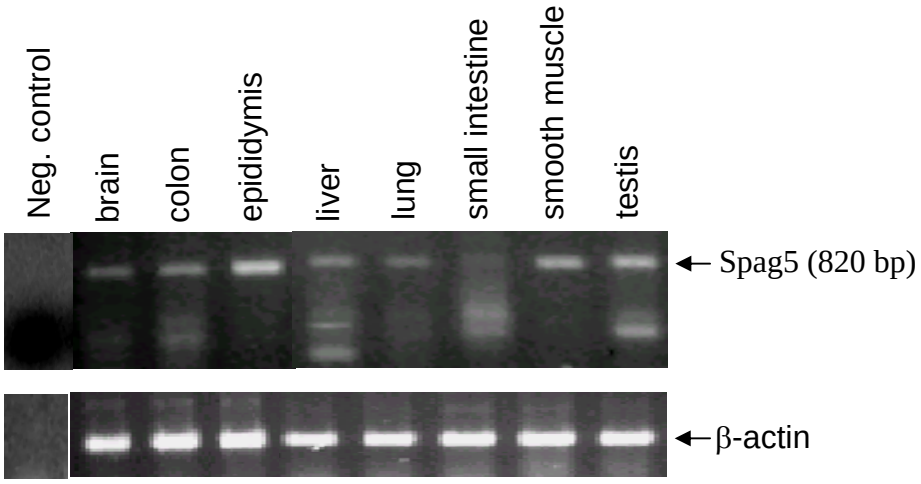
Neg. control
brain
colon
epididymis
liver
lung
small intestine
smooth muscle
testis
Spag5 (820 bp)
β-actin

Figure 16: Total testis RNA was isolated from rats 5 days old, 21 days old, 25 days old, 30 days old and adult rats and cDNA was made using random primers. PCR was performed using spag5-specific primers and 35 cycles. Spag5 was detected in all samples except 5 days old.

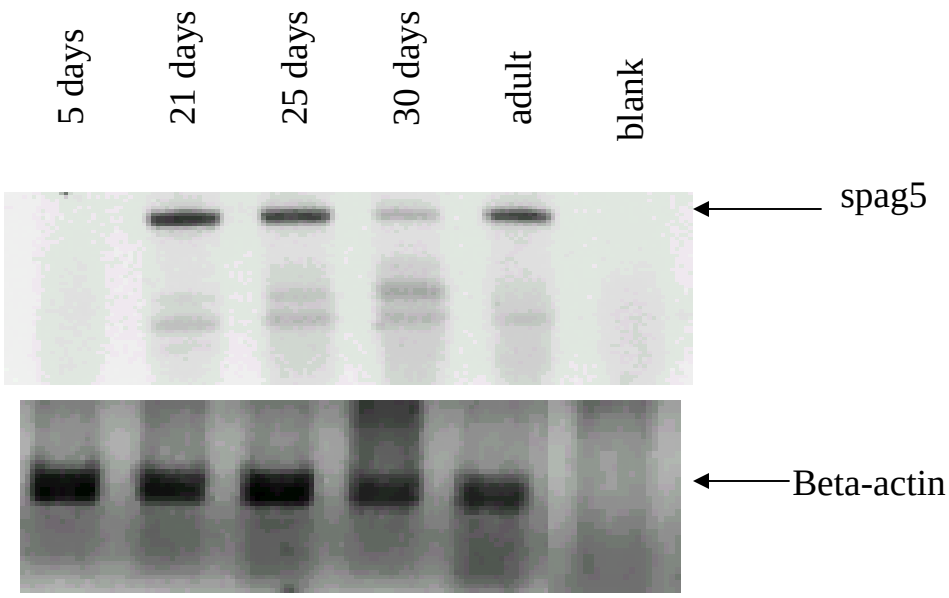
5 days
21 days
25 days
30 days
adult
blank
spag5
Beta-actin

Figure 17: Proteins were extracted from two different rat ODF fractions, two different rat sperm tail preparations, elutriated rat spermatids and spermatocytes, HeLa cells, mouse 3T3 cells and rat IEC-18 cells and analyzed with anti-Spag5 antibodies in western blot assays. Sperm tails show a single Spag5 protein, but somatic cells show two bands and male germ cells express multiple Spag5 proteins. Panel B shows the Coomassie staining of all the proteins. This experiment was repeated four times.

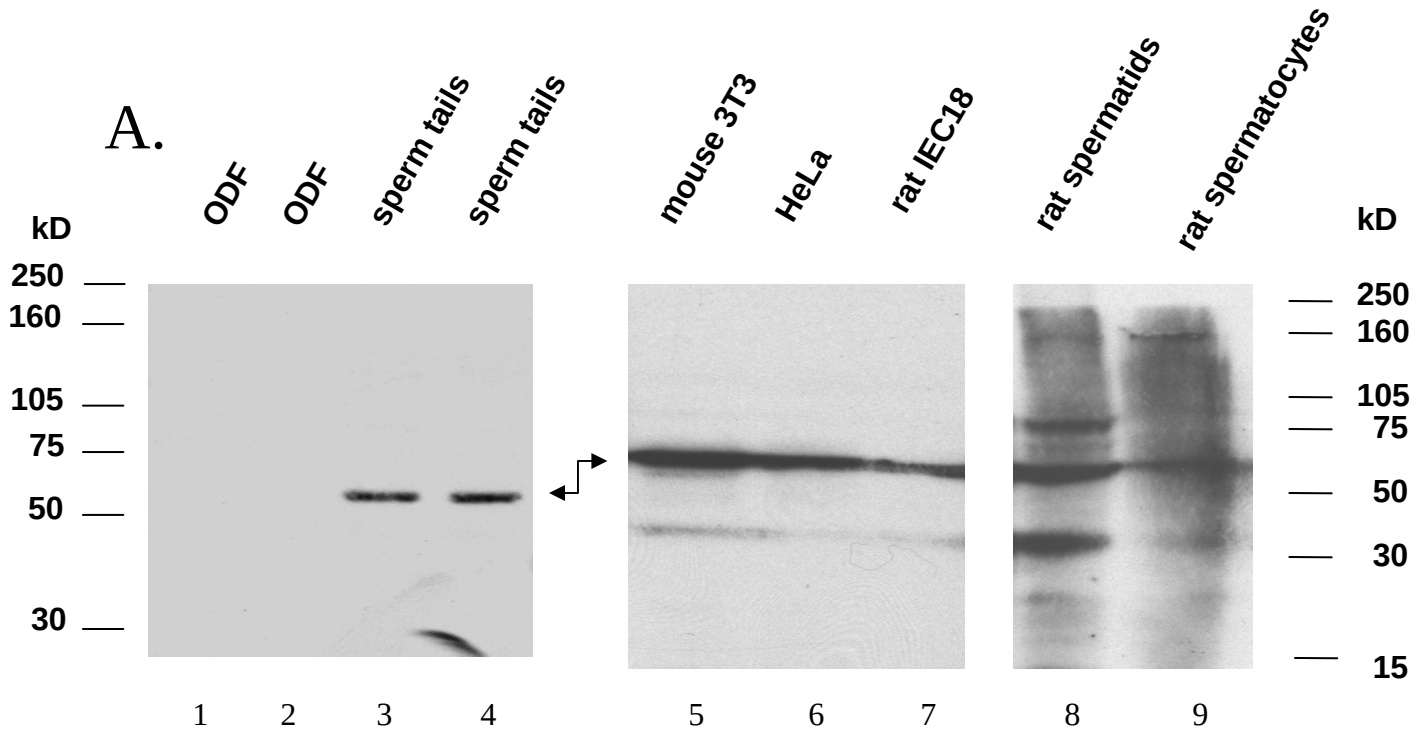
A.
ODF
ODF
sperm tails
sperm tails
mouse 3T3
HeLa
rat IEC18
rat spermatids
rat spermatocytes
kD
250
160
105
75
50
30
kD
250
160
105
75
50
30
15
1
2
3
4
5
6
7
8
9

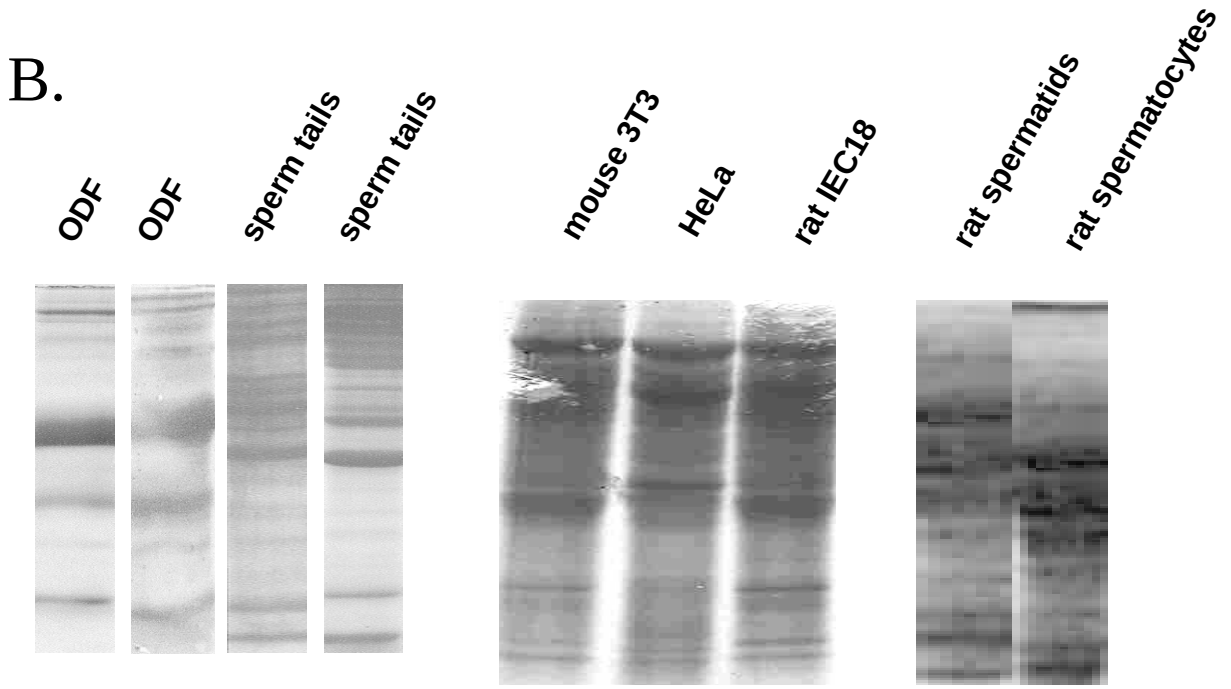
B.
ODF
ODF
sperm tails
sperm tails
mouse 3T3
HeLa
rat IEC18
rat spermatids
rat spermatocytes

Figure 18: A. Affinity purified anti-Spag5was used in blotting proteins isolated from both rat testis and sperm tails with a prominent band at ~55kDa in both sperm tails (only one band) and testis protein. B. Polyclonal anti-Astrin was used on the same extracts with many prominent bands in testis and three in sperm tails, a couple matching in size to Spag5. This experiment was repeated four times.

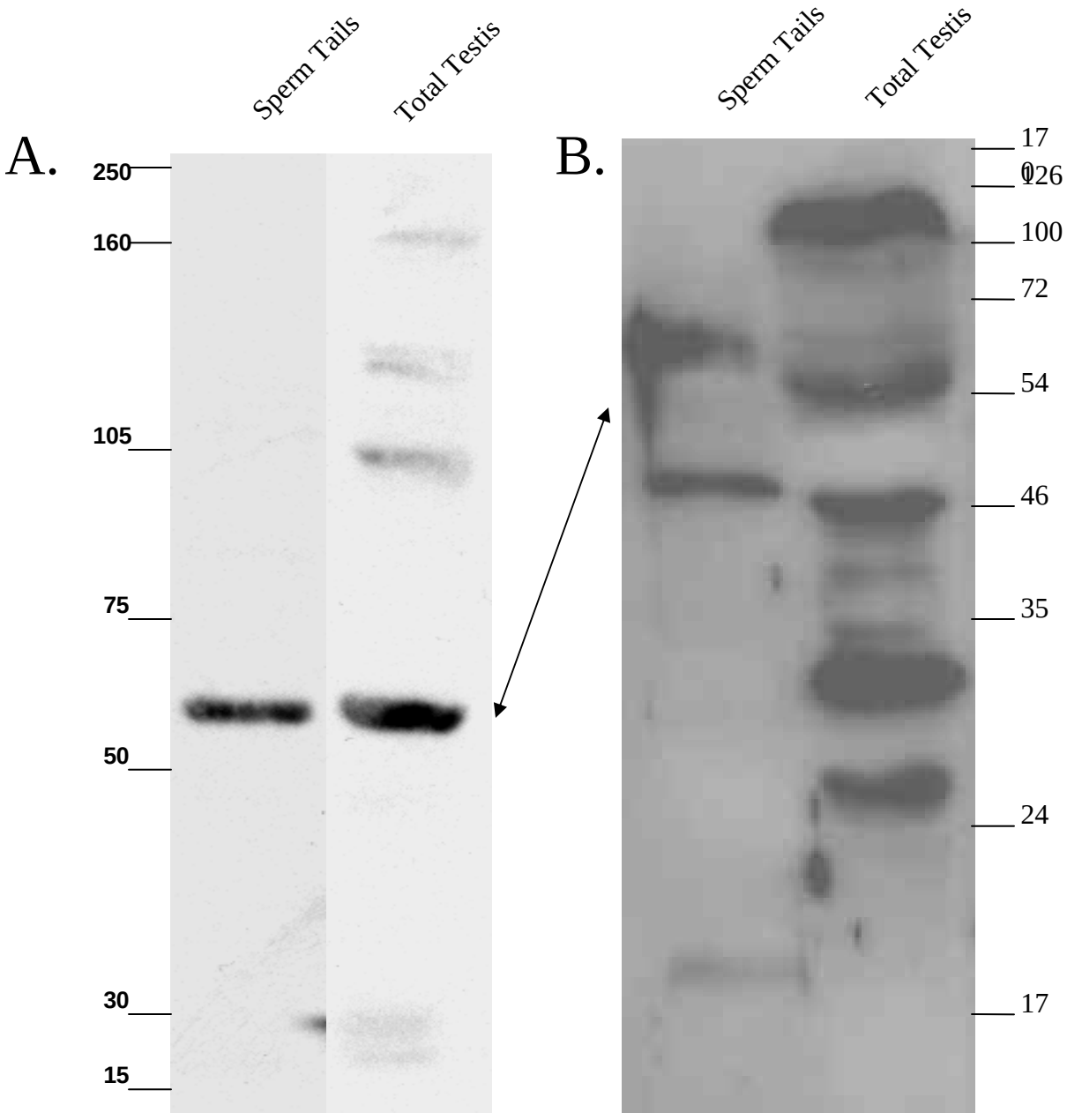
A.
Sperm Tails
Total Testis
250
160
105
75
50
30
15
B.
Sperm Tails
Total Testis
17
126
100
72
54
46
35
24
17
Anti-Spag5
Anti-Astrin

Figure 19: Mouse 3T3 fibroblasts were transfected with pEGFP-C2 vector containing spag5 sequence (panels B and C). Simultaneously, cells were also transfected with empty pEGFP-C2 vector (panel A). Expression of spag5 was detected by the green GFP signal. Spag5 was only detected in the cytoplasm, specifically surrounding the nucleus. No nuclear or mitotic spindle localization was detected for spag5. All cells were also stained for beta-tubulin using a monoclonal tubulin antibody and a Cy3-labelled secondary antibody. Beta-tubulin staining demonstrates cell and cytoskeleton integrity.

A.

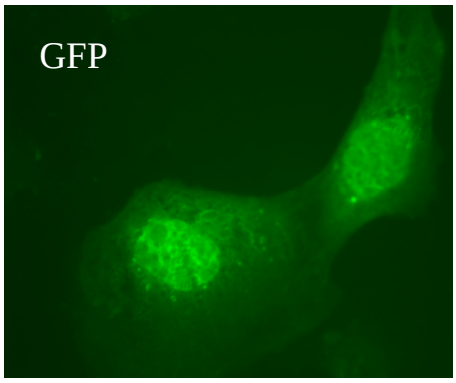

D.

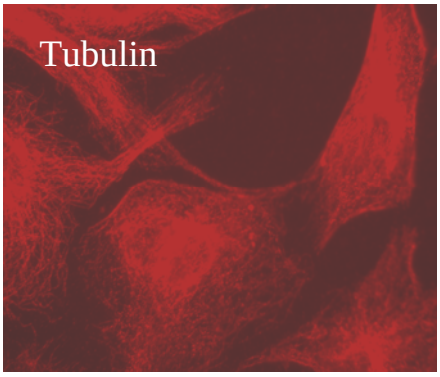

B.

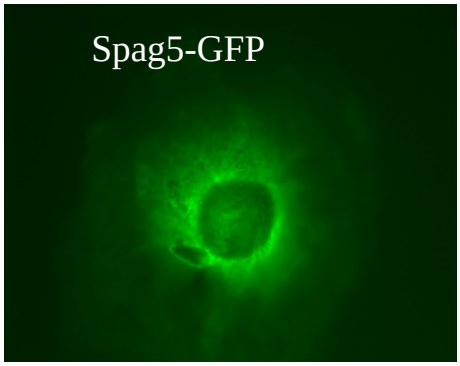

E.

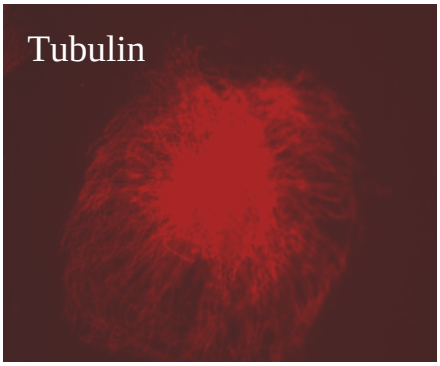

C.

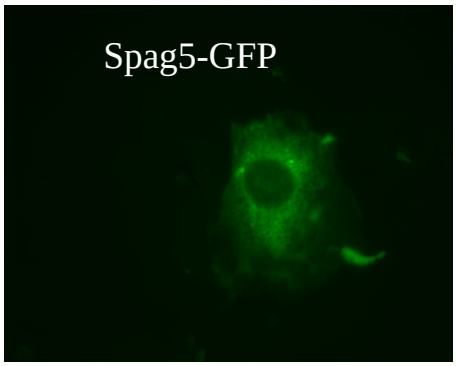

F.

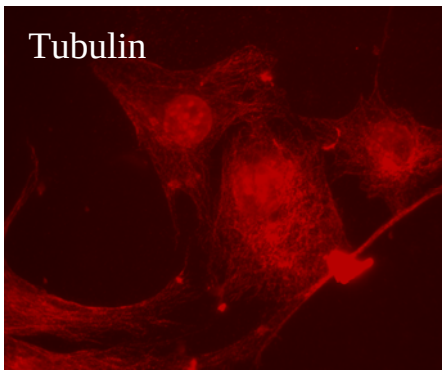

CHAPTER 4: SPAG5 DISCUSSION

4.a *Spag5 Summary*

Spag5 was initially identified as an Odf1-binding protein using the Odf1 leucine zipper motif as bait in a yeast two hybrid screen. Spag5 was thought to be a testis-specific protein which possibly functions as an ODF and axoneme binding protein similar to Spag4. Initial microtubule binding experiments verified that Spag5 binds microtubules *in vitro*, however, electron microscopy experiments revealed that Spag5 appears to only localize to the ODF and not the axoneme. Light microscopy experiments in rat testis sections revealed that Spag5 protein is found in elongating spermatid tails and the cytoplasm of round spermatids and spermatocytes. However, no localization to meiotic spindles was observed at this level. Blast searches revealed that Spag5 bears a 73% homology to the C-terminus of Astrin, a human non-motor mitotic spindle protein. Colocalization immunofluorescence with antibodies to both Spag5 and Astrin revealed that both localize to the mitotic spindle in dividing cells and both colocalize in a punctate pattern in the cytoplasm of interphase cells. While Spag5 and Astrin appear to colocalize, this does not appear to be 100% complete colocalization. Genomic analysis of both Astrin and Spag5 reveal that Spag5 is localized to rat chromosome 10 and is flanked by the Fructose-bisphosphate aldolase C (brain type aldolase) and the Phosphatidylinositol-glycan biosynthesis (class S protein) genes. Astrin is localized to human chromosome 17 and is flanked by these same two genes. The human gene is called Spag5 and these results indicate that Spag5 is the rat homolog of Astrin.

4.b *The role of spag5 in spermatogenesis*

Spag5 was originally thought to be testis-specific which RT-PCR and immunofluorescence studies have now refuted. However, it does appear that Spag5 may indeed play a role in the testis, specifically in the elongating spermatid tail and the mature spermatozoa tail. While light microscopy studies have revealed that Spag5 exists in the cytoplasm of spermatocytes and round spermatids, it is a possibility that Spag5 protein may be synthesized in these cells to be packaged and sent to the growing sperm tail where it functions as an ODF-interacting protein (function as of yet is unknown). Since Spag5 was found to bind to microtubules *in vitro*, it was hypothesized that Spag5 has a function similar to that of Spag4. Spag4 also interacts with microtubules *in vitro*, binds to Odf1 via leucine zippers and localizes to the ODF and axoneme of the rat sperm tail. There is another protein, Spag6, which has been found to be localized to the central microtubule pair of the human sperm axoneme. However, Spag6 does not appear to localize to the ODFs. Spag6 bears a significant homology to Chlamydomonas reinhardtii PF16 and contains eight contiguous armadillo repeats, which place them both in a family of proteins known to mediate protein-protein interactions (Neilson *et al*, 1999). It appears that Spag proteins may share similar localizations and possibly functions, while many do not. Electron microscopy experiments revealed that Spag5 only localizes to the ODF, but not to the axoneme in both the mature rat sperm tail and the elongating spermatid tail. Some gold particles were detected over the axoneme, FS and the mitochondrial sheath, but these observations were inconsistent and sparse. There was more Spag5 detected over the axoneme and mitochondrial sheath than over the fibrous sheath, but this was not major difference. This led to the hypothesis that Spag5 is an actual ODF protein. Western

blot analysis of isolated rat ODF protein using an affinity-purified Spag5 polyclonal antibody detected no protein bands. Therefore, it was concluded that the ODF isolation process leads to the solubilization of Spag5 and that Spag5 does not share the characteristics of the majority of ODF proteins, but instead associates with these cytoskeletal structures. Spag5 localizes to the ODFs in both mature spermatozoa tails and the elongating spermatid tail. Therefore, it is possible that Spag5 assists in the function of the ODFs in the mature, ejaculated sperm and/or assists in the formation of the ODFs in the elongating spermatid tail. Generating a full Spag5 knockout mouse would be extremely useful in elucidating the role of Spag5 in spermatogenesis, however, as will be discussed later, it is likely that knocking out the full Spag5 gene would not be possible due to its likely role in mitosis. Therefore, different methods would need to be generated in order to determine the function of Spag5 in spermatogenesis. One possibility is to immunoprecipitate Spag5-interacting proteins from elutriated cells to see if there are any other protein interactions other than Odf1.

Near the end of the project, the full length Spag5 mRNA and protein were published. We found that the Spag5 sequence that we had been working with was approximately less than half of that full sequence. Since most of the work performed on Spag5 in spermatogenesis was using an affinity-purified polyclonal antibody specific for Spag5 (C-terminus), the discovery of the full length Spag5 could affect these observations. It is possible that generation of an antibody to either the whole Spag5 protein or to the N-terminus could change the resulting Spag5 pattern detected in the IF, IP, immunocytochemistry and electron microscopy experiments. One other observation made in the immunocytochemistry experiments was that Spag5 does not appear to

localize to the meiotic spindle. In order to fully verify this observation, further experiments would need to be performed. Meiotic spindles can be visualized under light microscopy and no signal was observed in these structures for Spag5. Since Spag5 appeared to bind to microtubules *in vitro*, it was apparent that this possible function of Spag5 was utilized in a different environment, possibly in somatic cells. There have been many documented cases where a protein is involved both in mitotic spindles and meiotic spindles, both in spermatogenesis and oogenesis. However, there have also been cases where a protein has been necessary for mitotic spindle assembly and function, but has not been crucial for meiotic spindle assembly and function. Most studies to date on meiosis have been performed using the female model in many different species due to the ability to isolate and manipulate oocytes. One example of a protein which is essential for both meiotic and mitotic spindle assembly and function is MAPK (p42 mitogen-activated protein kinase). MAPK has been found to be essential for progression through meiotic M phase in Xenopus oocytes and also to be essential in maintaining the mitotic state (Guadagno and Ferrell, 1998).One interesting protein, PPH-4.1 (protein phosphatase 4.1), has been found to be required for the formation of spindles in mitosis and sperm meiosis in Caenorhabditis elegans. Also, besides promoting spindle formation, PPH-4.1 appears to play a role in either the establishment or the maintenance of chiasmata during meiotic prophase I. However, this phosphatase was apparently dispensable for female meiotic divisions, which do not depend on centrosomes (Sumiyoshi *et al*, 2002). Most of the work done on meiosis in spermatogenesis has not been performed in mammals, due to the difficulty in working with male germ cells and the results found in female systems can not always be applied to spermatogenesis. Male sperm cells can be isolated, but they

cannot be maintained in culture for more than a couple days. So, while it appears that Spag5 does not localize to the meiotic spindle of the rat, further work would need to be performed to verify this observation.

4.c *The role of spag5 in somatic cells*

The original Spag5 protein that we worked with was found to be 73% similar to the human non-motor mitotic spindle protein, astrin. The full length spag5 was found to be similar to astrin. Due to this similarity and the fact that Spag5 binds microtubules *in vitro*, it was hypothesized that Spag5 is the rat homolog of the human astrin. Even though the full length Spag5 was found to be more similar to astrin than the shorter Spag5, the amino terminal sequence of Spag5 did not match astrin. Spag5 comes from rat chromosome 10 and consists of 31 exons, while astrin comes form the human chromosome 17 and consists of 24 exons. Since Spag5 has more exons, the amino terminus of Spag5 contains more sequence than astrin and therefore would not be expected to match astrin in the amino terminus.

Using immunofluorescence, it was determined that Spag5 colocalizes with astrin in dividing IEC-18 rat cells, specifically in the mitotic spindle and also in the cytoplasm of interphase cells. This colocalization however, was not 100% and there was some astrin signal visualized that was separate from Spag5 signal. The punctate cytoplasmic staining found for both Spag5 and astrin in interphase cells has been demonstrated many times before (Mack and Compton, 2001; Gruber *et al*, 2002; Chang *et al*, 2003). Colocalization experiments revealed that this cytoplasmic staining matched that of ER staining. During interphase, the ER is closely associated with cytoplasmic microtubules and at the time of

nuclear envelope breakdown, this association diminishes and the ER dissociates with microtubules. It is possible that the cytoplasmic staining of Spag5 represents its association with microtubules, and not the ER directly. This hypothesis would have to be investigated further for verification.

The IF results for both Spag5 and astrin were supported by the protein analysis of Spag5 and astrin. In western blots of rat sperm tails and rat testis protein, many bands detected were similar between Spag5 and astrin, but astrin antibodies specifically detected more bands than Spag5. There are several explanations for these results. First, Spag5 polyclonal antibody was affinity purified on MBP-Spag5 protein while the Astrin polyclonal antibody was not affinity purified. This could account for the Astrin antibody detecting more protein bands than Spag5 and for detecting more protein in IEC-18 cells. Analysis of the protein sequences of Spag5 and astrin shows a difference in the amino terminal sequences which could account for the differing protein patterns in western blots and immunofluorescence. Astrin is documented as a 134 kDa protein, while Spag5 has been published as a 200 kDa protein. Both Spag5 and Astrin antibodies detected various protein bands of various sizes, however, no bands of either 134 kDa or 200 kDa were detected. However, protein bands close in size to 134 kDa and 200 kDa were detected and it is possible that the molecular weights of these proteins as estimated in gels were inaccurate. There were many other bands detected by both Astrin and Spag5 antibodies of varying sizes. It is possible that these antibodies are detecting proteins that are related to the Spag5/Astrin family. However, due to the large number of exons in both the Astrin and Spag5 genes, it is possible that these varying protein bands are alternatively spliced products of these genes. Another result that supports this possibility is the RT-PCR. In

many of the tissues tested for the presence of a Spag5 mRNA, the expected band size was detected, as well as other smaller products, supporting the possibility of alternatively spliced Spag5 products. One other possibility is that these smaller protein bands are processed products of the larger protein bands. Analysis of western blots of rat sperm tails and rat testis protein shows there are various protein bands detected by both Astrin and Spag5 antibodies in rat testis protein. However, in sperm tail protein, Spag5 only detects one band, and Astrin detects 3 bands. These proteins were both also detected in rat testis protein, leading to the hypothesis that these products are processed after translation in spermatocytes and round spermatids. A similar banding pattern was also identified between western blots of IEC-18 microtubules and Spag5 and Astrin testis immunoprecipitations, with protein bands of sizes similar to the rat testis and sperm tail western blots. Spag5 antibody was used to immunoprecipitate proteins from rat total testis protein and was then blotted with Astrin antibody. The opposite experiment was also performed. Both blots generated the same bands, leading to the conclusion that Spag5 and Astrin are the same proteins.

Since both Astrin and Spag5 colocalize to mitotic spindles and Spag5 binds microtubules *in vitro*, it was of interest to investigate whether Spag5 is binding microtubules in IEC-18 cells. Microtubules were isolated from IEC-18 cells and subjected to western blotting. Both Spag5 and Astrin were found to bind to microtubules. Spag5 antibodies detected one band of ~54 kDa in the microtubule extract, while Astrin detected many different bands. One possible explanation for this is that the Astrin antibody was not affinity purified. Spag5 antibodies detect many proteins in testis but only basically one in IEC-18 cells and one in rat sperm tails. Therefore, it is possible that

not all forms of Spag5 can or do bind to microtubules. All of this data points to the conclusion that Astrin is the human homolog of Spag5. Astrin has been published as a non-motor mitotic spindle protein, even though structural analysis of Astrin dimers resembles that of motor proteins. However, sequence analysis did not reveal any homology to motor domains, which have a well characterized and conserved protein module. Astrin has an alpha-helix content of 55% (elucidated by purified recombinant astrin protein) with a prominent globular head and a rod domain with a flexible hinge (determined by electron microscopy)(Gruber *et al*, 2002). The model proposed by Gruber *et al*, is that astrin forms parallel dimers via its alpha-helical coiled coil domains. Electron micrographs of recombinant Astrin in PBS reveal that astrin dimers associated into higher order structures of two to five dimers. Oligomerization was exclusively mediated by the head domains and higher oligomers resembled astral structures. The hypothesis is that Astrin may provide a scaffold for crosslinking regulatory and structural components at the mitotic spindle. Spag5 and Astrin are not 100% homologous, which leads to the question of whether Spag5 has the same structure as Astrin. One possible further direction would be to create a full length recombinant Spag5 protein for purification.

RNAi was used to silence Astrin in HeLa cells which caused the cells to arrest and become apoptotic. These cells also showed a phenotype with highly disordered spindles and chromosomes which did not congress to the spindle equator and remained dispersed (Gruber *et al*, 2002). In order to determine a possible function for Spag5, a mouse knockout was made, but these mice exhibited no phenotype(Xue *et al*, 2002). At the time the knockout was made, the full Spag5 gene was unknown. At the time, it was thought that the function of Spag5 may have been compensated for by another protein.

However, with the current discovery of the full length Spag5 gene, which consists of 31 exons, it is possible that the lack of phenotype in the knockout mice was due to the fact that not enough of the gene was knocked out and a Spag5 protein that contained functional motifs was still translated. With the current knowledge of the function of Astrin, it is possible that a full Spag5 knockout would not produce viable offspring (embryonic lethality) due to its likely role in mitosis and therefore a knockout mouse would not be worthwhile to pursue.

CHAPTER 5: 1017 AND 1038 RESULTS

5.a *1038 is a chimeric RNA*

Two cDNA clones had originally been isolated from a rat testicular library using an antibody that was raised against two proteins, FS14 and ODF14 in the laboratory of Dr. Richard Oko (Queen's University). These two cDNA clones were designated 1038 and 1017 respectively. FS14 and ODF14 are both approximately 14 kDa and share an identical amino terminal sequence. FS14 and ODF14 are major proteins of the fibrous sheath (FS) and outer dense fiber (ODF) structures. The ODF and FS are the structures which distinguish the sperm tail from a simple flagella. So, in order to determine the functions of these two structures, it is important to characterize all of their components (one example of which is the ODF-associated protein Spag5/Astrin). It was hypothesized that the 1038 and 1017 cDNAs encode FS14 and ODF14 respectively, but this needed to be verified. The 1017 sequence was found to be 100% homologous with ornithine decarboxylase antizyme 3 (Ivanov *et al*, 2000). This gene is localized to rat chromosome 2 and consists of 5 exons. However, the 1038 sequence was highly unusual. The amino-terminus of 1038 is identical to 1017 (first 2 exons of 1017 gene), so therefore was localized to rat chromosome 2 (189,360,686-189,359,911 bp). However, the carboxy-terminus of 1038 was found to localize to rat chromosome 4 and apparently contained no introns (61,713,543-61,714,042 bp). Using BLAST, no homologous sequence in mouse was found for this chromosome 4 region, however a homologous mouse gene was identified for the 1017 sequence.

5.b *1017 and 1038 are testis-specific mRNAs*

In order to prove that 1017 and 1038 indeed represent cDNAs of real mRNAs and not cloning artifacts, RT-PCR and Northern blotting was performed. Total rat testis RNA was isolated and used in RT-PCR reactions. The same 5' primer was used for both 1017 and 1038 with different 3' primers for each of them. Both 1017 and 1038 mRNAs were detected in total testis (Figure 20). Northern blotting was also performed using both rat and mouse RNA to verify the RT-PCR results and to also determine whether the C-terminal sequence of rat 1038 (chromosome 4 sequence) exists in mouse mRNA. Total RNA was isolated from the testis of rat and mouse and run on a gel, transferred to PVDF membrane and probed with double-stranded probes made by PCR to the common region of 1017 and the uncommon C-terminus of 1038 (Figure 21, top panel). It was found that both probes detected an RNA transcript of approximately 1 kb in both rat and mouse. The band detected in mouse with the 1038 probe was very faint, leading to the conclusion that the sequence does exist at the RNA level (and therefore the genomic level) but that the sequence has diverged compared to the rat sequence. Both Northern blots were exposed to film for the same amount of time (24h) however the C-terminal 1038 Northern in rat was fainter than for the amino terminal Northern. The common region probe could be detecting two different RNAs (1017 and 1038) while the uncommon C-terminus of 1038 could be detecting only the 1038 RNA, which could account for the difference in signal intensity. The size of the transcripts detected is approximately the same size as the transcripts detected previously using the whole 1017 and 1038 sequences as probes (Lawson, 1998).

5.c *Radiation Hybrid Mapping*

In order to verify the unusual finding of a real chimeric mRNA consisting of sequences from two different genes on two different chromosomes, radiation hybrid mapping was performed on both the amino-terminal sequence of 1038 (localized to rat chromosome 2 by bioinformatics and identical to the amino terminus of 1017) and the carboxy-terminal sequence of 1038 (localized to rat chromosome 4 by bioinformatics). Radiation hybrid mapping was performed on hamster cells that were irradiated and contain rat chromosomes. Since hamsters and rats are highly related, gradient PCR was performed to establish conditions where the unique 1038 sequences were detected in rat, but not in hamster, in order to detect the specific rat chromosome location and not the hamster chromosome location (Figure 22). For both primer sets, an annealing temperature of 65^{o}C generated a specific band in rat, but not in hamster. Once these conditions were determined, radiation hybrid mapping was performed, using the optimized PCR conditions. The two primer sets were linked to rat genomic markers and these results are depicted in figure 23. Radiation hybrid mapping verified the results of blast searches for 1038 and confirmed that 1038 was a chimeric cDNA containing sequences from two different genes localized on two different chromosomes in rat (Figure 23). Both the lod and theta scores of the genetic markers demonstrated a statistically significant linkage with both PCR products for 1017 and 1038. The genetic locations for all the genetic markers identified were close in genomic location to the BLAST search results for both 1017 and 1038.

Figure 20: RT-PCR was performed on total testis RNA using a primer specific to both 5’ 1017 and 1038 and then a specific 3’ primer for both clones. Lanes a and b show PCR using the same primers on two different testis RNA preps. Lane c is the negative control using the same primers with no cDNA. PCR generated a fragment for both 1017 and 1038 and these PCR fragments were sequenced to verify their identity. RT-PCR verifies the existence of both 1017 and 1038 at the mRNA level, which in turn verifies the existence of a chimeric mRNA from different genes on different chromosomes (1038). This experiment was repeated numerous times.

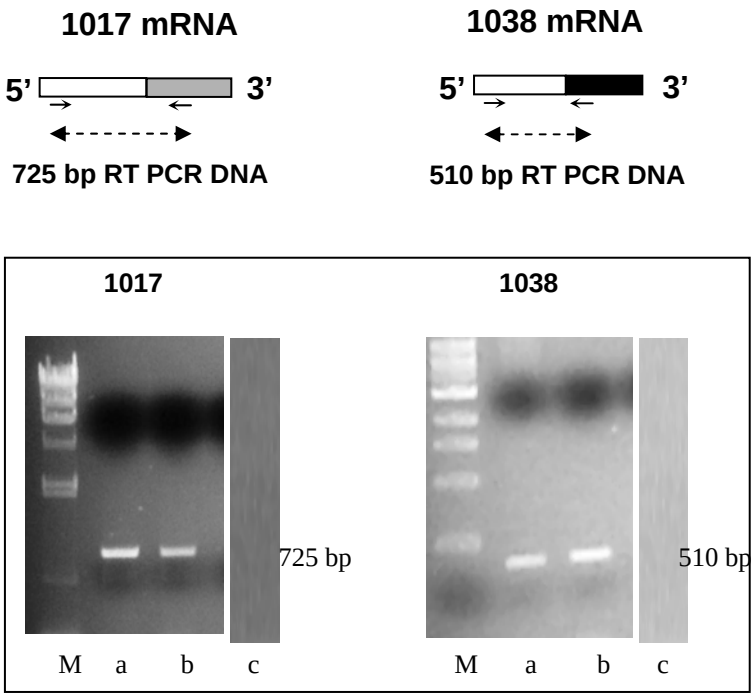
1017 mRNA
5'
3'
725 bp RT PCR DNA
1038 mRNA
5'
3'
510 bp RT PCR DNA
1017
1038
725 bp
510 bp
M a b c
M a b c

Figure 21: Northern blotting of total rat and mouse testis RNA was performed using two different probes, one homologous to the common region of 1017 and 1038 and one homologous to the unique region of 1038. Both probes detected an mRNA of approximately 1 kb in both rat and mouse. The blots were exposed to Kodak X-OMAT AR X-ray film at -70^{o}C for 24 hours. R-rat RNA, M-mouse RNA.

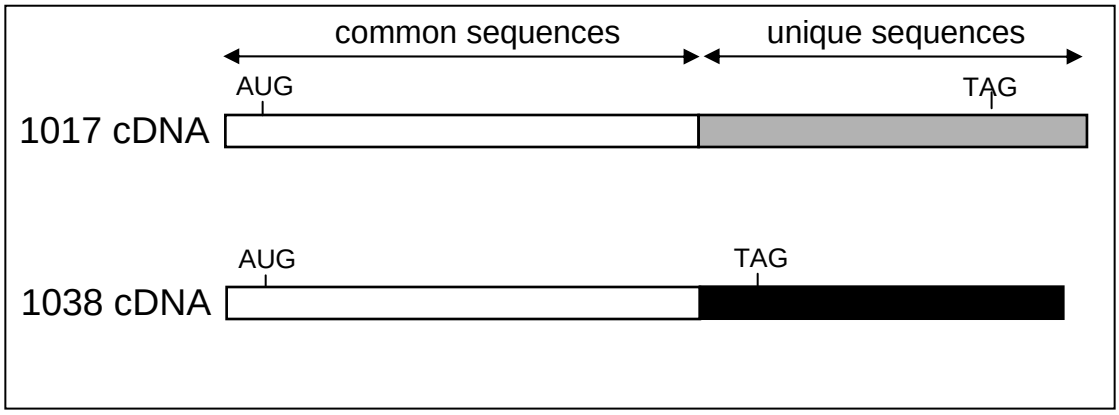
common sequences
unique sequences
AUG
TAG
1017 cDNA
AUG
TAG
1038 cDNA

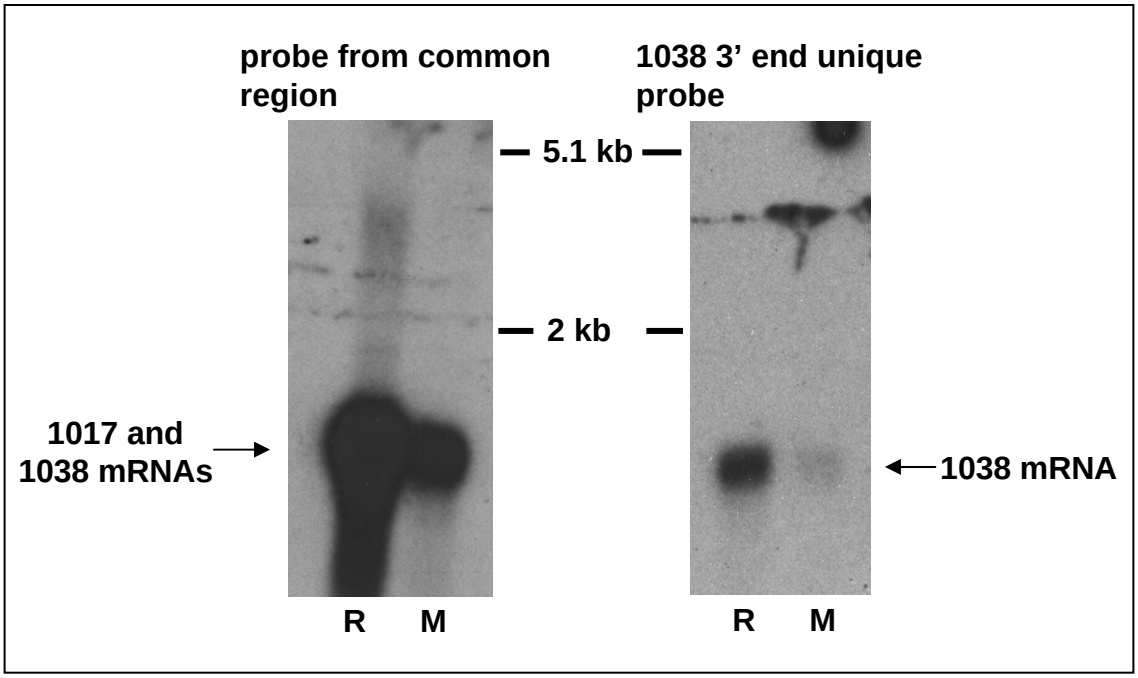
probe from common region
1038 3' end unique probe
5.1 kb
2 kb
1017 and 1038 mRNAs
1038 mRNA
R
M
R
M

5.d *Unique 1038 sequences derive from a larger transcription unit on rat chromosome 4*

Our results show that the 1038 mRNA derives from sequences on rat chromosomes 2 and 4. To learn more about the transcription unit on chromosome 4, we carried out RT-PCR experiments using nuclear RNA from spermatids. Nuclear RNA was isolated from elutriated spermatids and used in RT-PCR. The same 3' primer used for the previous RT-PCR for 1038 was used as well as a primer designed to the chromosome 4 genomic sequence, further upstream than the sequence known to be included in the 1038 transcript (Figure 24, top panel). A band was detected in elongating spermatids nuclear RNA (Figure 24, lane 1), leading to the conclusion that a chromosome 4 transcript exists. The use of an upstream 5' primer in a region not present in the mature 1038 mRNA shows that the chromosome 4 transcription unit is larger than the sequence included in the 1038 chimeric transcript. Since a larger chromosome 4 RNA exists in the nucleus compared to the chromosome 4 sequence included in 1038, there may be processing and/or recombination events in the nucleus. These results are depicted in figure 24.

5.e *FS14 and ODF14 Protein Analysis*

To attempt to correlate the FS14 and ODF14 proteins, total ODF and FS fractions were run on a 10%-20% gradient gel, stained with Coomassie brilliant blue dye and the 14 kDa bands were excised from each fraction. These bands were treated as described previously and subjected to MALDI-TOF and MS/MS analysis. These results are depicted in figure 25. As the table indicates, all of the peaks identified and sequenced matched to the amino terminus of both proteins. Therefore, no peaks were identified that matched the carboxy terminus of either protein. This could be because the proteins are

Figure 22: Gradient PCR was performed on both rat and hamster genomic DNA using 1017 and 1038 specific primers. Two primers specific to the 5' end of both 1017 and 1038 were used, (panel B) and two primers specific to the uncommon 3' end of 1038 (panel A) were used in PCR using an annealing temperature gradient from 45^{o}C-65^{o}C. Gradient PCR was performed in order to determine the annealing temperature needed to generate one band in rat genomic DNA with no bands generated in hamster DNA. For both primer sets (panels A and B) an annealing temperature of 65^{o}C generates one band for both primer sets with rat DNA and no bands with hamster DNA. All PCR reactions were cycled 35 times.

A.

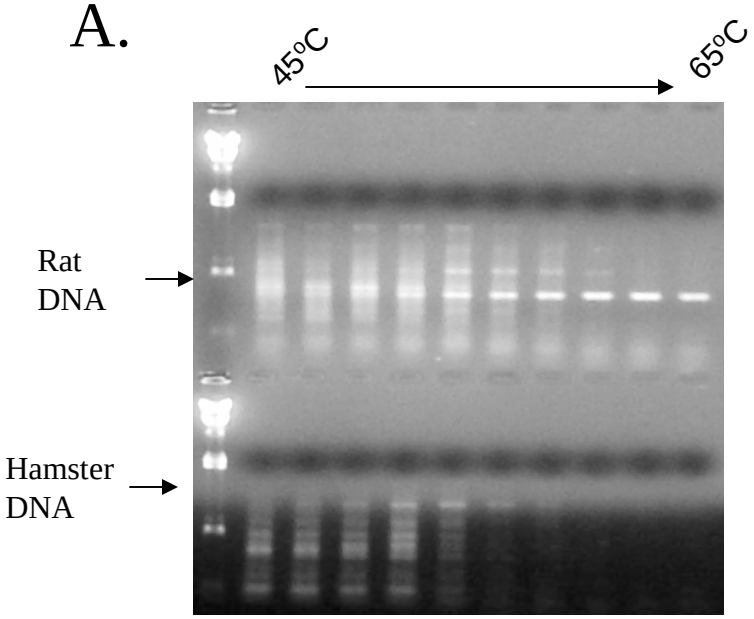

Unique 1038
sequence

B.

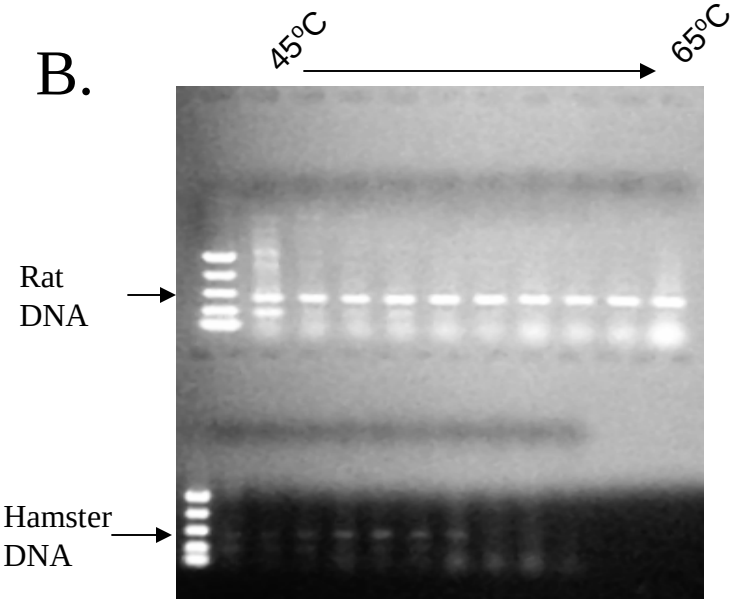

Common 1017/1038
sequence

Figure 23: Radiation hybrid mapping was performed using two primer sets complimentary to the common 5'end of 1017 and 1038 and to the uncommon 3'end of 1038. The T55 panel (hamster/rat hybrids) was screened using these primers in genomic PCR. Both primer sets generated fragments between 300-400bp which were then linked to rat genomic markers. The genomic location for the markers found to be linked to the PCR fragments are listed as follows: D4Rat22 – 65,021,998-65,022,162 bp (Chr.4); D4Rat20 – 63,712,339-63,712,478 bp (Chr.4); D4Rat96 – 69,506,218-69,506,315 bp (Chr.4); D4Got39 – 60,967,856-60,967,954 bp (Chr.4); D2Rat134 – 78,809 900 bp (Chr.2); D2Mgh9 – 191,340,897-191,341,025 bp (Chr.2); D8Got54 – 185,780,460-185,780,686 bp (Chr.2); D2Rat21 – 75,734,560-75,734,672 bp (Chr.2). The theta scores are the recombination frequencies with a 0 value meaning that the genes are linked and a maximum value of 1.0 meaning that the genes are not linked. The lod scores are the logarithm of the odds of genetic linkage. If there is a lod score of 3 or higher, the odds are 1000 to 1(or higher) in favour of a genetic linkage. All of the genetic markers detected in this experiment showed a statistically significant linkage with the two PCR products being tested as also demonstrated by the genomic location of the markers compared with the genomic locations of 1017 and 1038 as found with BLAST.

Radiation Hybrid Mapping Results

4.020-D4Rat22 theta = 0.083 lod = 8.132

4.019-D4Rat20 theta = 0.247 lod = 7.816

4.021-D4Rat96 theta = 0.321 lod = 6.681

4.018-D4Got39 theta = 0.414 lod = 4.970

Results for 3' end of 1038 (unusual region localized to chromosome 4)

2.039*-D2Rat134 theta = 0.299 lod = 7.558

2.040-D2Mgh9 theta = 0.471 lod = 5.001

8.022-D8Got54 theta = 0.467 lod = 4.980

2.022-D2Rat21 theta = 0.494 lod = 4.455

Results for 5' end of both 1017 and 1038 (common region localized to chromosome 2

quite small and any tryptic peptides produced in the C terminus were just not detected because of the small amount of peptide. MS/MS also detected a possible phosphorylation in the peptide SRPSLYSLSYIKR in one of the S/Y amino acids. Therefore, no peptides were identified which matched either FS14 or ODF14 to either 1017 or 1038. Further protein work would need to be completed. Amino terminal sequencing also identified that the start codon is a CTG, as opposed to the common ATG start codon (personal communication from Dr. Richard Oko). In a paper published on ornithine decarboxylase antizyme 3 (Ivanov *et al*, 2000), the authors identified the start codon to be a methionine further downstream from our proposed start codon, which is actually the first methionine in the sequence.

Figure 24: RT-PCR was performed on nuclear RNA isolated from spermatids and spermatocytes. In order to investigate the possibility of a larger chromosome 4 RNA than the sequence that is included in the 1038 sequence, a primer was designed further upstream on the chromosome 4 genomic sequence. Since this region is predicted to have no introns, an arbitrary location approximately 100bp further upstream from the 1038 junction site was chosen for primer design and location, called prom1038. Prom1038 and pr438 generated a PCR product in rat spermatid nuclear RNA, but not spermatocyte nuclear RNA (lane 1). 35 cycles of PCR were performed. A positive control PCR reaction was performed with primers located inside the 1038 chromosome 4 sequence (lane 3). Negative control RT-PCR reactions were performed for both primer sets using no reverse transcriptase (lanes 2 and 4).

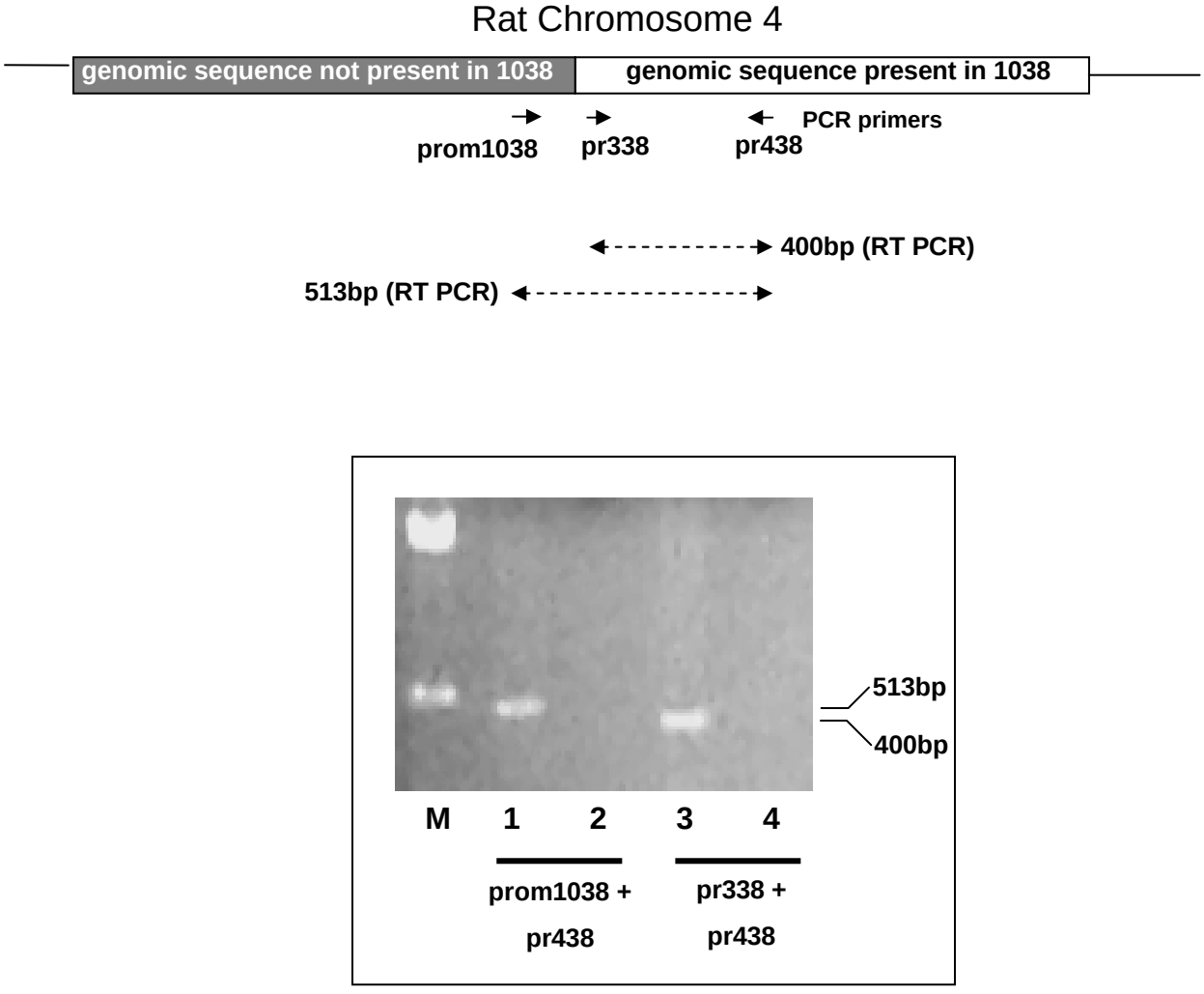
Rat Chromosome 4
genomic sequence not present in 1038
genomic sequence present in 1038
prom1038
pr338
pr438
PCR primers
400bp (RT PCR)
513bp (RT PCR)
513bp
400bp
M
1
2
3
4
prom1038 + pr438
pr338 + pr438

Figure 25: Mass spectrometry results for FS14 and ODF14. The peptides identified and sequenced match the amino terminus of both proteins. Note that one peptide, SRPSLYSLSYIKR contains a phosphorylation site at one of the S/Y positions.

Peptide Mass	Matched Sequence	Comments
951.31	mLPCCYR	fragment of 1015.23
999.25	MLPCCYR	
1015.23	mLPCCYR	oxidized form of 999.25, M oxidation
1208.60	EKmLPCCYR	M oxidation, fragment of 1272.37 which is the oxidized form of 1256.42
1413.62	SRPSLYSLSYIK	
1493.70	SRPSLYSLSYIK	phosphorylated form of 1413.62, one of the S/Y is phosphorylated
1551.86	SRPSLYSLSYIKR	fragment of 1649.76
1569.77	SRPSLYSLSYIKR	
1649.76	SRPSLYSLSYIKR	phosphorylated form of 1569.77, one of the S/Y is phosphorylated

CHAPTER 6: 1017 AND 1038 DISCUSSION

6.a *1017 and 1038 Summary*

1017 and 1038 were originally identified through the screen of a rat testicular library using an antibody that was specific to the ODF14 and FS14 proteins. ODF14 and FS14 share an identical amino terminal sequence, but have unshared epitopes. Blast searches revealed that the 1017 clone was 97% homologous to the mouse ornithine decarboxylase antizyme 3 gene which is found on rat chromosome 2. Blast searches of the 1038 clone revealed that the amino terminal sequence of 1038 localized to the first two exons of the ornithine decarboxylase antizyme 3 gene and the carboxy terminal sequence localized to an intronless gene on rat chromosome 4. In order to verify these results, RT-PCR, genomic PCR and radiation hybrid mapping were performed. These procedures confirmed that 1038 is a chimeric mRNA consisting of sequences from rat chromosomes 2 and 4. In order to determine if 1017 and 1038 encode FS14 and ODF14, mass spectrometry was performed on isolated coomassie stained bands for both proteins. Sequence analysis was performed on major peptides and sequence information was obtained. However, only sequence information was obtained for the amino terminus of both proteins (which is identical for FS14 and ODF14) so they were not distinguished.

6.b *1017 is homologous to mouse ornithine decarboxylase antizyme 3*

Of the two clones isolated from a rat testicular library, BLAST searches only revealed a homologous sequence for 1017. The 1017 cDNA was found to be 97% homologous to mouse ornithine decarboxylase antizyme 3 (OAZ3). OAZ3 is the third

antizyme characterized, the first two being OAZ1 and OAZ2. There is more information on OAZ1 and OAZ2 which are known to inhibit ornithine decarboxylase (ODC). Spermine is synthesized from spermidine for which the precursor is putrescine, which in turn comes from the decarboxylation of ornithine. ODC is in low abundance in mammals and is found in many different tissues. OAZ1 binds to it and inactivates it and targets it for degradation by the 26S proteosome without ubiquitination (Murakami *et al,* 1992 and Tokunaga *et al,* 1994). ODC mRNA and protein are present at some level in all testicular cells (Leydig, Sertoli, spermatogenic cells, etc.), but the levels of expression vary greatly. Several studies have shown that ODC expression during sperm development increases sharply (from earlier background levels) and peaks in late pachytene spermatocytes and early round spermatids (Kaipia *et al*, 1990 and Blackshear *et al*, 1989). Antizyme 3 mRNA expression is maximal during the middle and late stages (stages VIII through XII) of spermatid development, and then it disappears again in the mature spermatozoa. Most of the signal detected for OAZ3 mRNA was localized to the lumen of the seminiferous tubule, which is where the elongating tails project before the spermatids are completely released. Ivanov *et al*, did not investigate the localization of OAZ3 protein. The only work on OAZ3 protein was done by Tosaka *et al* (2000) where they produced a GFP-OAZ3 fusion protein and expressed it in hamster CHO cells. The expressed protein was found to be approximately 22 kDa. No work was done on endogenous OAZ3 protein. A study done by Lawson, (1998) on the proteins FS14 and ODF14 contains immunocytochemistry of rat seminiferous epithelium using an antibody to FS14 and ODF14 which was the same antibody used in the rat testicular library screen that pulled out the 1017 and 1038 cDNAs. The staining pattern for immunocytochemistry

is similar to the *in situ* study done on OAZ3 by Ivanov *et al*, 2000. Developmental Northern blots performed by Lawson found that 1017 and 1038 RNAs were both testis-specific and were both found to be expressed first in round spermatids with signal increasing until elongating spermatids. These results match those of the *in situ* hybridization experiments by Ivanov *et al*, 2000. It appears that the antizyme 3 wave of expression follows the wave of high ODC expression during spermatogenesis. This pattern of expression of the two genes implies that the physiological role of antizyme 3 is to quickly ‘‘extinguish’’ (prevent overaccumulation of) ODC activity after the stage at which ODC plays its role in spermatogenesis, most likely late spermatocytic/early spermatidal phase (Ivanov *et al*, 2000). OAZ1 and OAZ2 are least expressed in the testis compared with all the other tissues tested, while OAZ3 is only expressed in testis. It appears that OAZ3 is therefore important in regulating ODC in spermatogenesis, specifically in spermiogenesis (Ivanov *et al*, 2000). Interestingly, all three OAZs contain a frameshift of +1 in translation. All three sequences are similar with the most similarity in the second frame (after the frameshift). Since 1017 is almost completely homologous to OAZ3, it also contains this +1 translational frameshift. Analysis of the 1038 cDNA reveals that its homology with 1017 also includes this frameshift and the sequences of 1017 and 1038 actually diverge just past this frameshift site. This frameshift site occurs at a putative stop codon in OAZ3, 1017 and 1038. Analysis of the putative ORFs of both 1017 and 1038 reveal that if the stop codon is recognized instead of the frameshift, then both encoded proteins would be much smaller than 14 kDa (estimated size of FS14 and ODF14 by SDS-PAGE). Therefore, we predict that this frameshift in translation occurs in both possible proteins encoded by 1017 and 1038. The molecular weights and sequences

of FS14 and ODF14 will be discussed in the next section. Ivanov *et al*, predict the start codon for OAZ3 to be a methionine further downstream from our proposed start codon which would make sense since it is the first methionine in the sequence. However amino terminal sequencing of both FS14 and ODF14 (performed in the lab of Dr.Richard Oko, Queen's University), revealed that the protein starts further upstream, at the codon AUG.

6.c *1017 ORF predicts a protein of 28 kDa*

Interestingly, since 1017 contains the same frameshift site as OAZ3, the open reading frame (ORF) of 1017 would encode a protein of approximately 28 kDa. However, both FS14 and ODF14 run at approximately 14 kDa on SDS-PAGE. One explanation for this discrepancy could be that the 1017 gene has different spliced variants which are either the FS14 or the ODF14. However, a 28 kDa 1017 protein has never been identified, but the OAZ3 protein is predicted to be 22 kDa, but this protein size has never been identified in endogenous protein. The 22 kDa OAZ3 protein product was translated from a start codon further downstream from the start codon we propose, which would account for the discrepancy between the full length OAZ3/1017 protein. The more likely explanation however is that the 14 kDa protein is a processed product of the full length 1017 28 kDa protein. This possibility leads to the idea that the 1017 gene likely encodes FS14, and not ODF14, since it has been demonstrated numerous times that FS proteins are processed before assembling in the forming sperm tail. ODF proteins have never been shown to be processed before assembling in the sperm tail. One example of a processed FS protein is p82 (mentioned in the introduction). P82 is first synthesized as a precursor

protein of approximately 92 kDa (840 amino acids) but the mature form of the protein is 72 kDa (Carrera *et al*, 1994). One other example of a processed FS protein is TSGA10, a FS protein in humans which is not expressed in testes of two infertile patients. TSGA10 encodes a spermatid protein of approximately 65 kDa which is processed to a 27 kDa protein in the FS (Modarressi *et al*, 2004). Mass spectroscopy did not result in the designation of one cDNA with either FS14 or ODF14, so the possibility that the 1017 mRNA encodes FS14 would need to be further investigated. Analysis of the 1038 ORF reveals that it would encode a protein of approximately 16 kDa. On SDS-PAGE, both FS14 and ODF14 appear to run at approximately 14 kDa, which is an approximation and could actually be 16 kDa. The exact molecular weight of FS14 and ODF14 could be determined by mass spectroscopy and is a possible further direction for this project.

6.d *1038 is a chimeric RNA*

The amino terminus of 1038 is homologous to 1017 and is derived from the first two exons of the ornithine decarboxylase antizyme 3 gene on rat chromosome 2. However the carboxy terminus of 1038 was mapped to an unknown gene on rat chromosome 4. This unusual result had to first be verified by RT-PCR and northern blotting to determine that 1038 was indeed an intact RNA and not a cloning artifact from the testicular library. After verifying the existence of the 1038 RNA, it was hypothesized that 1038 was the result of a trans-splicing event, however, sequence analysis revealed no known splice sites within the 1038 genomic sequence. It is possible that trans-splicing does occur to produce the 1038 mRNA, however this would be via an unknown splice site. A 3’ consensus splice site (CAGG) exists in the overlapping junction between the

chromosome 2 and 4 transcripts, however, no consensus 5’ splice site exists due to the lack of a T in the sequence, which occurs in most 5’ splice sites. One other possibility is that the 1038 RNA is produced by a recombination event. Analysis of the 1038 sequence did not reveal any known recombination sites, however, RNA recombination is not a well characterized event. Trans-splicing also is not a well characterized event in mammalian systems, and the cases that are known are mostly concerning the splicing of RNAs from two different genes on the same chromosome. There are two published cases in mammalian systems of trans-splicing occurring which results in a chimeric mRNA containing sequences from two different chromosomes. One of these examples is human acyl-coenzyme A:cholesterol acyltransferase 1 (acat1) which contains sequences from human chromosomes 1 and 7. The common form of acat1 is 50 kDa and a rare form of acat1 was discovered which contained an extra 5’ untranslated and translated region and was derived from both chromosomes 1 and 7. The rare acat1 form was found to encode a protein of approximately 56 kDa and was found to have the same function as the common acat1 form. This rare acat1 mRNA was found to form via known spliceosome motifs (Yang *et al*, 2004). The other example of transplicing involving different chromosomes in mammals is the rat Leukocyte Common Antigen-Related (LAR) tyrosine phosphatase receptor. An alternative LAR cDNA was identified with an untranslated 3’ sequence. FISH and radiation hybrid mapping demonstrated that loci encoding LAR and its alternative 3' UTR are present on distinct chromosomes. Analysis of the exon/intron sequences of this alternative LAR transcript revealed that they contain nonconsensus splice junctions along with elements known to promote both cis- and trans-splicing (Zhang *et al*, 2003). The 1038 genomic DNA sequences do not contain any

known splice sites, which is different from the rare acat1 and LAR transcripts. The other possibility already mentioned is that 1038 is produced from an RNA recombination event. One supporting piece of data for the recombination possibility is the presence of a larger RNA originating from rat chromosome 4 in the nucleus than is found in the 1038 RNA (Figure 24, lane 1). The chromosome 4 genomic sequence is predicted by BLAST to not contain introns, which makes it difficult to predict possible splicing or recombination sites. RNA recombination in mammalian systems has not been well investigated or defined. The RNA recombination events that have been investigated in mammals have involved the reverse transcription of a chimeric RNA that has been incorporated back in to the genome. In a study done by Buzdin *et al*, 2003, it was found that the human genome contains many types of chimeric retrogenes generated through *in vivo* RNA recombination. However, in our study, the 1038 RNA does not exist intact in the genome, which was verified by radiation hybrid mapping. Therefore, if RNA recombination is responsible for the formation of the 1038 RNA, then it is via unknown mechanisms. However, one interesting finding is that at the junction site between the chromosome 2 and 4 sequences in the 1038 RNA, there is an overlapping 16 nucleotides (CAGGAAAACAGCCAGC). This small sequence does not share homology with any splicing or recombination sites, however, this could be involved in the formation of the chimeric 1038 RNA. Future studies may define if recombination occurs in the nucleus or cytoplasm.

6.e *FS14 and ODF14 share an identical amino terminal sequence*

The amino terminal sequence of both FS14 and ODF14 was identified in the lab of Dr.Richard Oko (Queen's University) previous to the start of this study. In order to determine if the 1017 and 1038 RNAs encode FS14 and/or ODF14, mass spectrometry was performed on both proteins. The objective of the mass spectrometry experiment was to identify peptide peaks that distinguish between FS14 and ODF14, which are located in the carboxy termini. The results of mass spectrometry revealed peptide sequences only for the amino termini of FS14 and ODF14 which verified the earlier results. This was an expected result because of genomic analysis of 1017 and 1038 which revealed that both clones contain the same first two exons from the ornithine decarboxylase antizyme 3 gene on rat chromosome 2. Mass spectrometry did not generate any data for the carboxy termini of FS14 and ODF14. Possible further experiments that could be performed to determine the origin of FS14 and ODF14 will be discussed in the next section.

6.f ***Further directions and conclusions***

The original main objective for the 1017 and 1038 project was to determine if these two RNAs encode FS14 and ODF14. In the course of the study, it was found that 1017 is homologous to rat ornithine decarboxylase antizyme 3 and 1038 is a chimeric RNA consisting of sequences from rat chromosomes 2 and 4. Mass spectrometry revealed that both FS14 and ODF14 share the same amino terminal sequence (expected result) however, no peptide information was generated in the carboxy terminus of either protein. One proposed experiment to elucidate this carboxy terminus information is to digest FS14 and ODF14 with carboxypeptidase and submit these samples for MALDI-TOF analysis. This experiment could generate differing amino acid information for FS14

and ODF14. One other possibility is to generate an antibody to a peptide region that differs between the deduced amino acid sequences from 1017 and 1038 which can be used in western blotting and electron microscopy (in progress). Also, as was mentioned previously, the exact molecular weights of FS14 and ODF14 could be determined using mass spectroscopy.

The 1038 RNA was determined to be a chimeric RNA, however the mechanism of how 1038 is formed is still unknown. It was determined from RT-PCR of spermatid nuclear RNA that the chromosome 4 sequence of 1038 could actually generate a larger transcript (Figure 24, lane 1). The size of the larger full length chromosome 4 transcript is unknown and it is of interest to know if this transcript encodes another protein, apart from FS14 or ODF14. Northern blotting of rat and mouse testis RNA revealed that the chromosome 4 sequence from 1038 detected an RNA of approximately 1 kb, which was the same size of RNA detected by the chromosome 2 sequence from 1038 (Figure 21). If the larger chromosome 4 transcript encodes another protein in testis, it would be expected that Northern blotting would have revealed another RNA band unless it is the same size as the 1038 RNA. Using 5'RACE, it would be possible to determine the full size of the larger chromosome 4 transcript. Additionally, using the same primers as were used in figure 24, RT-PCR could be performed on spermatid cytoplasmic RNA to determine whether the larger transcript exists only in the nucleus. If it exists only in the nucleus, then it likely is processed into 1038 and the larger transcript does not encode another protein since the recombination or splicing event that produces the 1038 RNA would occur in the nucleus and not the cytoplasm. However, if the larger chromosome 4 transcript exists in the cytoplasm, then it could likely encode another protein.

In conclusion, we determined the origin of the 1017 and 1038 RNAs, however, it is still unclear which proteins they encode, which could be FS14 and ODF14. The 1038 RNA is a chimeric RNA containing sequences from rat chromosomes 2 and 4. Our original hypothesis was that FS14 and ODF14 were alternatively spliced products of the same gene, due to their identical amino terminal sequence, however our results refute this possibility. If 1017 and 1038 encode FS14 and ODF14, then 1017 and 1038 are separate RNAs and therefore are not alternatively spliced products of the same gene.

References Listed

Alexandropoulos K, Cheng G, Baltimore D. Proline-rich sequences that bind to Src homology 3 domains with individual specificities. Proc Natl Acad Sci U S A. 1995; 92(8): 3110-4.

Baltz JM, Williams PO, Cone RA**.** Dense fibers protect mammalian sperm against damage. Biol Reprod 1990; 43(3): 485-91.

Banks JD, Heald R. Chromosome movement: dynein-out at the kinetochore. Curr Biol. 2001; 11(4): R128-31.

Blackshear PJ, Manzella JM, Stumpo DJ, Wen L, Huang JK, Oyen O, Young WS 3rd. High level, cell-specific expression of ornithine decarboxylase transcripts in rat genitourinary tissues. Mol Endocrinol. 1989; 3(1): 68-78.

Bunch DO, Welch JE, Magyar PL, Eddy EM, O'Brien DA. Glyceraldehyde 3-phosphate dehydrogenase-S protein distribution during mouse spermatogenesis. Biol Reprod. 1998; 58(3): 834-41.

Burfeind P, Hoyer-Fender S. Sequence and developmental expression of a mRNA encoding a putative protein of rat sperm outer dense fibers. Dev Biol 1991; 148:195-204.

Burmester S, Hoyer-Fender S. Transcription and translation of the outer dense fiber gene (Odf1) during spermiogenesis in the rat. A study by in situ analyses and polysome fractionation. Mol Reprod Dev 1996; 45(1):10-20.

Buzdin A, Gogvadze E, Kovalskaya E, Volchkov P, Ustyugova S, Illarionova A, Fushan A, Vinogradova T, Sverdlov E. The human genome contains many types of chimeric retrogenes generated through in vivo RNA recombination. Nucleic Acids Res. 2003; 31(15): 4385-90.

Carrera A, Gerton GL, Moss SB. The major fibrous sheath polypeptide of mouse sperm: structural and functional similarities to the A-kinase anchoring proteins. Dev Biol. 1994; 165(1): 272-84.

Carrera A, Moos J, Ning XP, Gerton GL, Tesarik J, Kopf GS, Moss SB. Regulation of protein tyrosine phosphorylation in human sperm by a calcium/calmodulin-dependent mechanism: identification of A kinase anchor proteins as major substrates for tyrosine phosphorylation. Dev Biol. 1996; 180(1): 284-96.

Catalano RD, Hillhouse EW, Vlad M. Developmental expression and characterization of FS39, a testis complementary DNA encoding an intermediate filament-related protein of the sperm fibrous sheath. Biol Reprod. 2001; 65(1): 277-87.

Chang MS, Huang CJ, Chen ML, Chen ST, Fan CC, Chu JM, Lin WC, Yang YC. Cloning and characterization of hMAP126, a new member of mitotic spindle-associated proteins. Biochem Biophys Res Commun 2001; 287:116-121.

Clermont Y. Renewal of spermatogonia in man. American Journal of Anatomy 1966; 118: 509.

Clermont Y, Oko R, Hermo L. Immunocytochemical localization of proteins utilized in the formation of outer dense fibers and fibrous sheath in rat spermatids. An electron microscope study. Anat Rec 1990; 227: 447-457.

Compton DA. Spindle assembly in animal cells. Annu Rev Biochem 2000; 69: 95-114.

Dacheux J, Gatti JL, Dacheux F. Contribution of epididymal secretory proteins for spermatozoa maturation. Microscopy Research and Technique 2003; 61: 7-17.

Dictenberg JB, Zimmerman W, Sparks CA, Young A, Vidair C, Zheng Y, Carrington W, Fay FS, Doxsey SJ. Pericentrin and gamma-tubulin form a protein complex and are organized into a novel lattice at the centrosome. J Cell Biol. 1998; 141(1): 163-74.

Edde B, Rossier J, Le Caer JP, Desbruyeres E, Gros F, Denoulet P. Posttranslational glutamylation of alpha-tubulin. Science. 1990; 247(4938): 83-5.

Eddy EM, Toshimori K, O'Brien DA. Fibrous sheath of mammalian spermatozoa. Microsc Res Tech 2003; 61:103-115.

El-Alfy M, Moshonas D, Morales CR, Oko R. Molecular cloning and developmental expression of the major fibrous sheath protein (FS 75) of rat sperm. J Androl. 1999 Mar-Apr;20(2):307-18.

Fawcett DW. The mammalian spermatozoa. Dev Biol 1975; 44: 394.

Fawcett DW. The mammalian spermatozoon. Dev Biol 1975; 44:394-436.
Baltz JM, Williams PO, Cone RA. Dense fibers protect mammalian sperm against damage. Biol Reprod 1990; 43:485-491.

Fawcett DW, Ito S, Slautterback D. The occurrence of intercellular bridges of groups of cells exhibiting synchronous differentiation. Journal of Biophys Biochem Cytol 1959; 5: 453-460.

Fouquet JP, Kann ML, Combeau C, Melki R. Gamma-tubulin during the differentiation of spermatozoa in various mammals and man. Mol Hum Reprod. 1998; 4(12): 1122-9.

Friend KS. Spermatozoan membrane organization. Immunobiology of Gametes, Edidin M, Johnson MG, Eds. 1977; 5.

Friend KS, Fawcett DW. Membrane differentiations in freeze-fractured mammalian sperm. J Cell Biol 1974; 63(2 Pt 1): 641-64.

Fujita A, Nakamura K, Kato T, Watanabe N, Ishizaki T, Kimura K, Mizoguchi A, Narumiya S. Ropporin, a sperm-specific binding protein of rhophilin, that is localized in the fibrous sheath of sperm flagella. J Cell Sci. 2000; 113 (Pt 1): 103-12.

Fulcher KD, Mori C, Welch JE, O'Brien DA, Klapper DG, Eddy EM. Characterization of Fsc1 cDNA for a mouse sperm fibrous sheath component. Biol Reprod. 1995; 52(1): 41-9.

Garcia MA, Vardy L, Koonrugsa N, Toda T. Fission yeast ch-TOG/XMAP215 homologue Alp14 connects mitotic spindles with the kinetochore and is a component of the Mad2-dependent spindle checkpoint. EMBO J. 2001; 20(13): 3389-401.

Gandhi R, Bonaccorsi S, Wentworth D, Doxsey S, Gatti M, Pereira A. The Drosophila kinesin-like protein KLP67A is essential for mitotic and male meiotic spindle assembly. Mol Biol Cell. 2004; 15(1): 121-31.

Gruber J, Harborth J, Schnabel J, Weber K, Hatzfeld M. The mitotic-spindle-associated protein astrin is essential for progression though mitosis. J Cell Sci 2002; 115(Pt21):4053-4059.

Guadagno TM, Ferrell JE Jr. Requirement for MAPK activation for normal mitotic progression in Xenopus egg extracts. Science. 1998; 282(5392): 1312-5.

He X, Rines DR, Espelin CW, Sorger PK. Molecular analysis of kinetochore-microtubule attachment in budding yeast. Cell. 2001; 106(2): 195-206.

Hecht NB, Distel RJ, Yelick PC, Tanhauser SM, Driscoll CE, Goldberg E, Tung KS. Localization of a highly divergent mammalian testicular alpha tubulin that is not detectable in brain. Mol Cell Biol. 1988; 8(2): 996-1000.

Hirokawa N, Noda Y, Okada Y. Kinesin and dynein superfamily proteins in organelle transport and cell division. Curr Opin Cell Biol 1998; 10(1): 60-73.

Inoue YH, do Carmo Avides M, Shiraki M, Deak P, Yamaguchi M, Nishimoto Y, Matsukage A, Glover DM. Orbit, a novel microtubule-associated protein essential for mitosis in Drosophila melanogaster. J Cell Biol. 2000; 149(1): 153-66.

Irons M. Synthesis and assembly of connecting piece proteins as revealed by radioautography. J Ultrastructure Res 1983; 82: 27.

Irons M, Clermont Y. Kinetics of fibrous sheath formation in the rat spermatid. Am J Anat 1982a; 165: 121-130.

Irons M, Clermont Y. Formation of the outer dense fibers during spermiogenesis in the rat. Anat Rec 1982b; 202: 463-471.

Ivanov IP, Rohrwasser A, Terreros DA, Gesteland RF, Atkins JF. Discovery of a spermatogenesis stage-specific ornithine decarboxylase antizyme: antizyme 3. Proc Natl Acad Sci U S A. 2000; 97(9): 4808-13.

Johnson AD, Gomes WR (Editors). The testis. Academic press. Vols 1-4:1970-1977.

Joshi HC. Microtubule dynamics in living cells. Curr Opin Cell Biol. 1998; 10(1): 35-44.

Kaipia A, Toppari J, Mali P, Kangasniemi M, Alcivar AA, Hecht NB, Parvinen M. Stage- and cell-specific expression of the ornithine decarboxylase gene during rat and mouse spermatogenesis. Mol Cell Endocrinol. 1990; 73(1): 45-52.

Kim AJ, Endow SA. A kinesin family tree. J Cell Sci. 2000; 113 Pt 21: 3681-2.

Lawson V. The molecular cloning and developmental expression of two novel mRNAs encoding putative 14 kDa ODF and FS proteins of the rat sperm tail. Master of Science thesis, Queen’s University 1998.

Leblond C, Clermont Y. Definition of the stages of the cycle of the seminiferous epithelium in the rat. Annals of The New York Academy of Science 1952; 55:548-573.

Lemos CL, Sampaio P, Maiato H, Costa M, Omel'yanchuk LV, Liberal V, Sunkel CE. Mast, a conserved microtubule-associated protein required for bipolar mitotic spindle organization. EMBO J. 2000; 19(14): 3668-82.

Lewis SA, Cowan NJ. Complex regulation and functional versatility of mammalian alpha- and beta-tubulin isotypes during the differentiation of testis and muscle cells. J Cell Biol. 1988; 106(6): 2023-33.

Mack GJ and Compton DA. Analysis of mitotic microtubule-associated proteins using mass spectrometry identifies astrin, a spindle-associated protein. PNAS 2001; 98(25):14434-144439.

Maekawa H, Schiebel E. CLIP-170 family members: a motor-driven ride to microtubule plus ends. Dev Cell. 2004; 6(6): 746-8.

Manandhar G, Sutovsky P, Joshi HC, Stearns T, Schatten G. Centrosome reduction during mouse spermiogenesis. Dev Biol. 1998; 203(2): 424-34.

Mandal A, Naaby-Hansen S, Wolkowicz MJ, Klotz K, Shetty J, Retief JD, Coonrod SA, Kinter M, Sherman N, Cesar F, Flickinger CJ, Herr JC. FSP95, a testis-specific 95-kilodalton fibrous sheath antigen that undergoes tyrosine phosphorylation in capacitated human spermatozoa. Biol Reprod. 1999; 61(5): 1184-97.

Mary J, Redeker V, Le Caer JP, Rossier J, Schmitter JM. Posttranslational modifications in the C-terminal tail of axonemal tubulin from sea urchin sperm. J Biol Chem. 1996; 271(17): 9928-33.

Mei X, Singh IS, Erlichman J, Orr GA. Cloning and characterization of a testis-specific, developmentally regulated A-kinase-anchoring protein (TAKAP-80) present on the fibrous sheath of rat sperm. Eur J Biochem. 1997; 246(2): 425-32.

Messinger SM, Albertini DF. Centrosome and microtubule dynamics during meiotic progression in the mouse oocyte. J Cell Sci. 1991; 100 (Pt 2): 289-98.

Modarressi MH, Behnam B, Cheng M, Taylor KE, Wolfe J, van der Hoorn FA. Tsga10 encodes a 65-kilodalton protein that is processed to the 27-kilodalton fibrous sheath protein. Biol Reprod. 2004; 70(3): 608-15.

Morales CR, Oko R, Clermont Y. Molecular cloning and developmental expression of an mRNA encoding the 27 kDa outer dense fiber protein of rat spermatozoa. Mol Reprod Dev 1994; 37:229-240.

Mori C, Nakamura N, Welch JE, Gotoh H, Goulding EH, Fujioka M, Eddy EM. Mouse spermatogenic cell-specific type 1 hexokinase (mHk1-s) transcripts are expressed by alternative splicing from the mHk1 gene and the HK1-S protein is localized mainly in the sperm tail. Mol Reprod Dev. 1998; 49(4): 374-85.

Murakami Y, Matsufuji S, Kameji T, Hayashi S, Igarashi K, Tamura T, Tanaka K, Ichihara A. Ornithine decarboxylase is degraded by the 26S proteasome without ubiquitination. Nature. 1992; 360(6404): 597-9.

Naaby-Hansen S, Mandal A, Wolkowicz MJ, Sen B, Westbrook VA, Shetty J, Coonrod SA, Klotz KL, Kim YH, Bush LA, Flickinger CJ, Herr JC. CABYR, a novel calcium-binding tyrosine phosphorylation-regulated fibrous sheath protein involved in capacitation. Dev Biol. 2002; 242(2): 236-54.

Nakamura K, Fujita A, Murata T, Watanabe G, Mori C, Fujita J, Watanabe N, Ishizaki T, Yoshida O, Narumiya S. Rhophilin, a small GTPase Rho-binding protein, is abundantly expressed in the mouse testis and localized in the principal piece of the sperm tail. FEBS Lett. 1999; 445(1): 9-13.

Nakaseko Y, Goshima G, Morishita J, Yanagida M. M phase-specific kinetochore proteins in fission yeast: microtubule-associating Dis1 and Mtc1 display rapid separation and segregation during anaphase. Curr Biol. 2001; 11(8): 537-49.

Neilson LI, Schneider PA, Van Deerlin PG, Kiriakidou M, Driscoll DA, Pellegrini MC, Millinder S, Yamamoto KK, French CK, Strauss JF 3rd. cDNA cloning and characterization of a human sperm antigen (SPAG6) with homology to the product of the Chlamydomonas PF16 locus. Genomics. 1999; 60(3): 272-80.

Oko R. Comparative analysis of proteins from the fibrous sheath and outer dense fibers of rat spermatozoa. Biol Reprod 1988; 39:169-182.

Oko R. Occurrence and formation of cytoskeletal proteins in mammalian spermatozoa. Andrologia 1998; 30:193-206.

Oko R, Clermont Y. Light microscope immunocytochemical study of fibrous sheath and outer dense fiber formation in the rat spermatid. Anat Rec 1989; 46.

Oko R, Clermont Y. Mammalian spermatozoa: structure and assembly of the tail. In: Gagnon C (ed), Controls of Sperm Motility: Biological and Clinical Aspects. Ann Arbor, MI: CRC Press; 1990:3-28.

Oko RJ, Jando V, Wagner CL, Kistler WS, Hermo LS. Chromatin reorganization in rat spermatids during the disappearance of testis-specific histone, H1t, and the appearance of transition proteins TP1 and TP2. Biol Reprod 1996:54:1141-1157.
Parra MT, Page J, Yen TJ, He D, Valdeolmillos A, Rufas JS, Suja JA. Expression and behaviour of CENP-E at kinetochores during mouse spermatogenesis. Chromosoma. 2002; 111(1): 53-61.

Pasqualone D, Huffaker TC. STU1, a suppressor of a beta-tubulin mutation, encodes a novel and essential component of the yeast mitotic spindle. J Cell Biol. 1994; 127(6 Pt 2): 1973-84.

Pfarr CM, Coue M, Grissom PM, Hays TS, Porter ME, McIntosh JR. Cytoplasmic dynein is localized to kinetochores during mitosis. Nature 1990 May; 345(6272): 263-5.

Rechsteiner M, Rogers SW. PEST sequences and regulation by proteolysis. Trends Biochem Sci. 1996; 21(7): 267-71.

Redeker V, Levilliers N, Schmitter JM, Le Caer JP, Rossier J, Adoutte A, Bre MH. Polyglycylation of tubulin: a posttranslational modification in axonemal microtubules. Science. 1994; 266(5191): 1688-91.

Rogers S, Wells R, Rechsteiner M. Amino acid sequences common to rapidly degraded proteins: the PEST hypothesis. Science. 1986; 234(4774): 364-8.

Rosenbaum J, Moulder J, Ringo D. Flagellar elongation and shortening in chlamydomonas: the use of cycloheximide and colchicines to study the synthesis and assembly of flagellar proteins. J Cell Biol 1969; 41: 600.

Rudiger M, Plessmann U, Rudiger AH, Weber K. Beta tubulin of bull sperm is polyglycylated. FEBS Lett. 1995; 364(2): 147-51.

Sablin EP, Fletterick RJ. Coordination between motor domains in processive kinesins. J Biol Chem. 2004 Apr; 279(16): 15707-10.

Saxton WM, Stemple DL, Leslie RJ, Salmon ED, Zavortink M, McIntosh JR. Tubulin dynamics in cultured mammalian cells. J Cell Biol. 1984; 99(6): 2175-86.

Schalles U, Shao X, van der Hoorn FA, Oko R. Developmental expression of the 84-kDa ODF sperm protein: localization to both the cortex and the medulla of outer dense fibers and to the connecting piece. Dev Biol 1998: 199:250-260.

Schatten H, Schatten G, Mazia D, Balczon R, Simerly C. Behavior of centrosomes during fertilization and cell division in mouse oocytes and in sea urchin eggs. Proc Natl Acad Sci U S A. 1986; 83(1): 105-9.

Shao X, Tarnasky HA, Lee JP, Oko R, van der Hoorn FA. Spag4, a novel sperm protein, binds outer dense-fiber protein ODF1 and localizes to microtubules of manchette and axoneme. Dev Biol 1999; 211:109-123.

Shao X, Tarnasky HA, Schalles U, Oko R, van der Hoorn FA. Interactional cloning of the 84-kDa major outer dense fiber protein Odf84. Leucine zippers mediate associations of Odf84 and Odf27. J Biol Chem 1997; 272:6105-6113.

Shao X, van der Hoorn FA. Self-interaction of the major 27-kilodalton outer dense fiber protein is in part mediated by a leucine zipper domain in the rat. Biol Reprod 1996; 55:1343-1350.

Shao S, Xue J, van der Hoorn FA. Testicular protein Spag5 has similarity to mitotic spindle protein Deepest and binds outer dense fiber protein Odf1. Mol Reprod Dev 2001; 59:410-416.

Sharp DJ, Rogers GC, Scholey JM. Cytoplasmic dynein is required for poleward chromosome movement during mitosis in Drosophila embryos. Nat Cell Biol. 2000; 2(12): 922-30.

Sharp DJ, Rogers GC, Scholey JM. Roles of motor proteins in building microtubule-based structures: a basic principle of cellular design. Biochim Biophys Acta 2000; 496(1): 128-41.

Sumiyoshi E, Sugimoto A, Yamamoto M. Protein phosphatase 4 is required for centrosome maturation in mitosis and sperm meiosis in C. elegans. J Cell Sci. 2002; 115(Pt 7): 1403-10.

Tokunaga F, Goto T, Koide T, Murakami Y, Hayashi S, Tamura T, Tanaka K, Ichihara A. ATP- and antizyme-dependent endoproteolysis of ornithine decarboxylase to oligopeptides by the 26 S proteasome. J Biol Chem. 1994; 269(26): 17382-5.

Tosaka Y, Tanaka H, Yano Y, Masai K, Nozaki M, Yomogida K, Otani S, Nojima H, Nishimune Y**.** Identification and characterization of testis specific ornithine decarboxylase antizyme (OAZ-t) gene: expression in haploid germ cells and polyamine-induced frameshifting. Genes to Cells 2000; 5(4): 265.

Turner RM, Musse MP, Mandal A, Klotz K, Jayes FC, Herr JC, Gerton GL, Moss SB, Chemes HE. Molecular genetic analysis of two human sperm fibrous sheath proteins, AKAP4 and AKAP3, in men with dysplasia of the fibrous sheath. J Androl. 2001; 22(2): 302-15.

Vera JC, Brito M, Zuvic T, Burzio LO. Polypeptide composition of the rat sperm outer dense fibers. A simple procedure to isolate the fibrillar complex. J Biol Chem 1984; 259:5970-5977.

Villasante A, Wang D, Dobner P, Dolph P, Lewis SA, Cowan NJ. Six mouse alpha-tubulin mRNAs encode five distinct isotypes: testis-specific expression of two sister genes. Mol Cell Biol. 1986; 6(7): 2409-19.

Visconti PE, Johnson LR, Oyaski M, Fornes M, Moss SB, Gerton GL, Kopf GS. Regulation, localization, and anchoring of protein kinase A subunits during mouse sperm capacitation. Dev Biol. 1997; 192(2): 351-63.

Xue J, Tarnasky HA, Rancourt DE, van der Hoorn FA. Targeted disruption of the testicular SPAG5/Deepest protein does not affect spermatogenesis or fertility. Mol Cell Biol 2002; 22(7):1993-1997.

Yang L, Lee O, Chen J, Chen J, Chang CC, Zhou P, Wang ZZ, Ma HH, Sha HF, Feng JX, Wang Y, Yang XY, Wang L, Dong R, Ornvold K, Li BL, Chang TY.

Human acyl-coenzyme A:cholesterol acyltransferase 1 (acat1) sequences located in two different chromosomes (7 and 1) are required to produce a novel ACAT1 isoenzyme with additional sequence at the N terminus. J Biol Chem. 2004; 279(44): 46253-62.

Yu H, Chen JK, Feng S, Dalgarno DC, Brauer AW, Schreiber SL. Structural basis for the binding of proline-rich peptides to SH3 domains. Cell. 1994; 76(5): 933-45.

Zhang C, Xie Y, Martignetti JA, Yeo TT, Massa SM, Longo FM. A candidate chimeric mammalian mRNA transcript is derived from distinct chromosomes and is associated with nonconsensus splice junction motifs. DNA Cell Biol. 2003; 22(5): 303-15.